Supporting information

[1,5]-Hydride shift-cyclization *versus* C(sp^2)-H Functionalization in the Knoevenagel-Cyclization Domino Reactions of 1,4- and 1,5-Benzoxazepines

Dóra Szalóki Vargáné [1,2,†], László Tóth [1,3,†], Balázs Buglyó [1], Attila Kiss-Szikszai [1], Attila Mándi [1], Péter Mátyus [4], Sándor Antus [1,*], Yinghan Chen [5], Dehai Li [5], Lingxue Tao [6], Haiyan Zhang [6] and Tibor Kurtán [1,*]

[1] Department of Organic Chemistry, University of Debrecen, Debrecen, P. O. Box 400, Debrecen 4002, Hungary; szalokido@gmail.com (D.S.V.); tothlaszlochemist@gmail.com (L.T.); buglyo.balazs@science.unideb.hu (B.B.); kiss.attila@science.unideb.hu (A.K.-S.); mandi.attila@science.unideb.hu (A.M.)
[2] Doctoral School of Chemistry, University of Debrecen, Egyetem tér 1, Debrecen 4032, Hungary
[3] Department of Organic Chemistry, Semmelweis University, Budapest 1094, Hungary
[4] Institute of Digital Health Sciences, Faculty of Health and Public Services, Semmelweis University, Ferenc tér 15, Budapest 1094, Hungary; peter.maty@gmail.com
[5] Key Laboratory of Marine Drugs, Chinese Ministry of Education, School of Medicine and Pharmacy, Ocean University of China, Qingdao 266003, China; qd_yinghan@163.com (Y.C.); dehaili@ouc.edu.cn (D.L.);
[6] CAS Key Laboratory of Receptor Research, Shanghai Institute of Materia Medica, Chinese Academy of Sciences, 555 Zu Chong Zhi Road, Zhang Jiang Hi-Tech Park, Shanghai 201203, China; lingxuetao@simm.ac.cn (L.T.); hzhang@simm.ac.cn (H.Z.)
* Correspondences: kurtan.tibor@science.unideb.hu (T.K.), antus.sandor@science.unideb.hu (S.A.)
† These authors contributed equally to this work.

Table of content

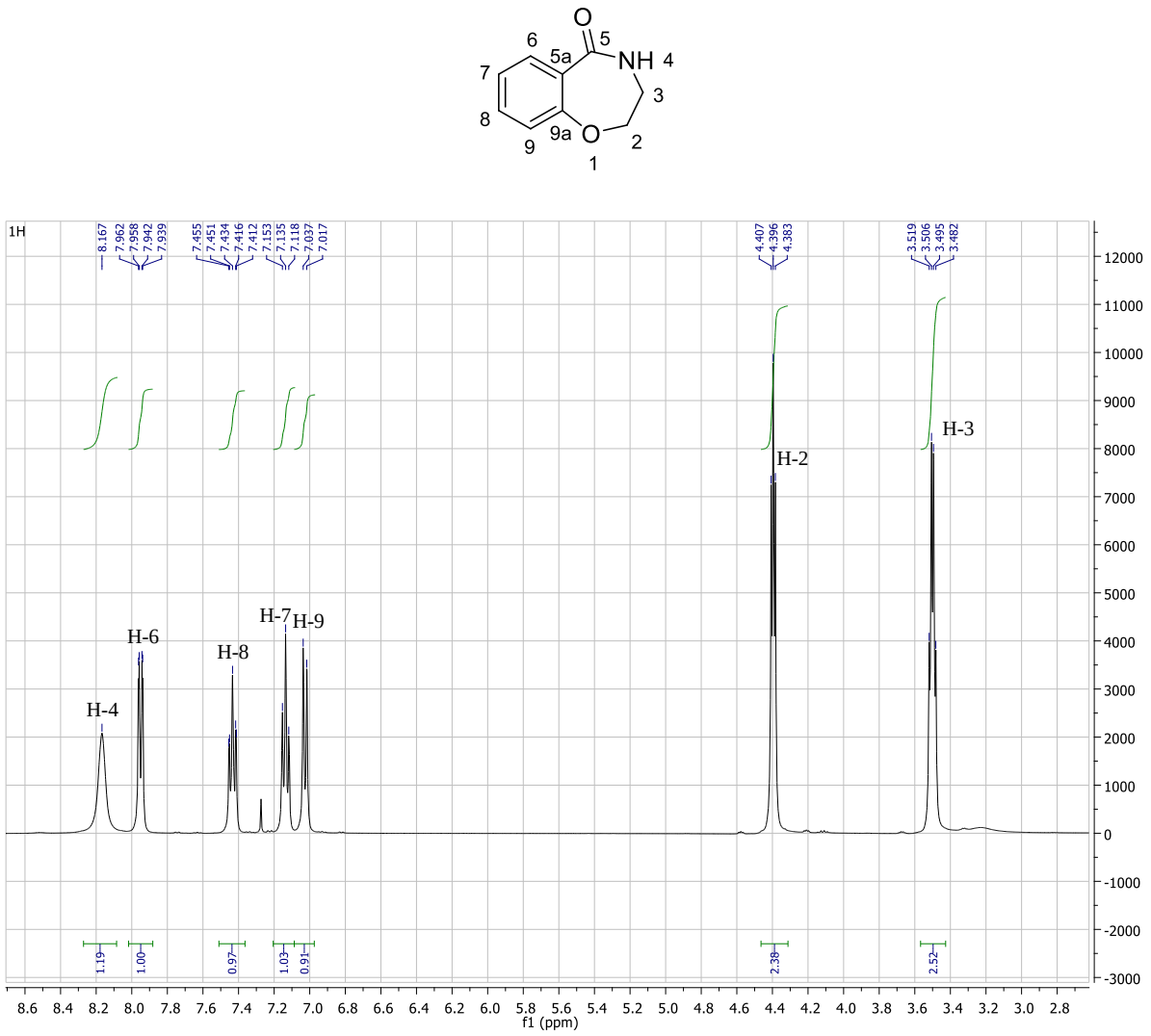

Figure S1. ^{1}H-NMR spectrum of *rac*-**8a** measured in $CDCl_3$ (400 MHz).

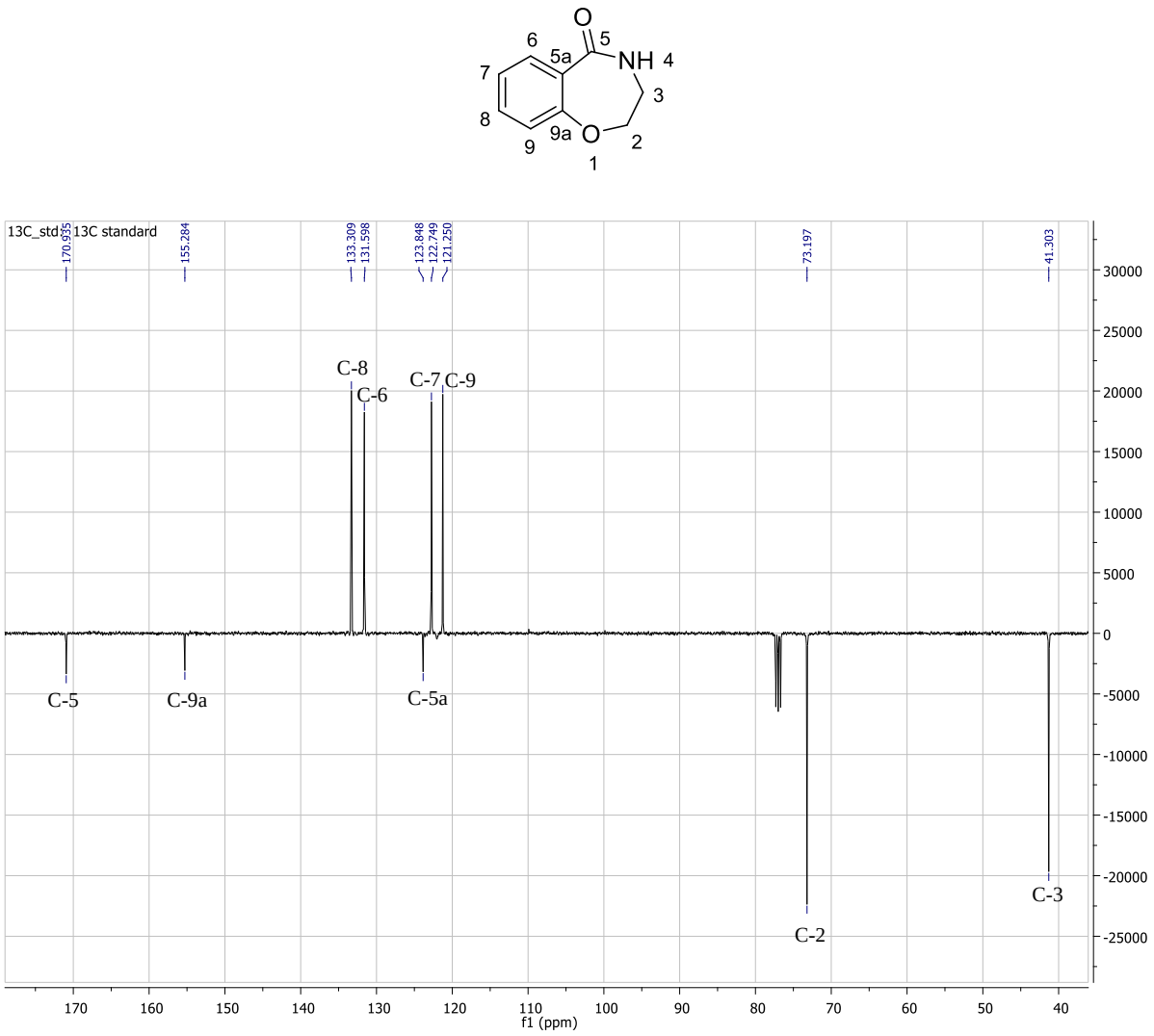

Figure S2. J-modulated ^{13}C-NMR spectrum of *rac*-**8a** measured in $CDCl_3$ (100 MHz).

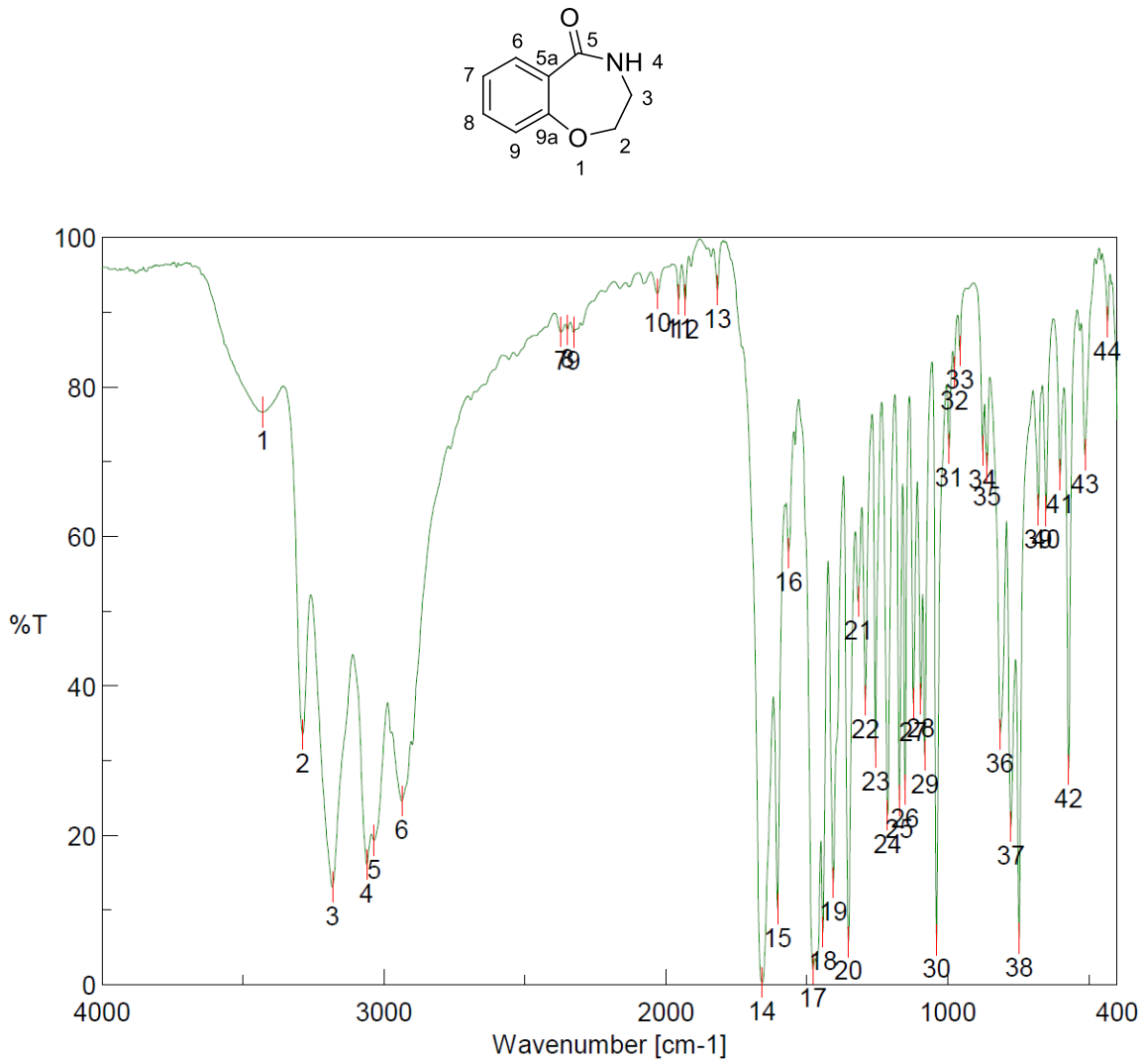

Figure S3. IR spectrum of *rac*-**8a** recorded as KBr disc.

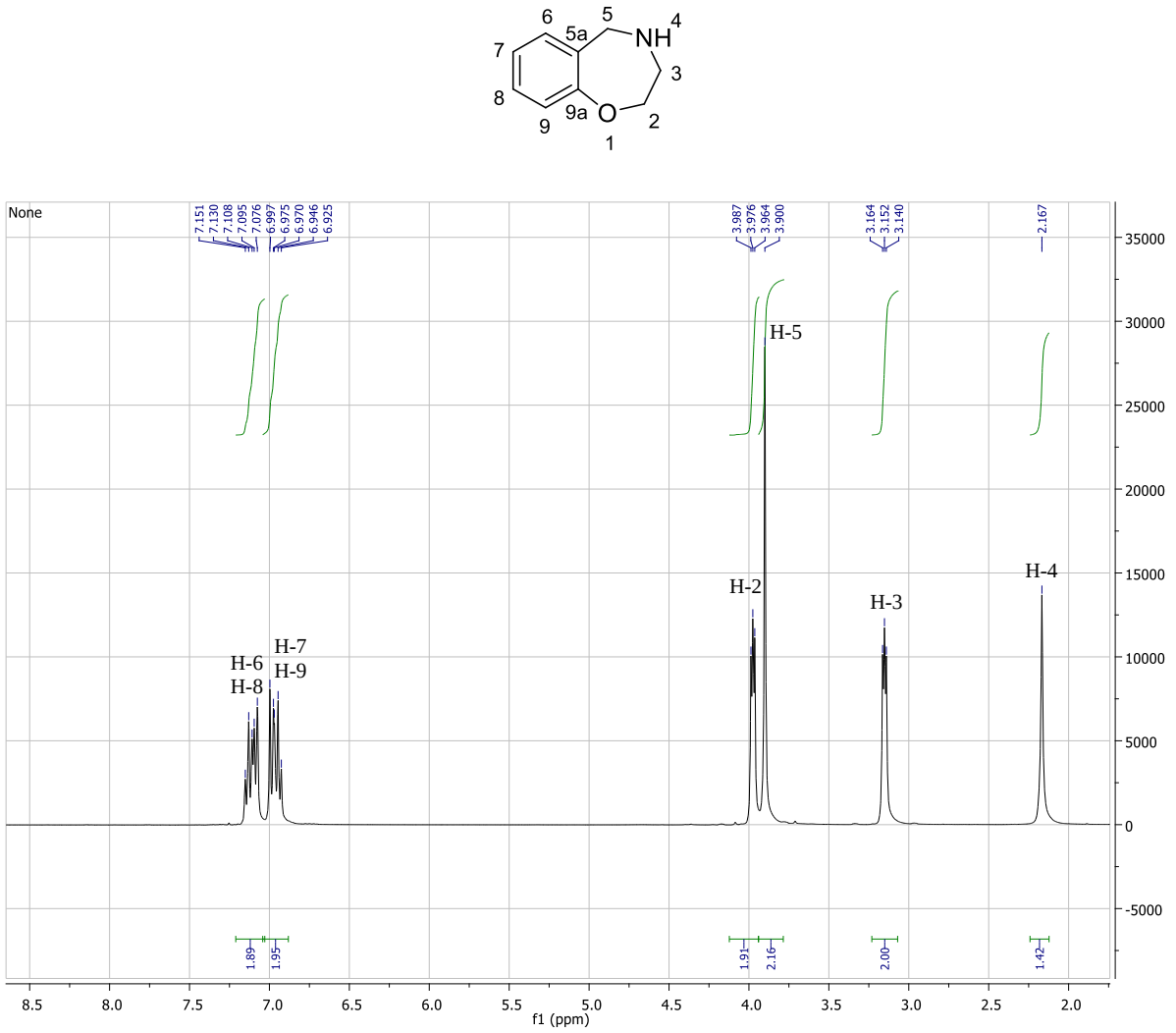

Figure S4. ^{1}H-NMR spectrum of *rac*-**9a** measured in $CDCl_3$ (400 MHz).

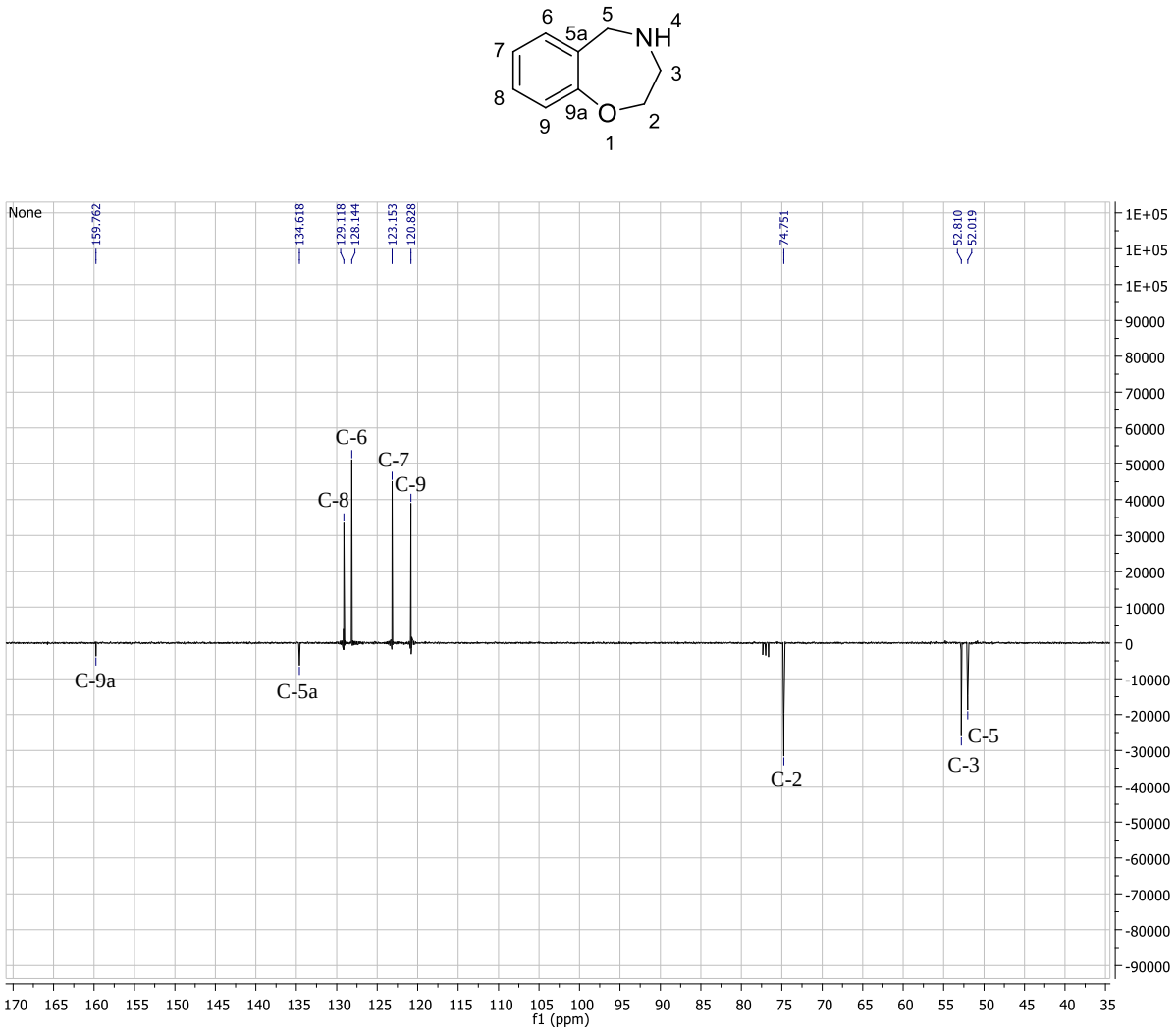

Figure S5. J-modulated ^{13}C-NMR spectrum of *rac*-**9a** measured in $CDCl_3$ (100 MHz).

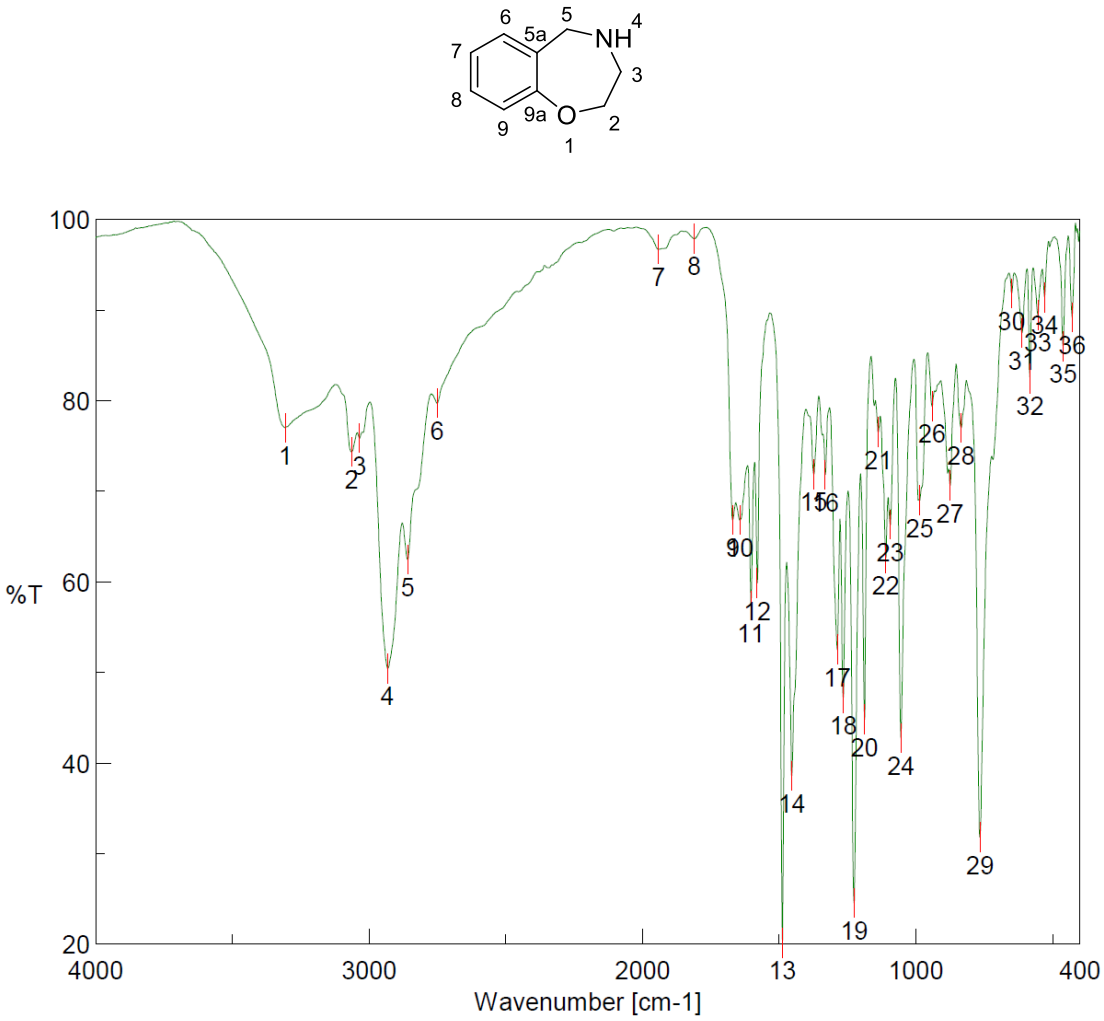

Figure S6. IR spectrum of *rac*-**9a** recorded as KBr disc.

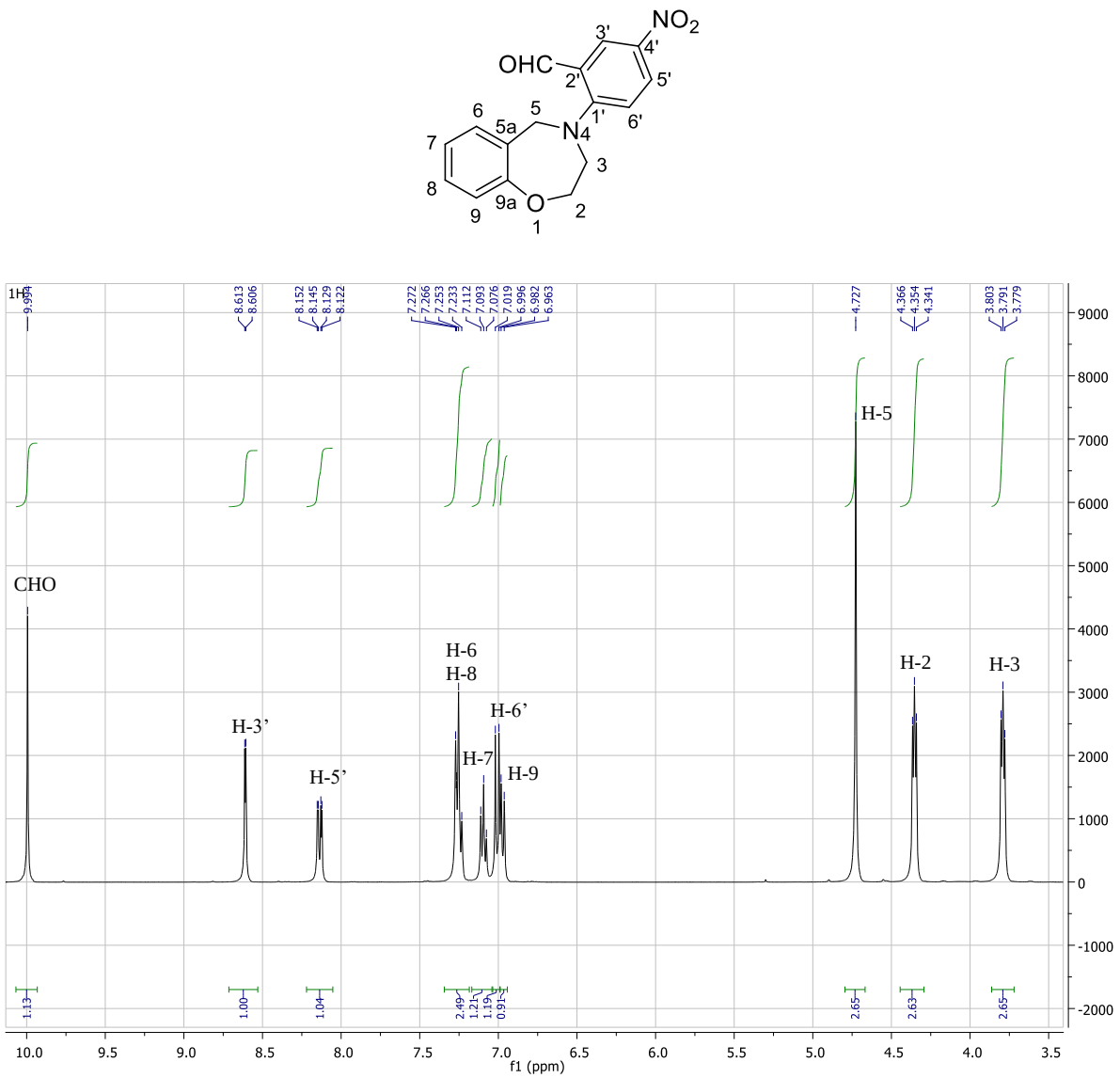

Figure S7. ^{1}H-NMR spectrum of *rac*-**1a** measured in $CDCl_3$ (400 MHz).

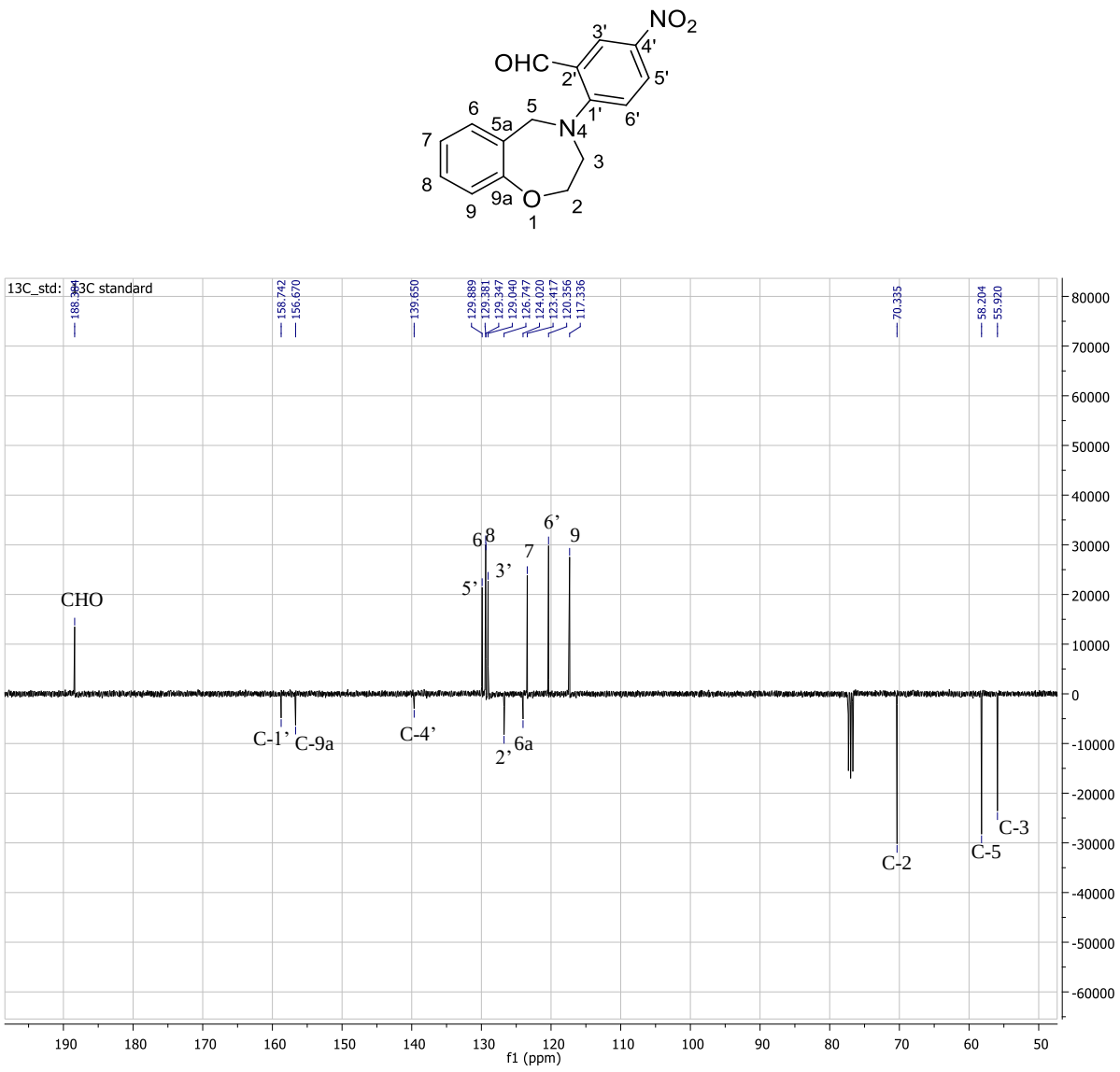

Figure S8. J-modulated ^{13}C-NMR spectrum of *rac*-**1a** measured in $CDCl_3$ (100 MHz).

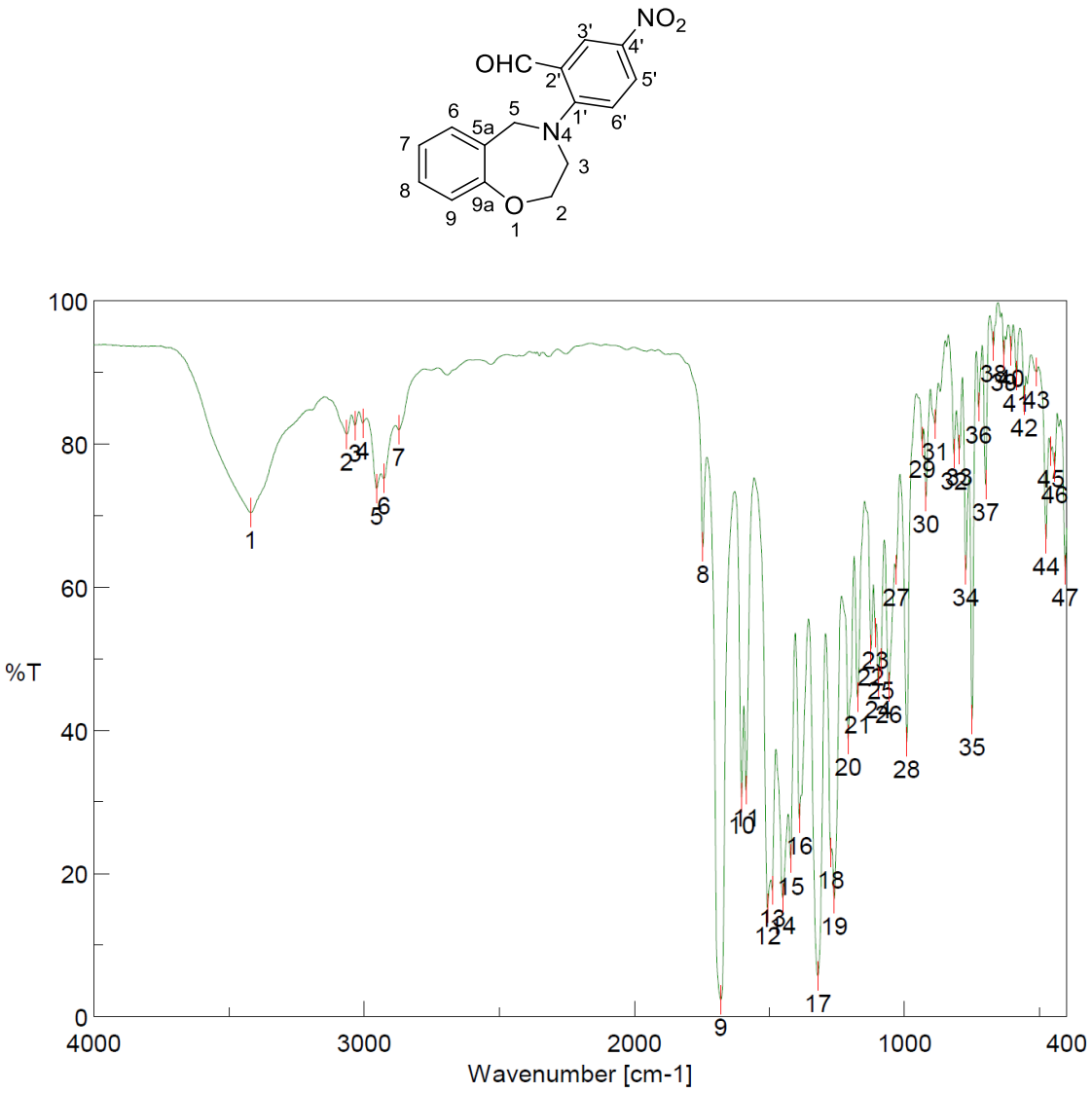

Figure S9. IR spectrum of *rac*-**1a** recorded as KBr disc.

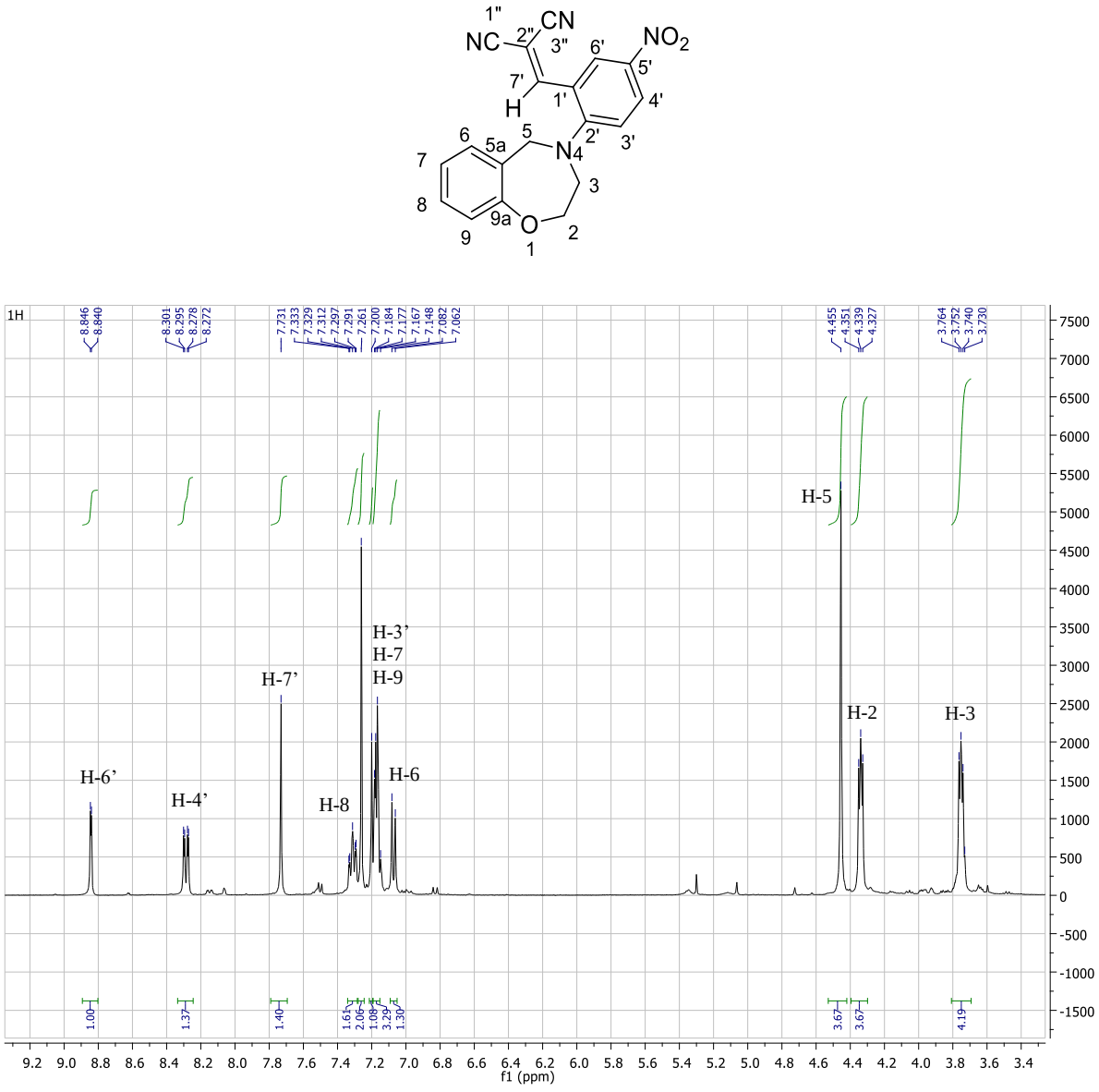

Figure S10. ^{1}H-NMR spectrum of *rac*-**12a** measured in $CDCl_3$ (400 MHz).

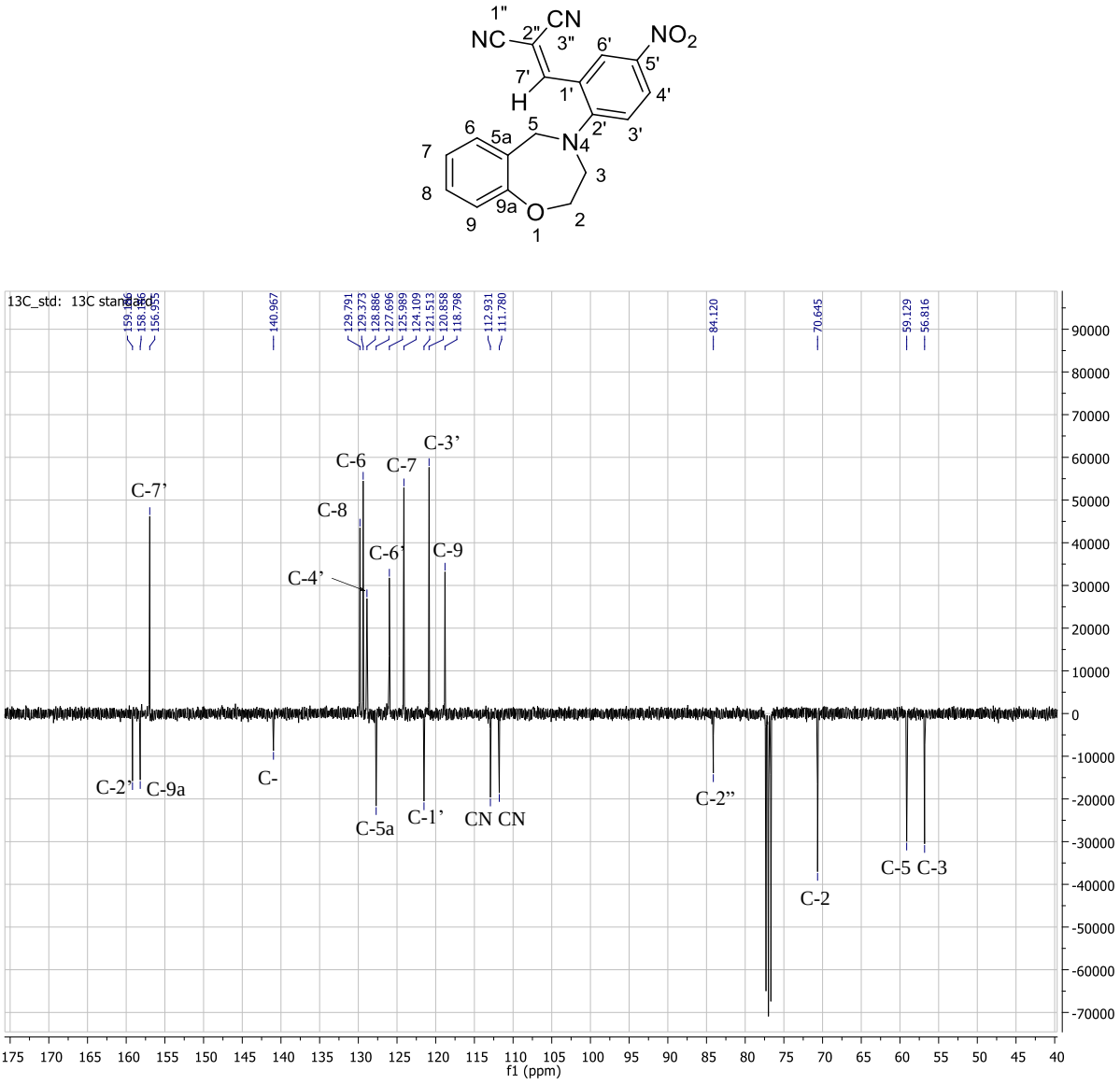

Figure S11. J-modulated ^{13}C-NMR spectrum of *rac*-**12a** mesured in $CDCl_3$ (100 MHz).

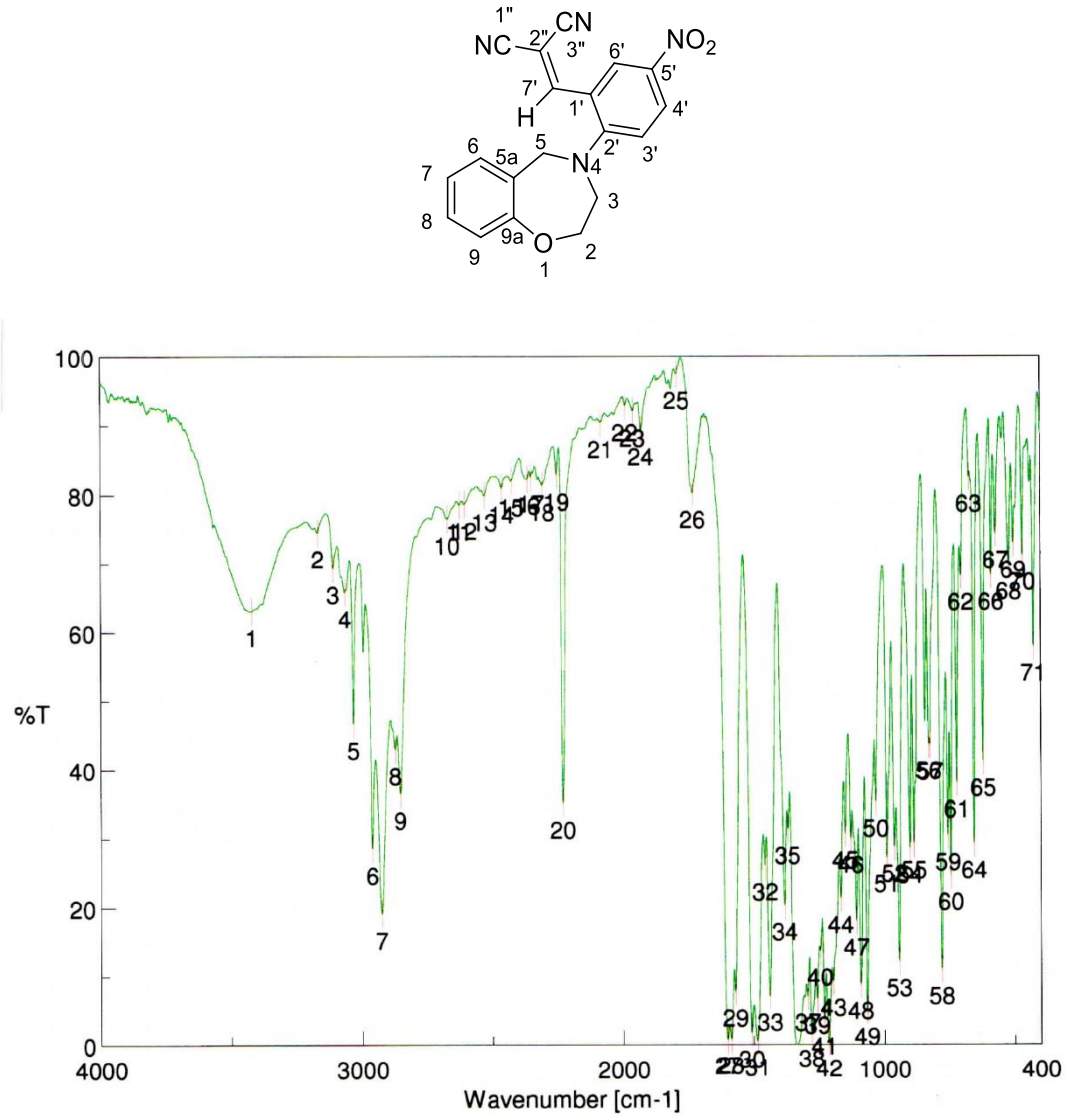

Figure S12. IR spectrum of *rac*-**12a** recorded as KBr disc.

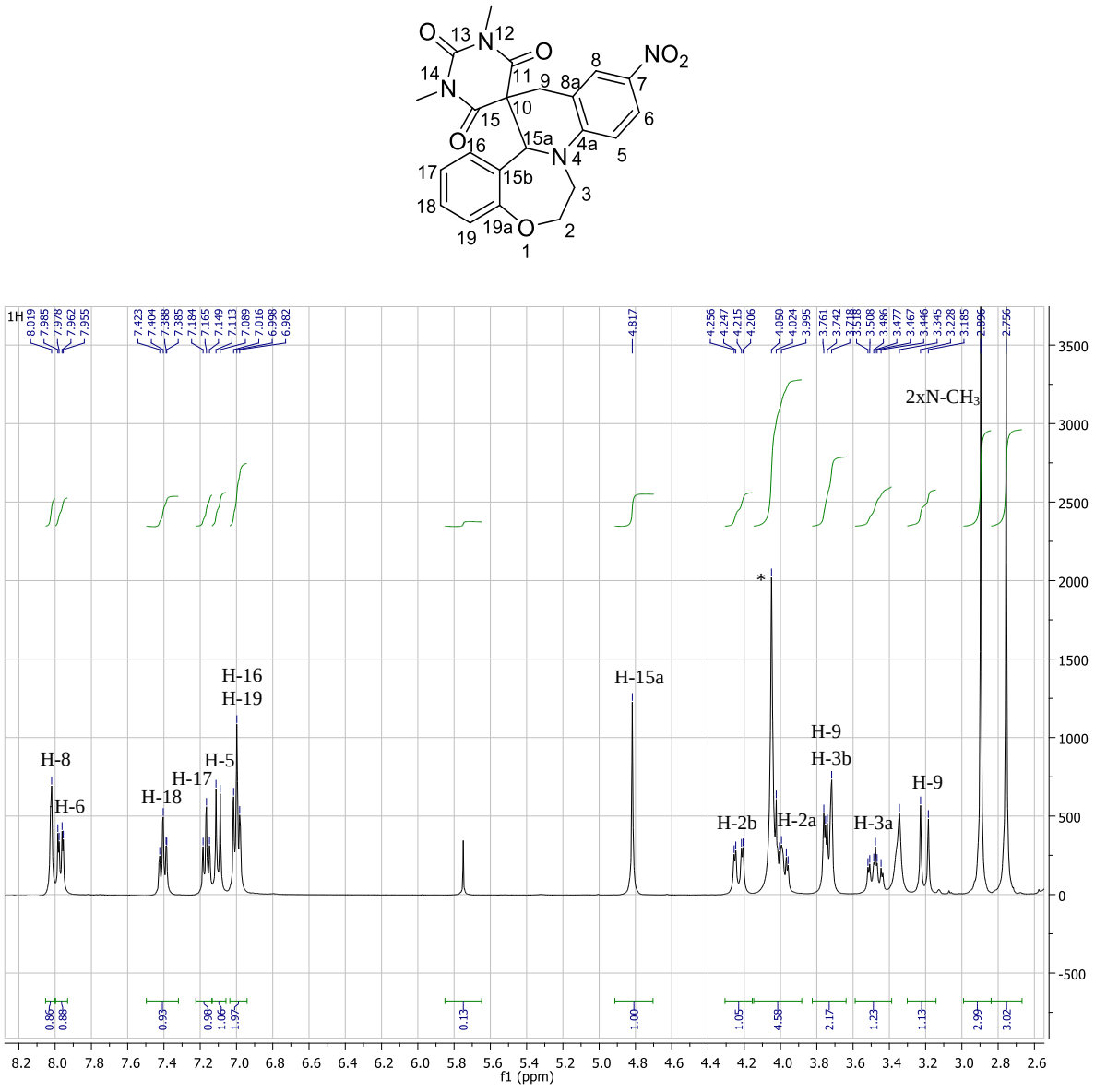

Figure S13. ^{1}H-NMR spectrum of *rac*-**10a** measured in $CDCl_3$ (400 MHz).

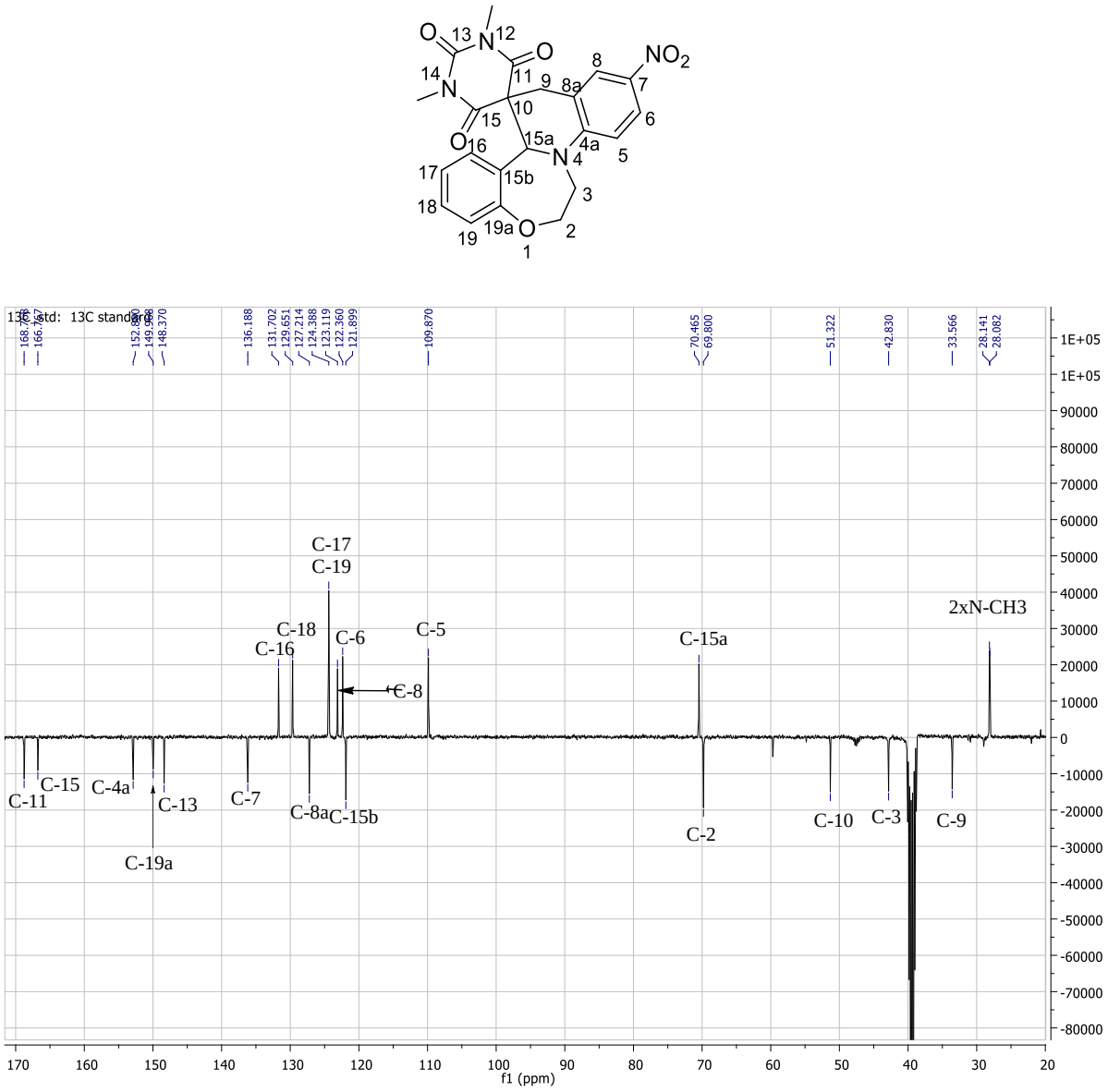

Figure S14. J-modulated ^{13}C-NMR spectrum of *rac*-**10a** measured in $CDCl_3$ (100 MHz).

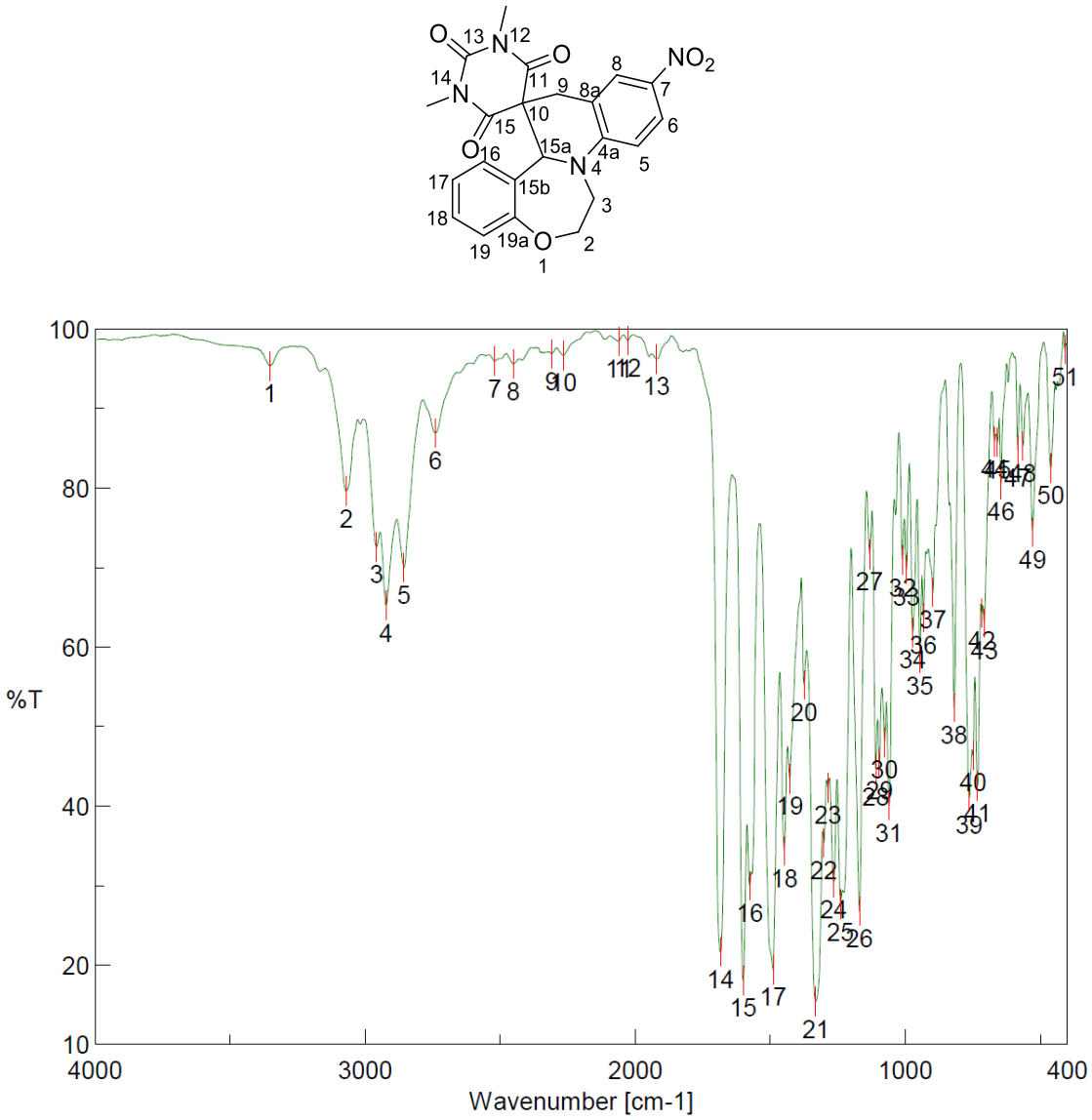

Figure S15. IR spectrum of *rac*-**10a** recorded as KBr disc

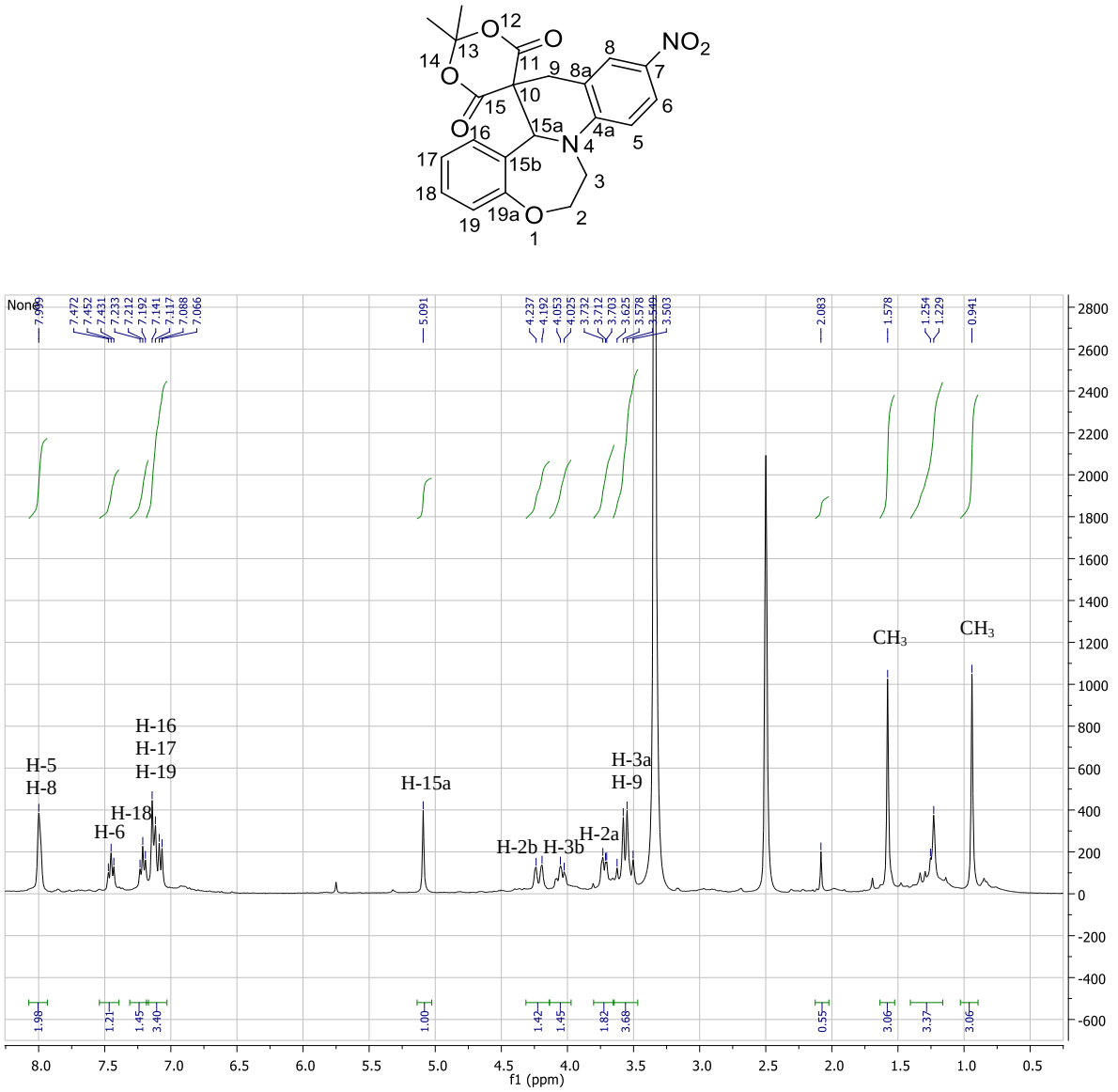

Figure S16. ^{1}H-NMR spectrum of *rac*-**11a** measured in DMSO-d_6 (400 MHz)

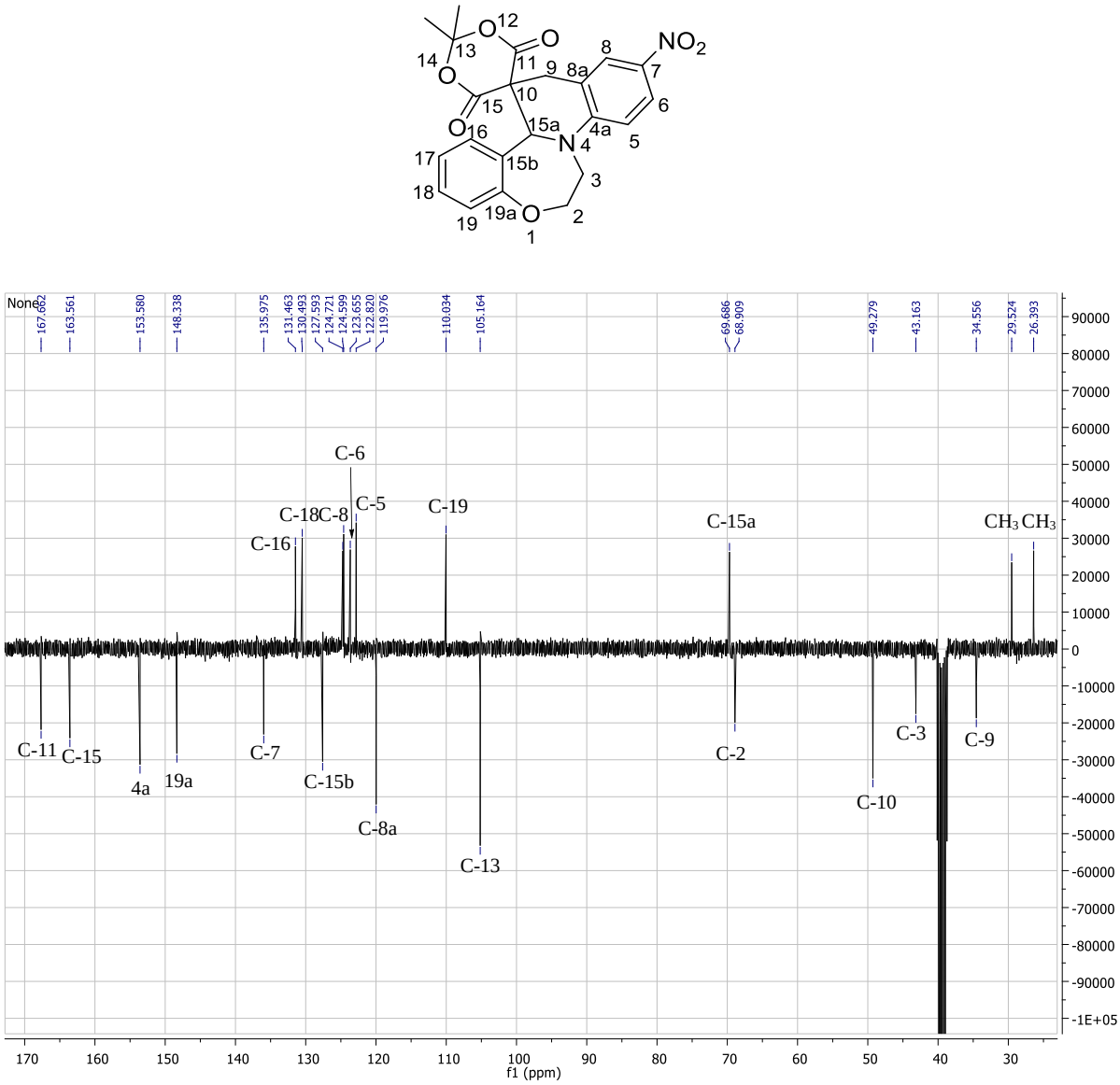

Figure S17. J-modulated ^{13}C-NMR spectrum of *rac*-**11a** measured in DMSO-d_6 (100 MHz)

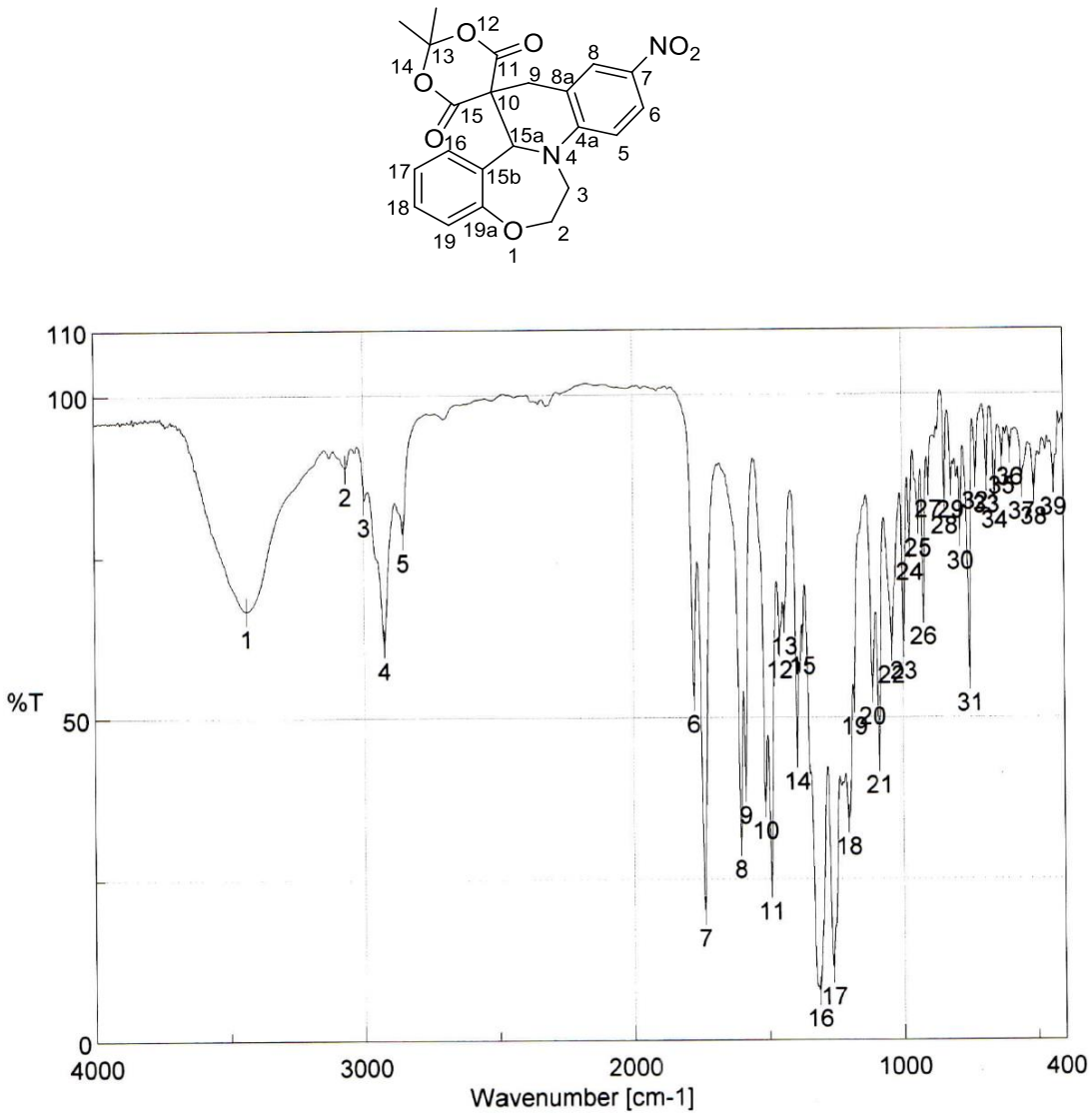

Figure S18. IR spectrum of *rac*-**11a** recorded as KBr disc

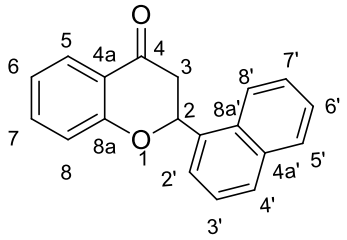

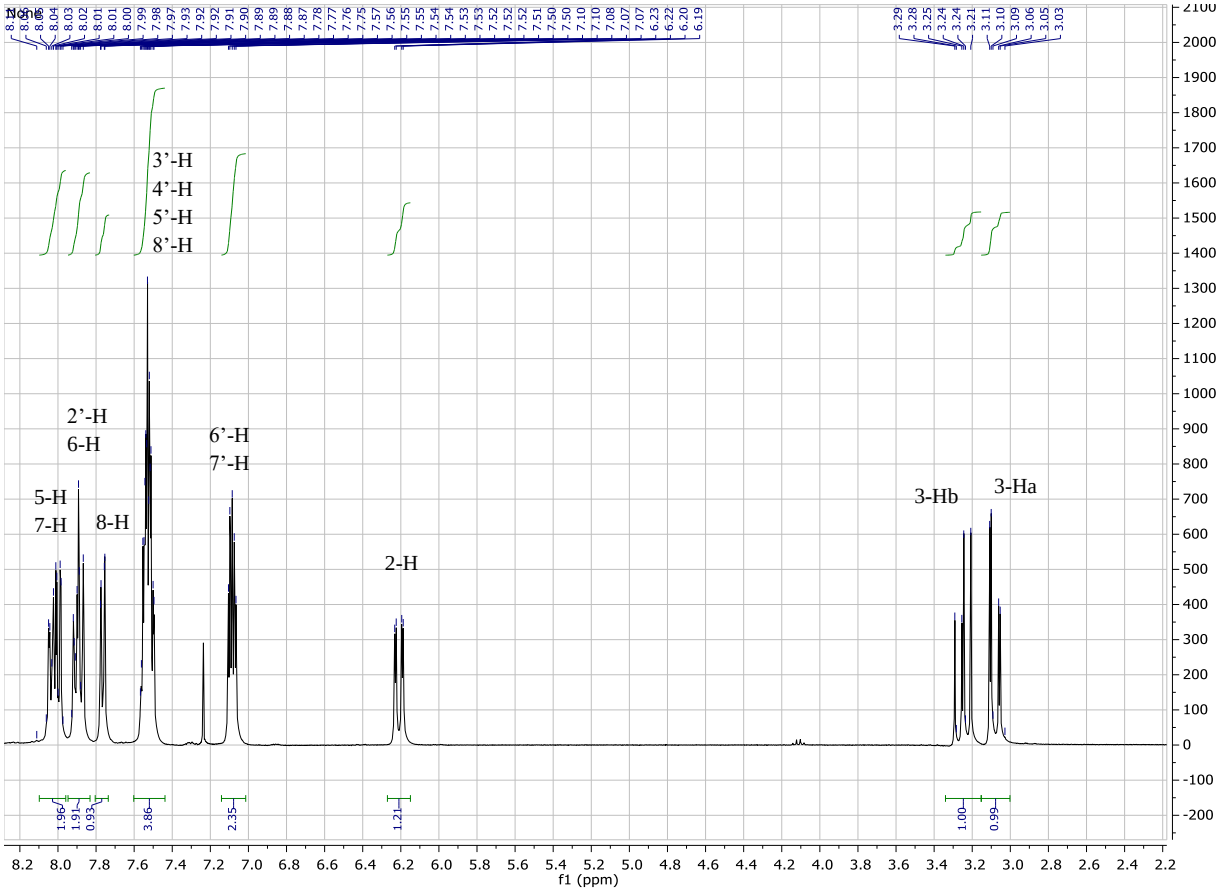

Figure S19. ^{1}H-NMR spectrum of *rac*-**7b** measured in $CDCl_3$ (360 MHz)

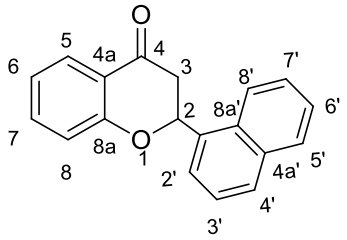

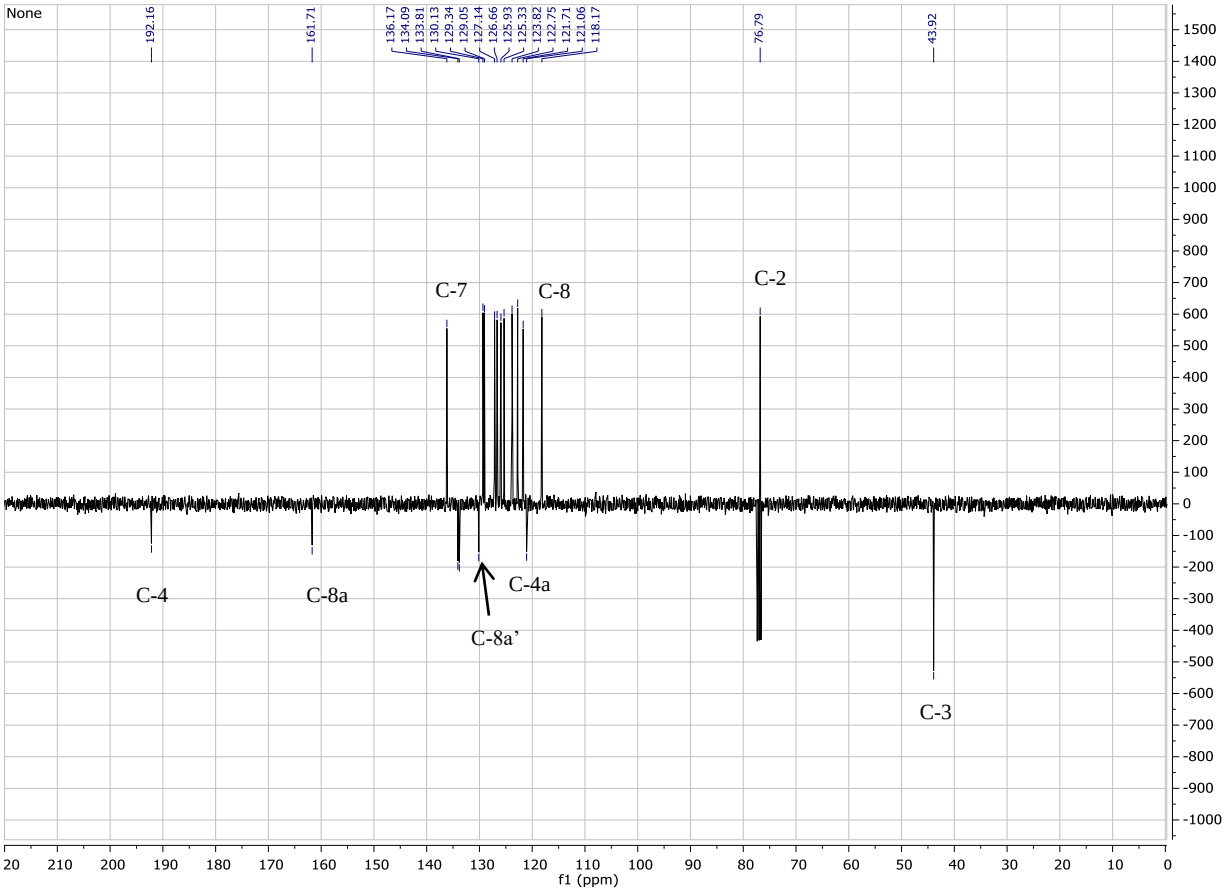

Figure S20. J-modulated ^{13}C-NMR spectrum of *rac*-**7b** measured in $CDCl_3$ (90 MHz)

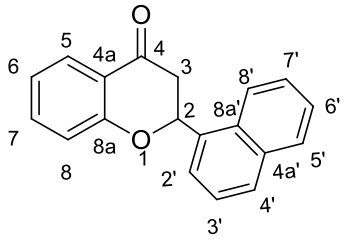

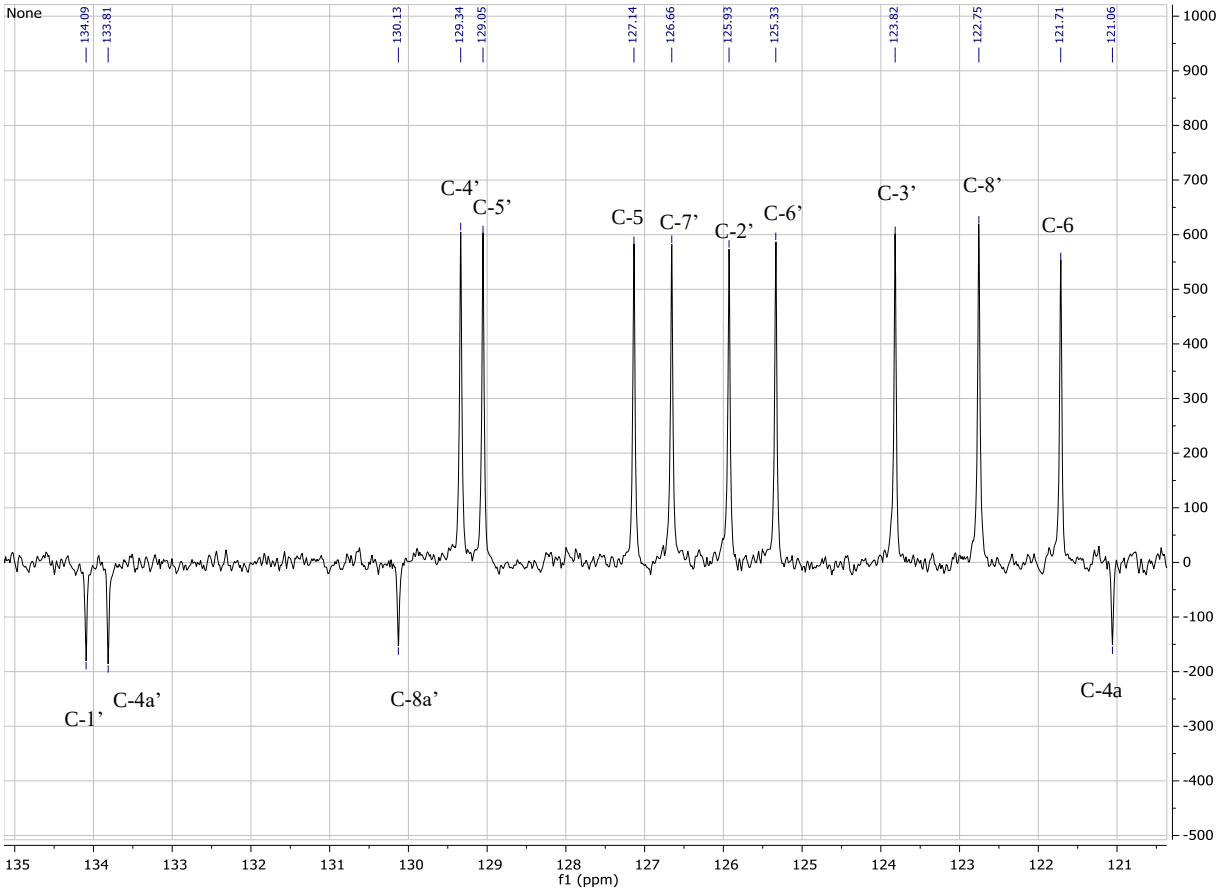

Figure S21. J-modulated ^{13}C-NMR spectrum of *rac*-**7b** measured in $CDCl_3$ (90 MHz)

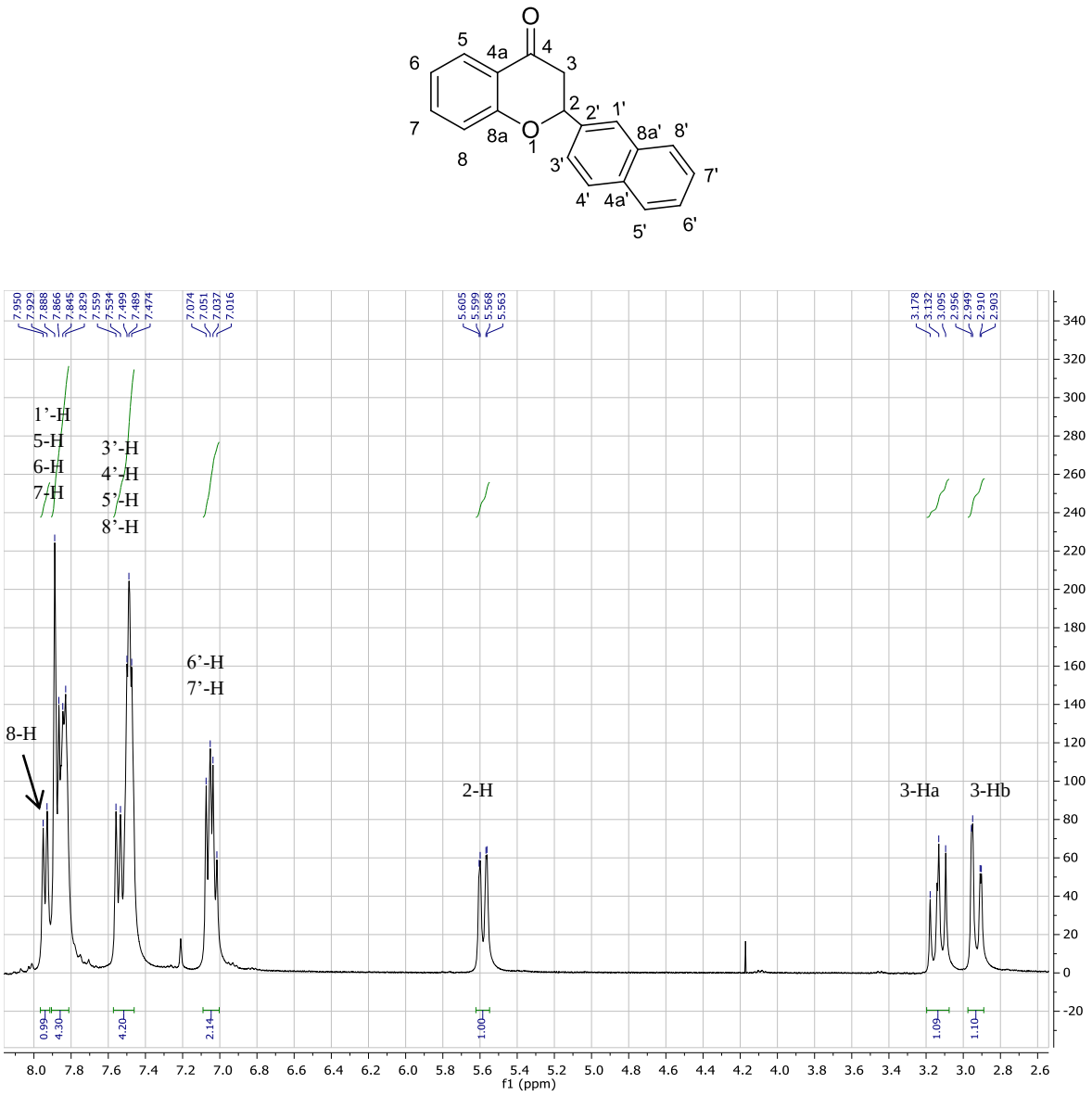

Figure S22. ^{1}H-NMR spectrum of *rac*-**7c** measured in $CDCl_3$ (360 MHz)

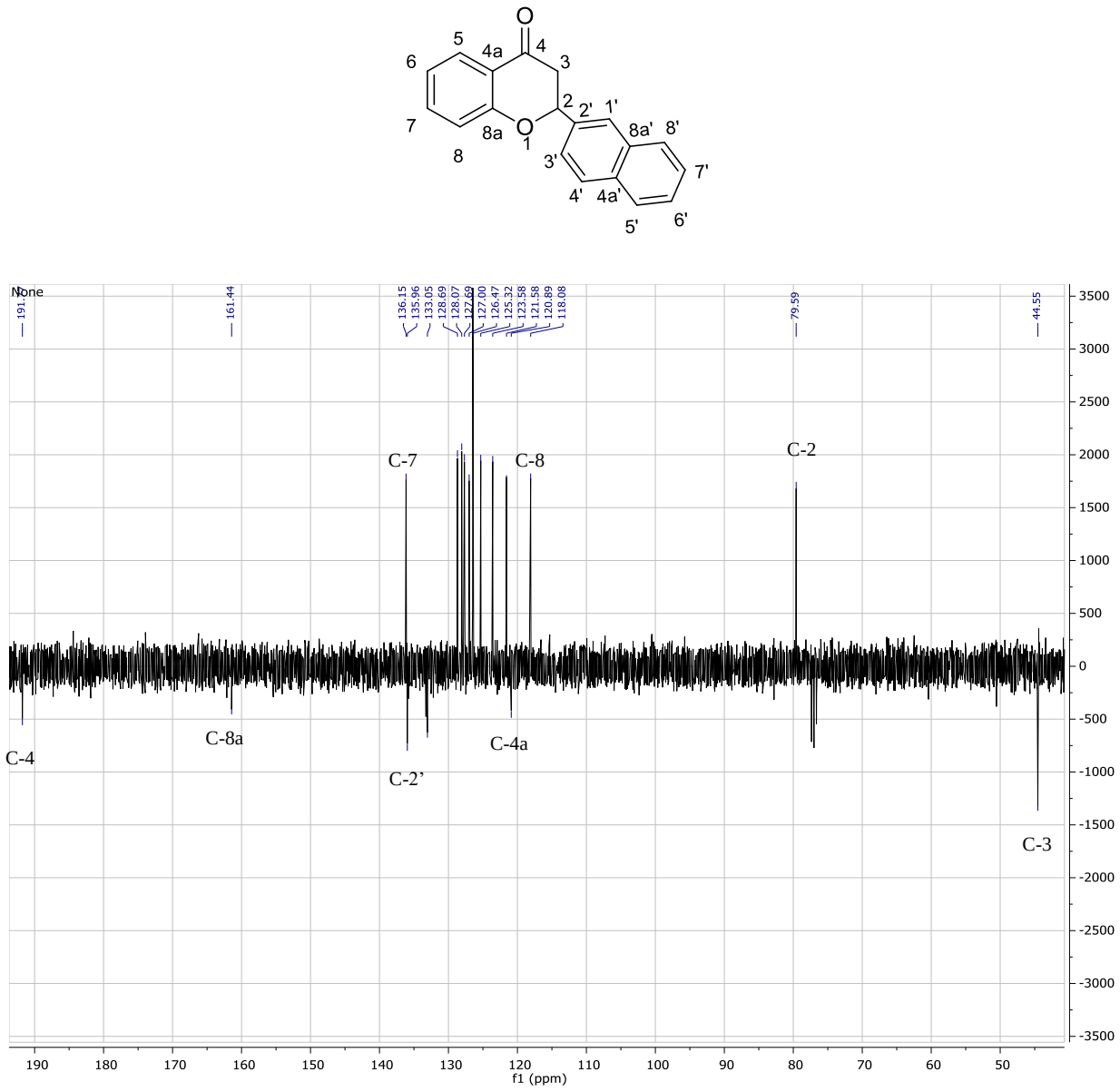

Figure S23. J-modulated ^{13}C-NMR spectrum of *rac*-**7c** measured in $CDCl_3$ (90 MHz)

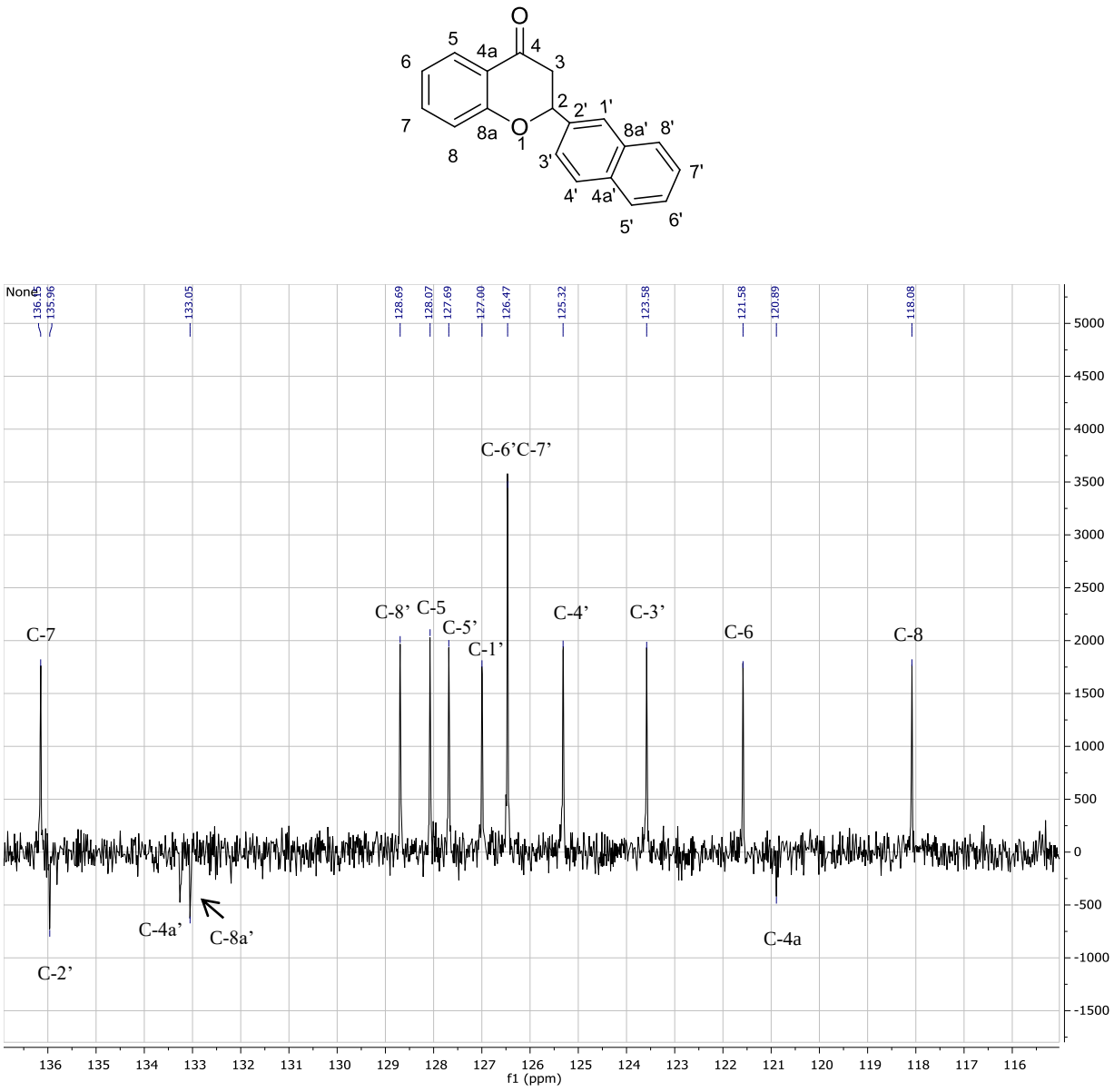

Figure S24. J-modulated ^{13}C-NMR spectrum of *rac*-**7c** measured in $CDCl_3$ (90 MHz)

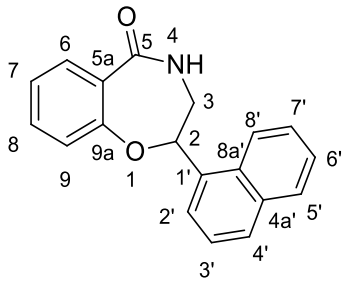

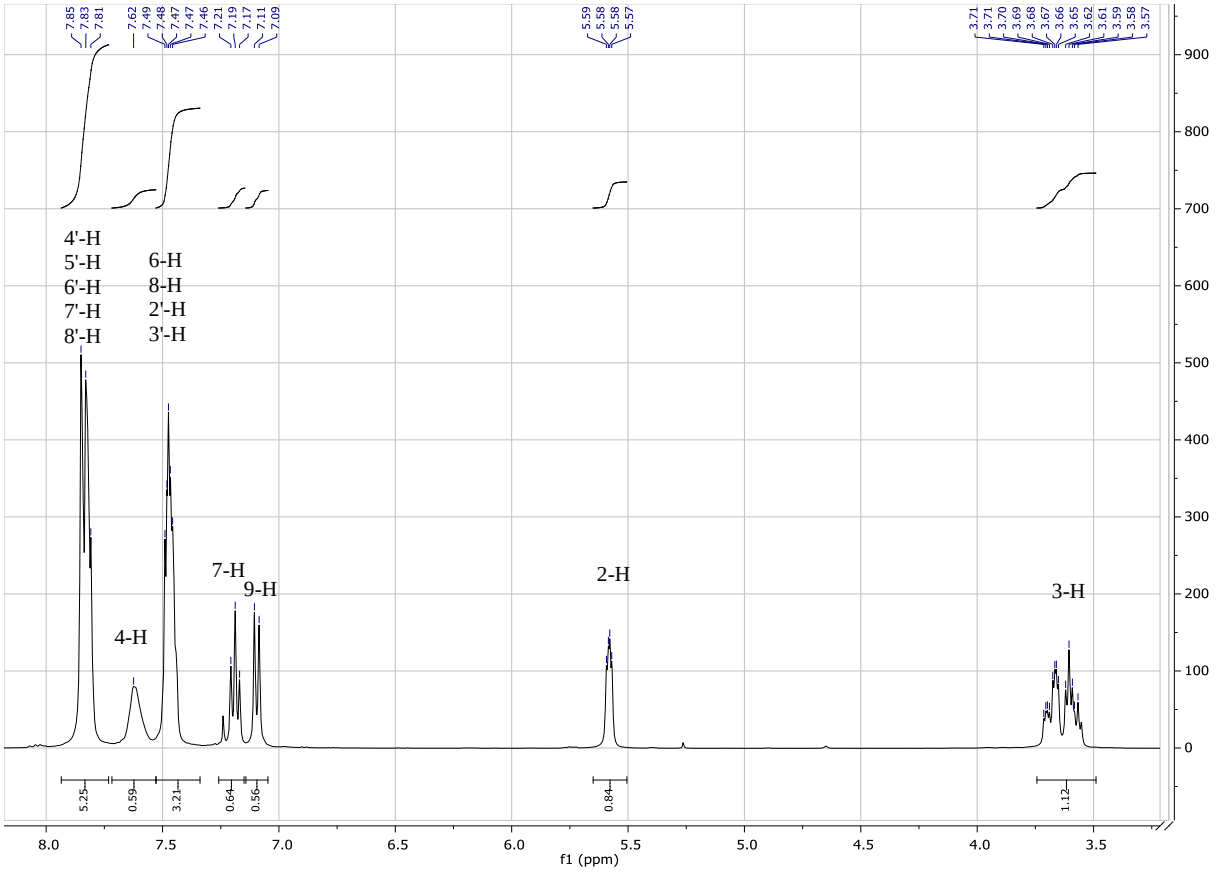

Figure S25. ^{1}H-NMR spectrum of *rac*-**8b** measured in $CDCl_3$ (400 MHz)

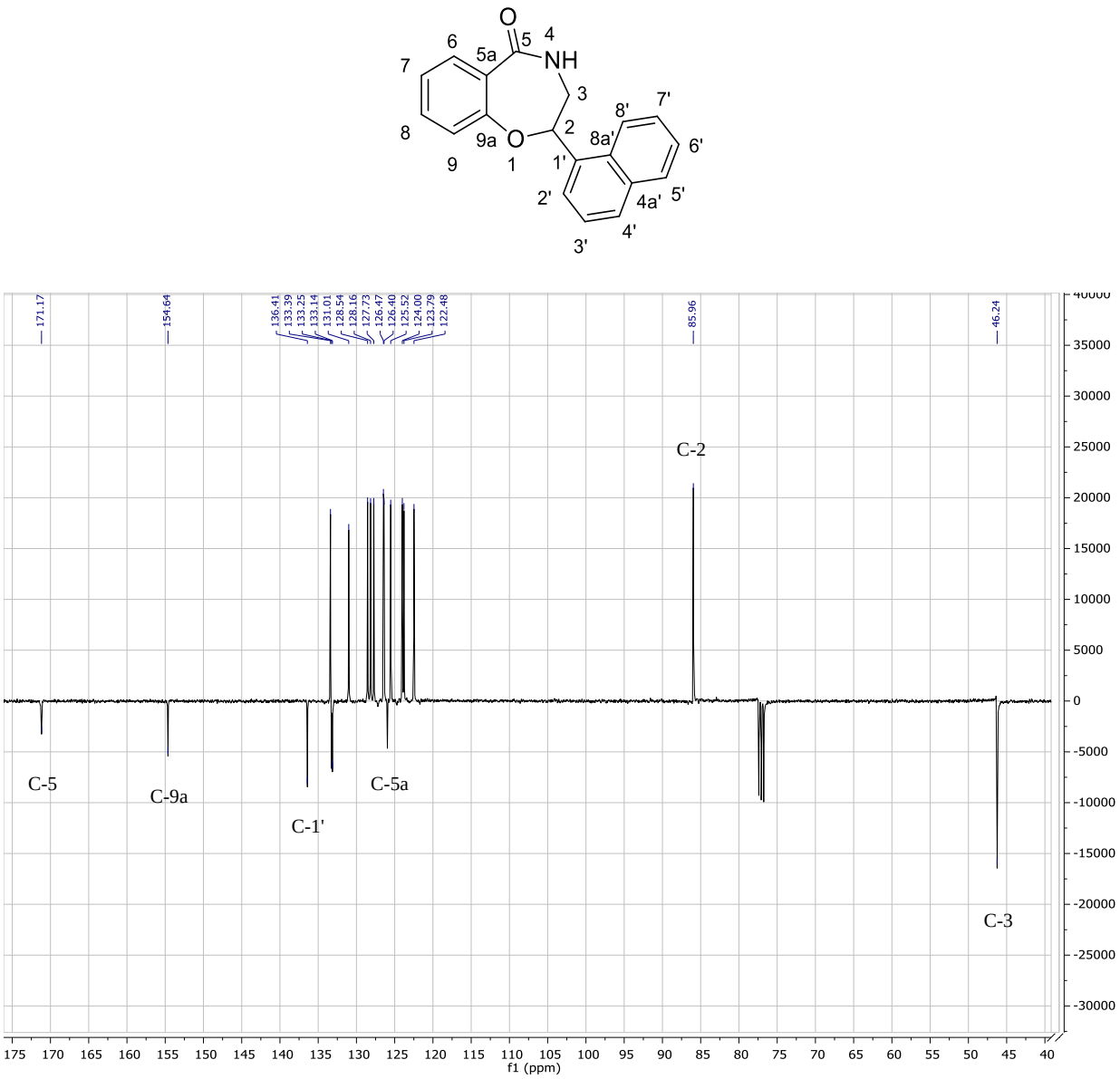

Figure S26. J-modulated ^{13}C-NMR spectrum of *rac*-**8b** measured in $CDCl_3$ (100 MHz)

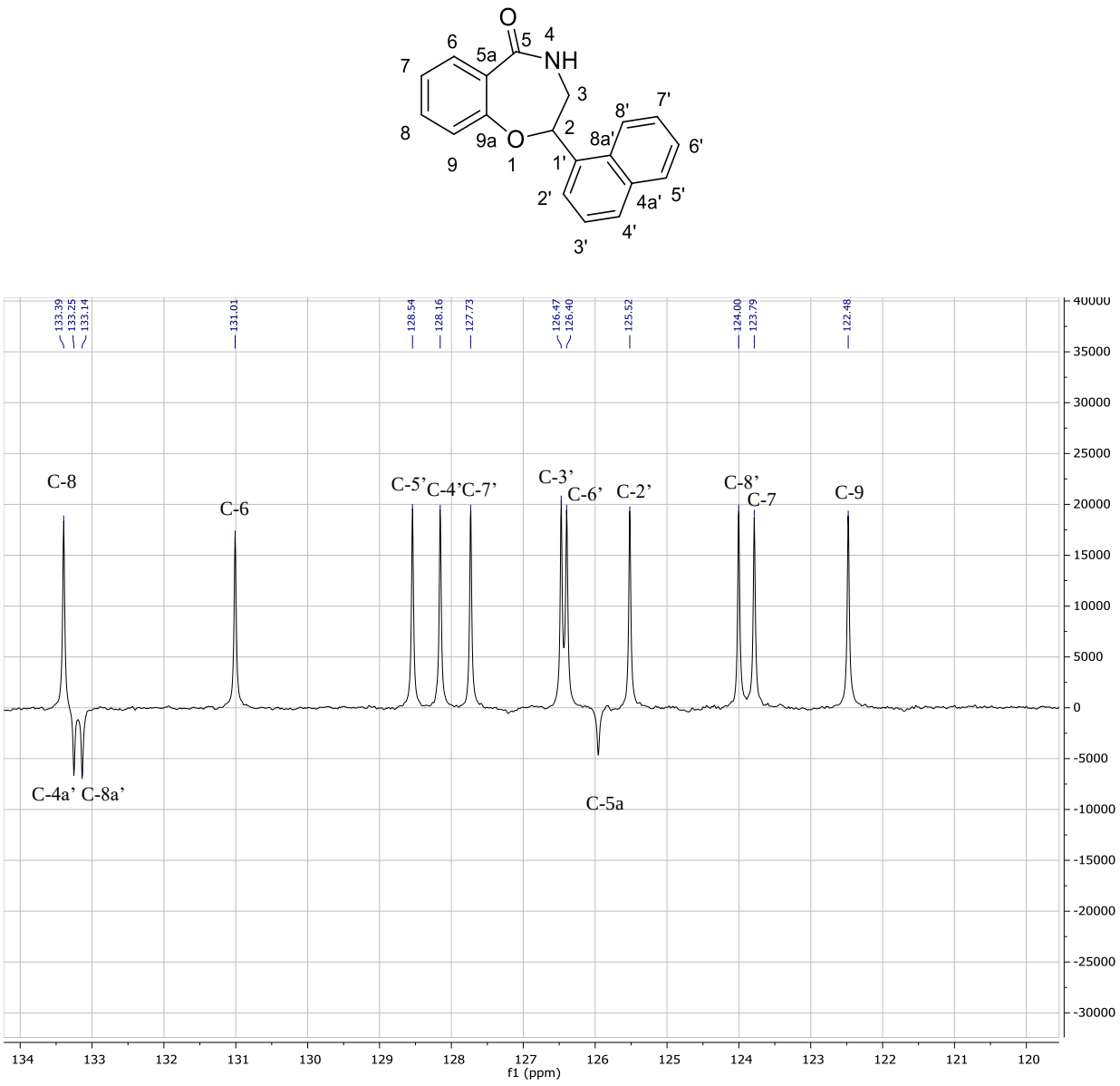

Figure S27. J-modulated ^{13}C-NMR spectra of *rac*-**8b** measured in $CDCl_3$ (100 MHz)

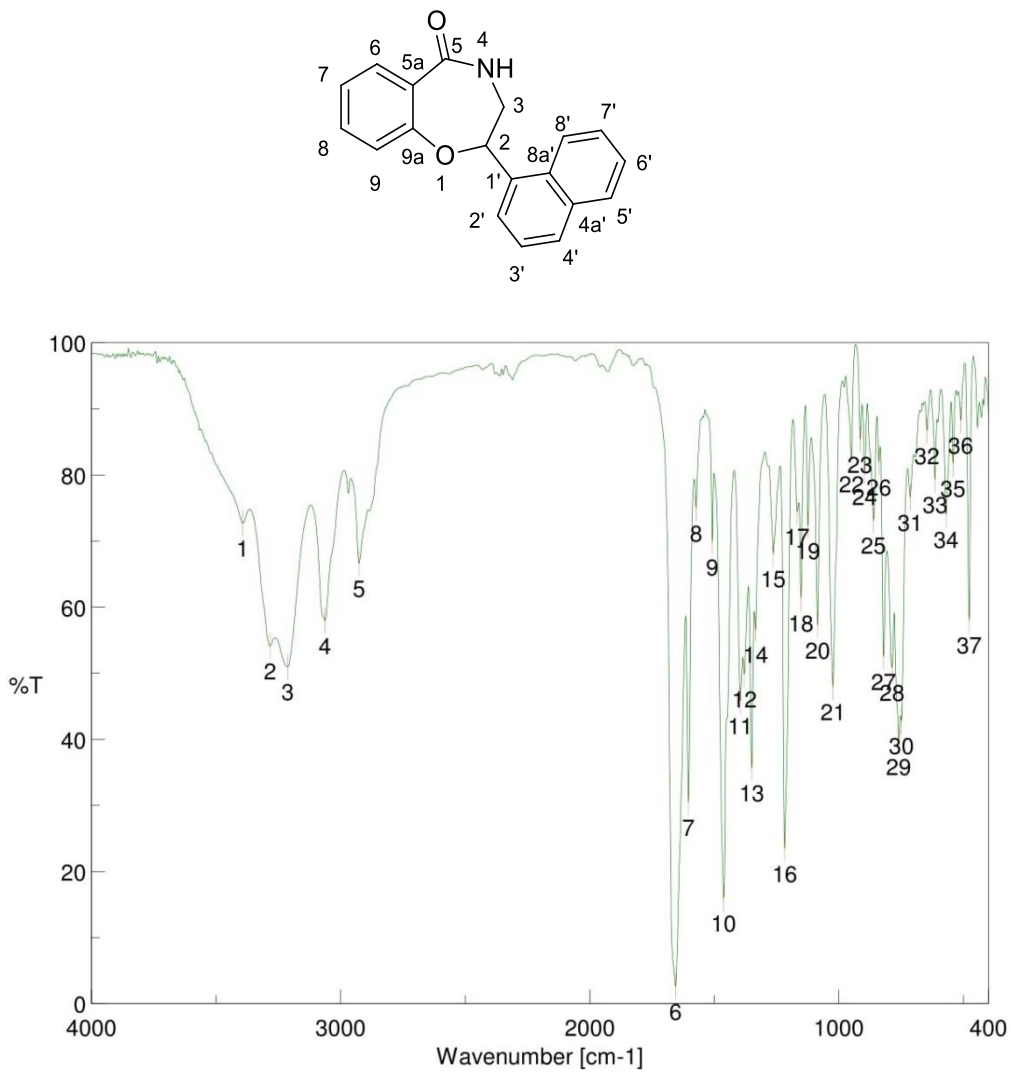

Figure S28 IR spectra of *rac*-**8b** recorded as KBr disc

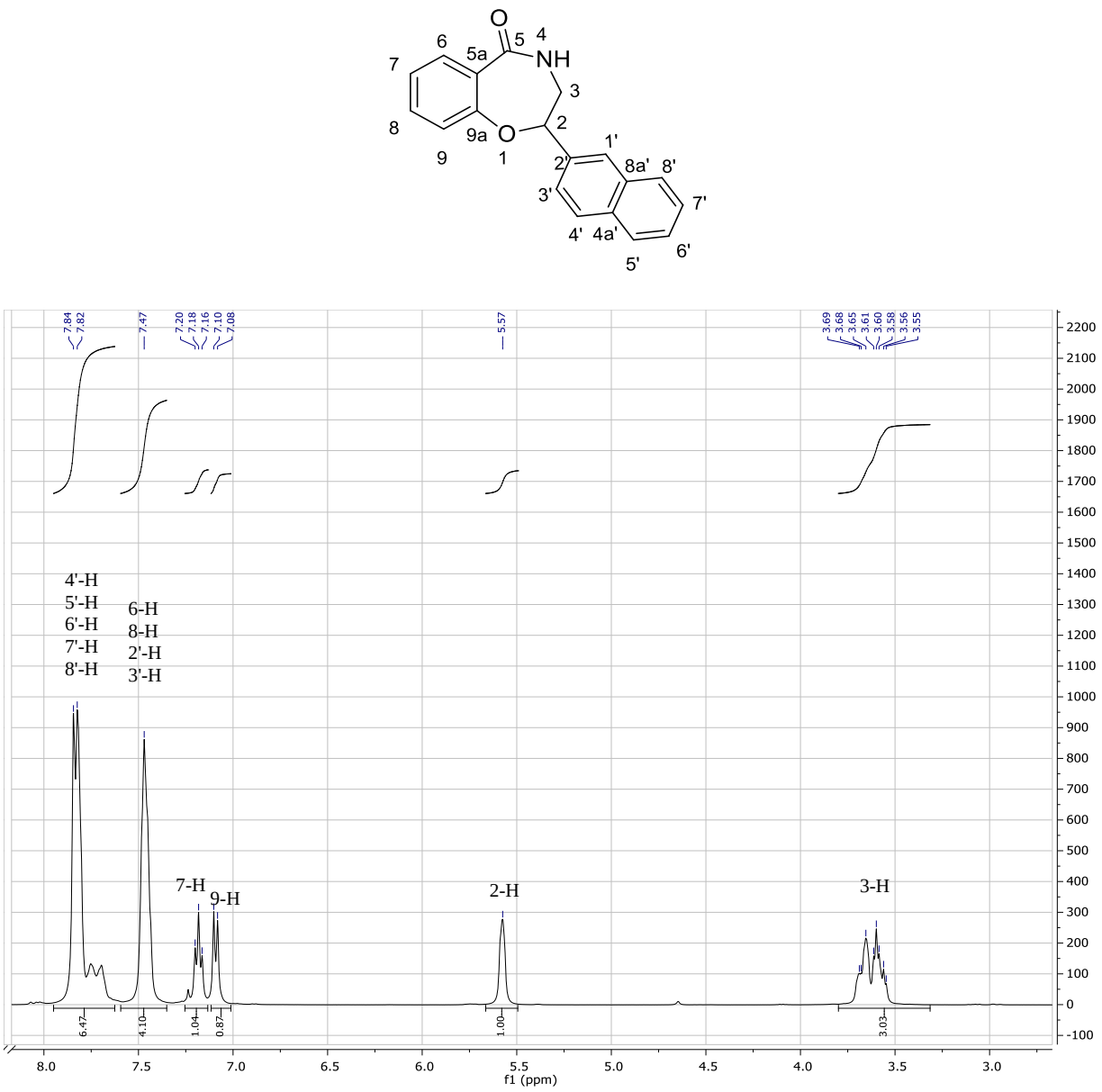

Figure S29. ^{1}H-NMR spectrum of *rac*-**8c** measured in $CDCl_3$ (400 MHz)

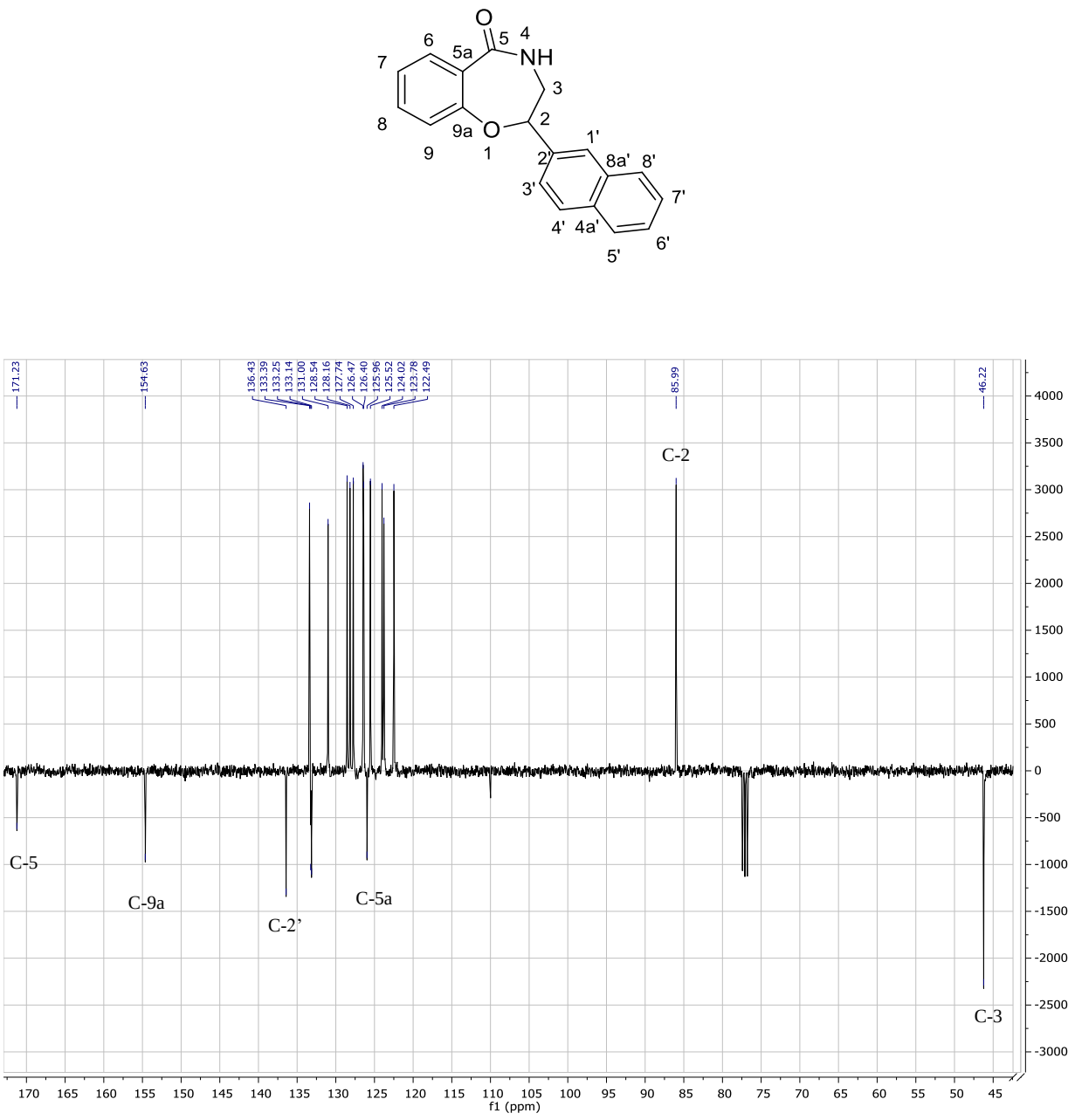

Figure S30. J-modulated ^{13}C-NMR spectrum of *rac*-**8c** measured in $CDCl_3$ (100 MHz)

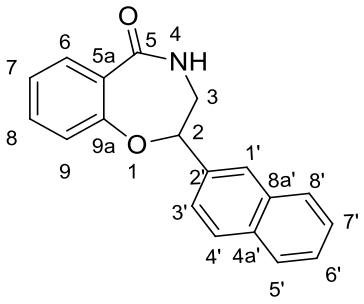

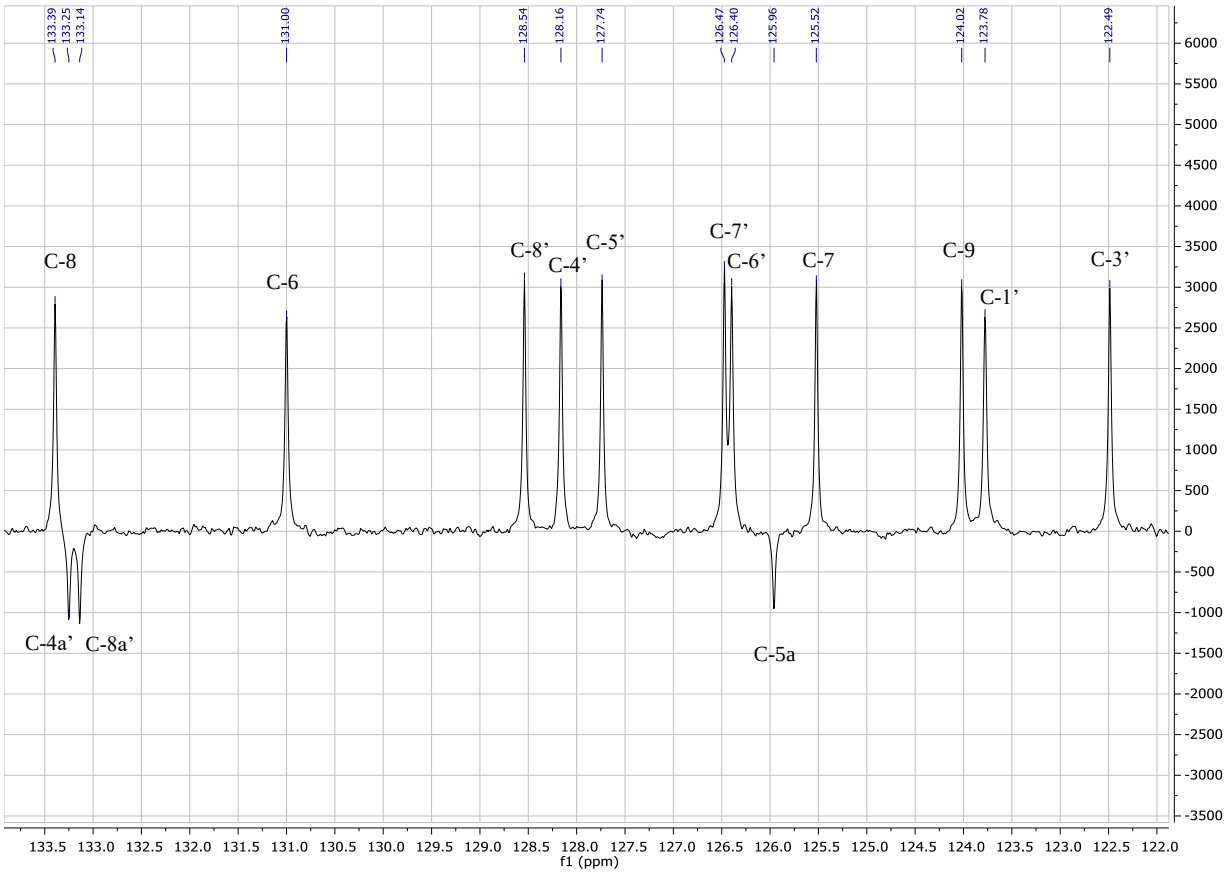

Figure S31 J-modulated ^{13}C-NMR spectrum of *rac*-**8c** measured in $CDCl_3$ (100 MHz)

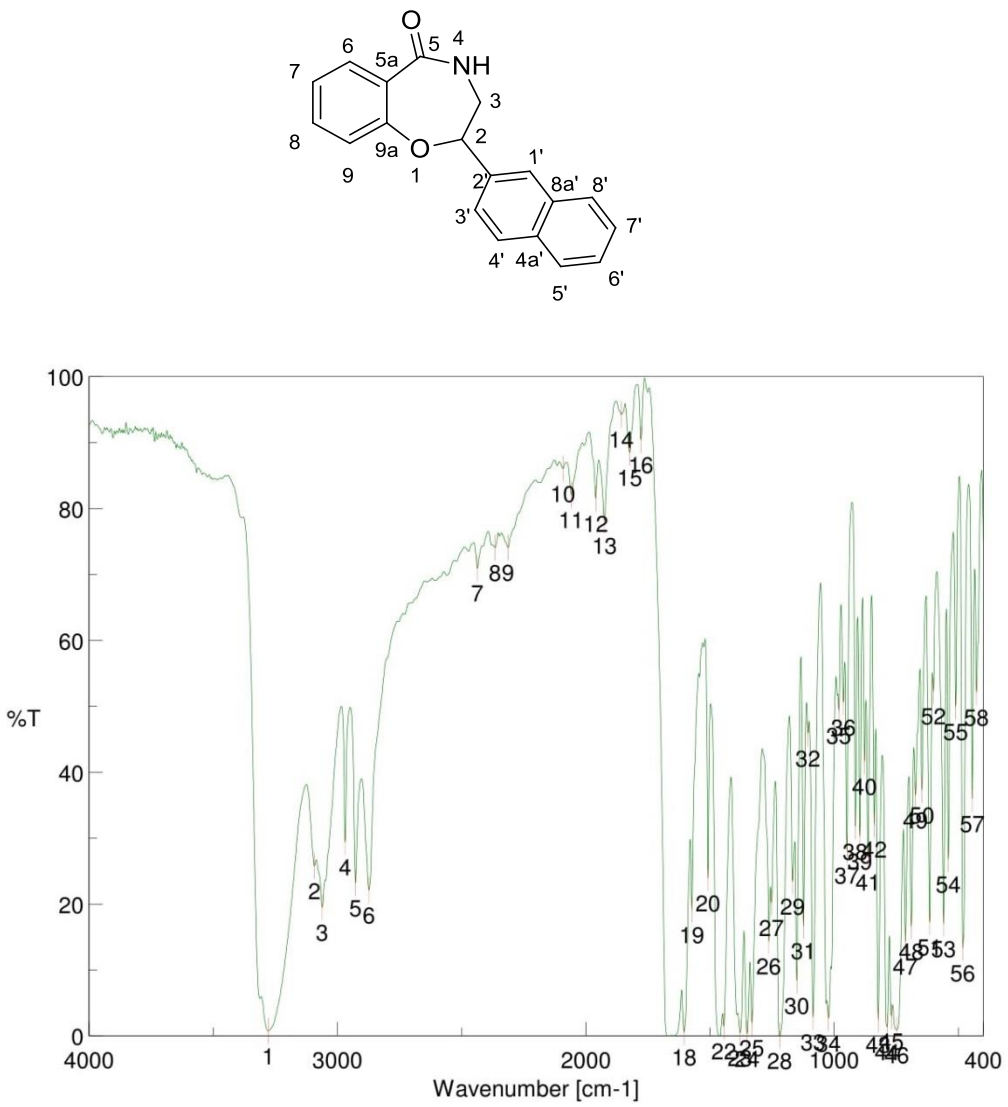

Figure S32 IR spectrum of *rac*-**8c** recorded as KBr disc

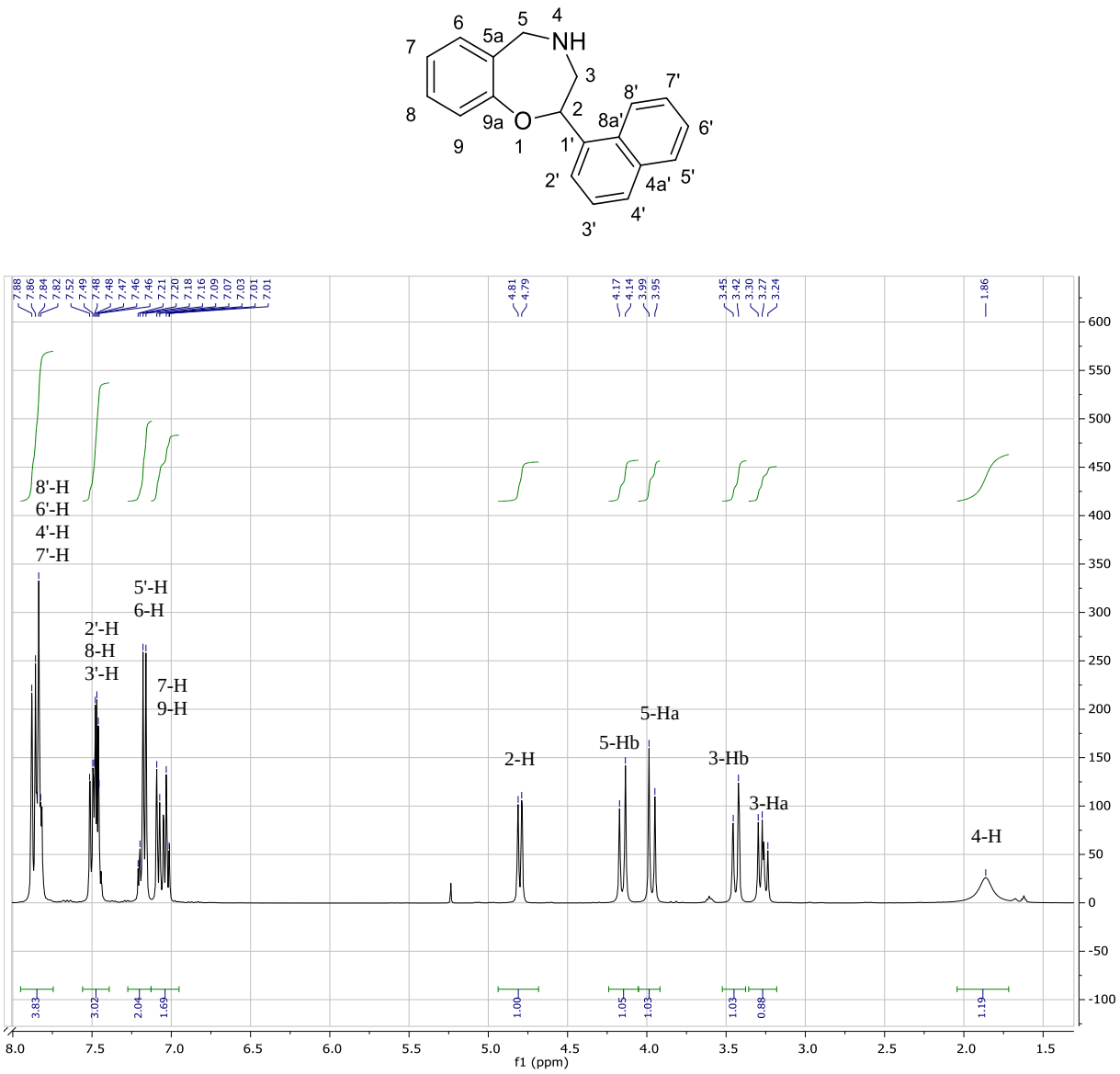

Figure S33. ^{1}H-NMR spectrum of *rac*-**9b** measured in $CDCl_3$ (400 MHz)

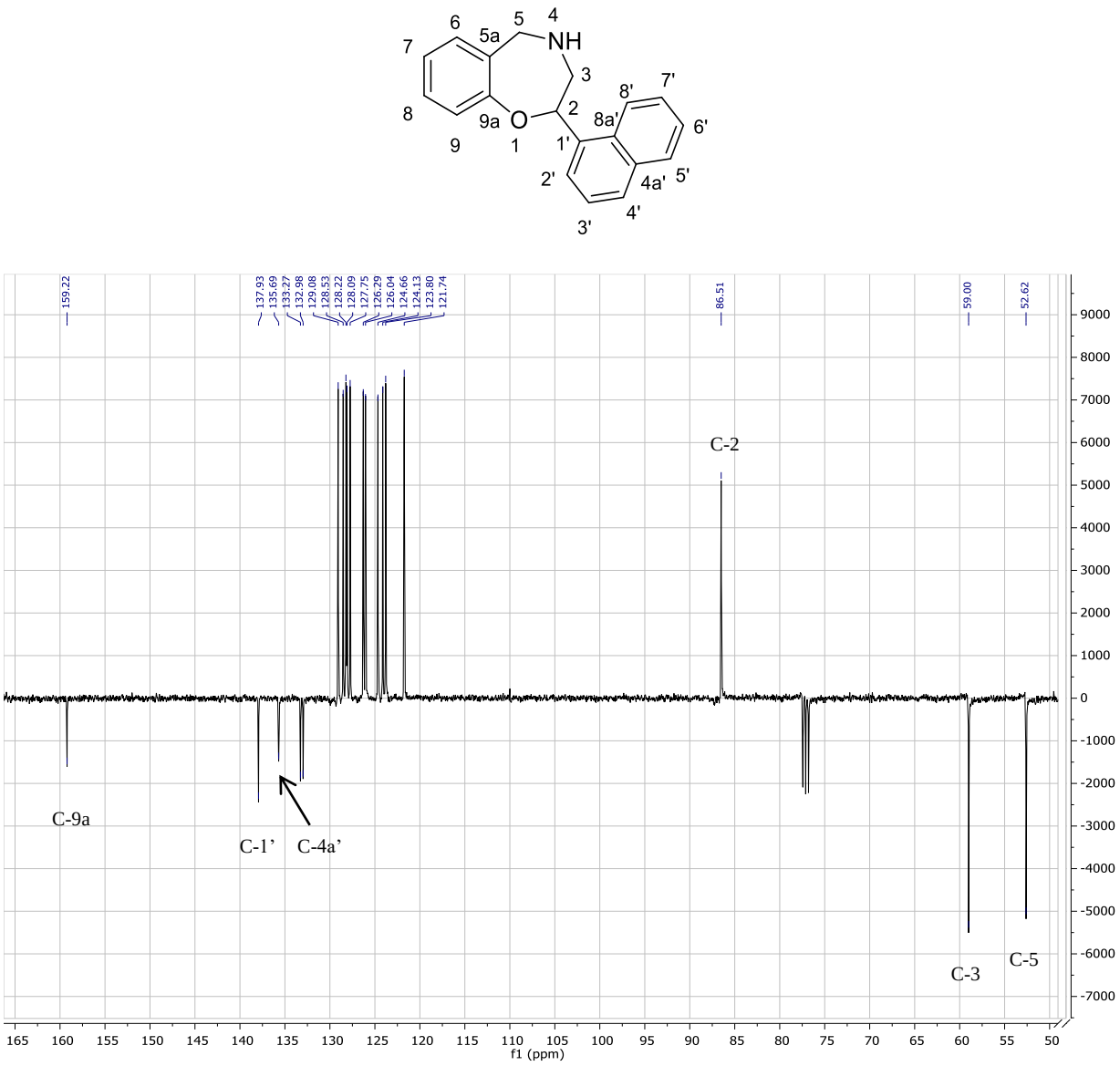

Figure S34. J-modulated ^{13}C-NMR spectrum of *rac*-**9b** measured in $CDCl_3$ (100 MHz)

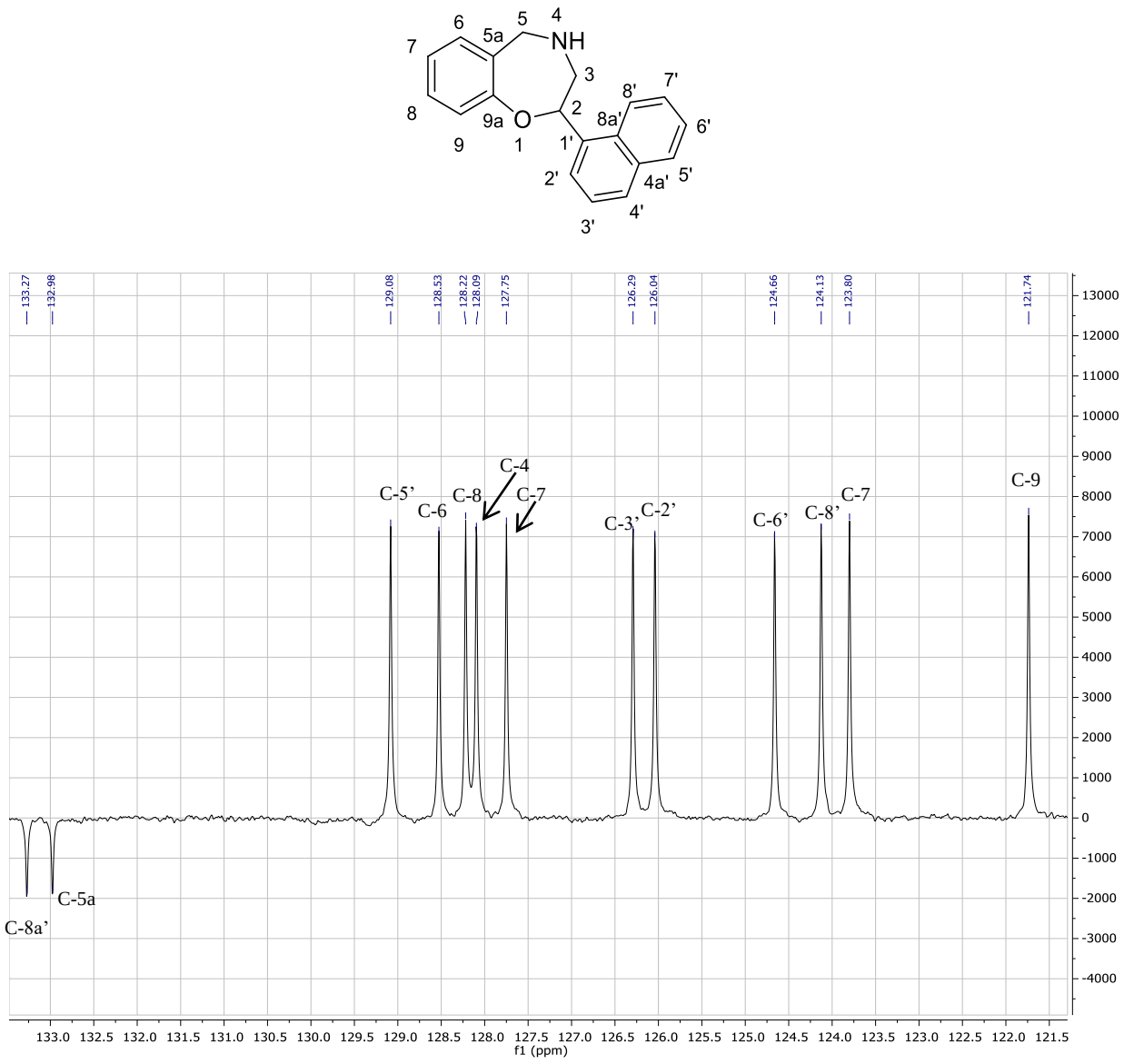

Figure S35. J-modulated ^{13}C-NMR spectrum of *rac*-**9b** measured in $CDCl_3$ (100 MHz)

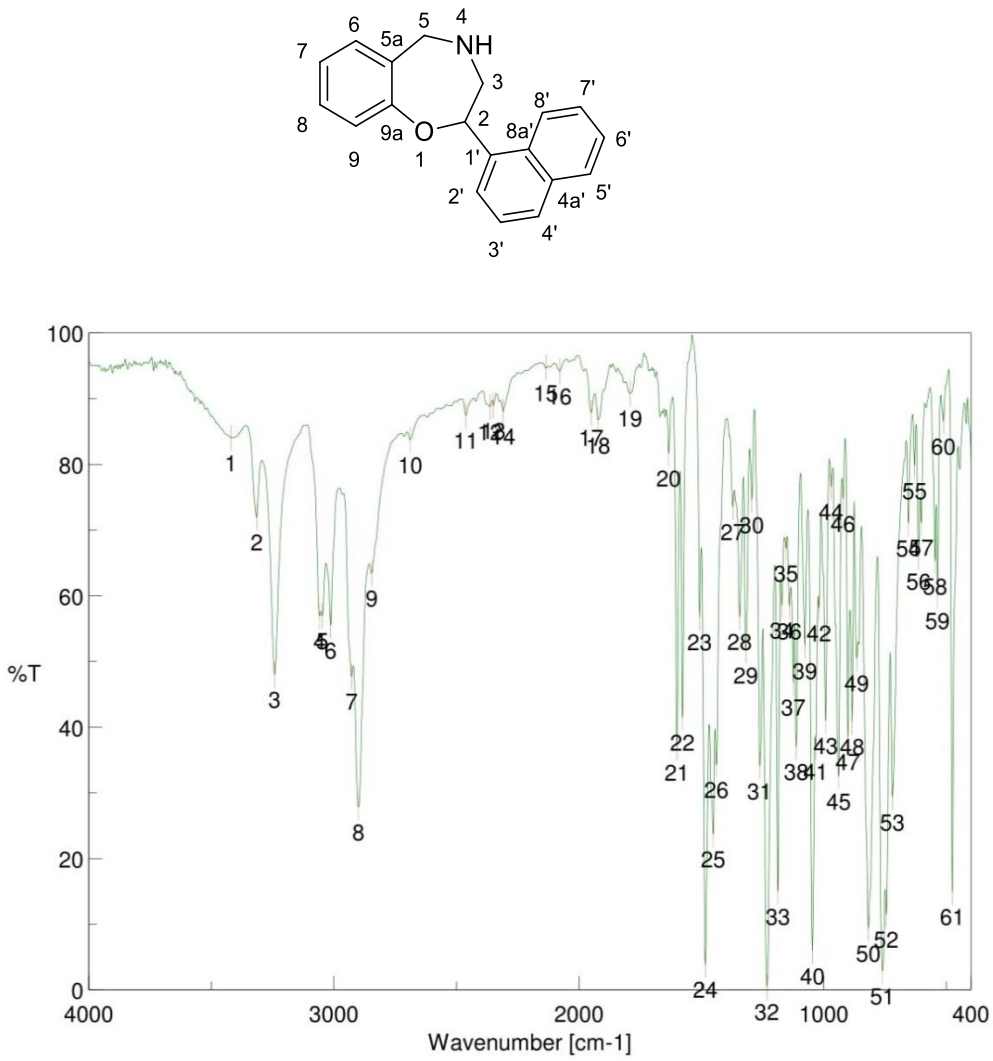

Figure S36. IR spectrum of *rac*-**9b** recorded as KBr disc

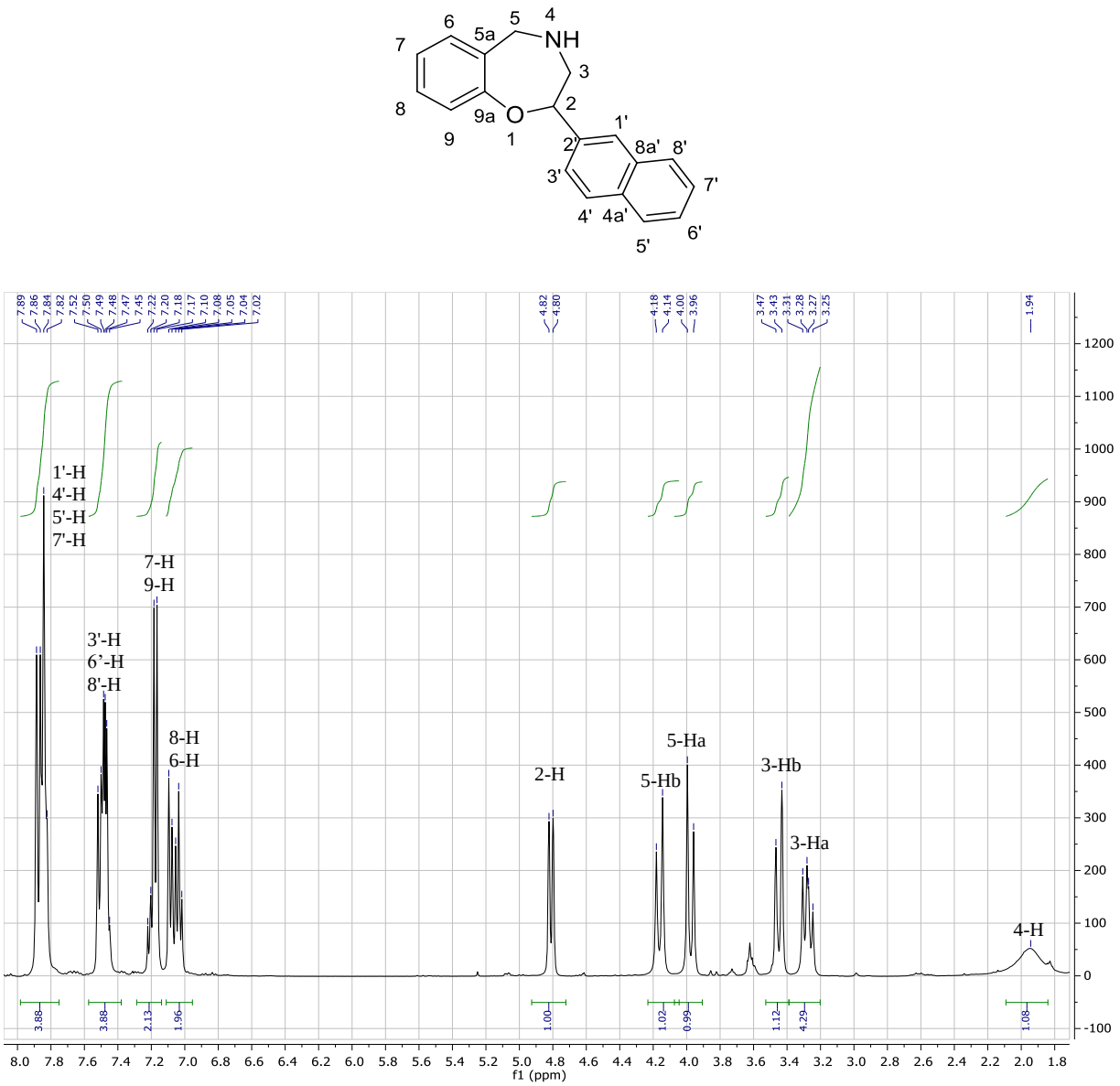

Figure S37. ^{1}H-NMR spectrum of *rac*-**9c** measured in $CDCl_3$ (400 MHz)

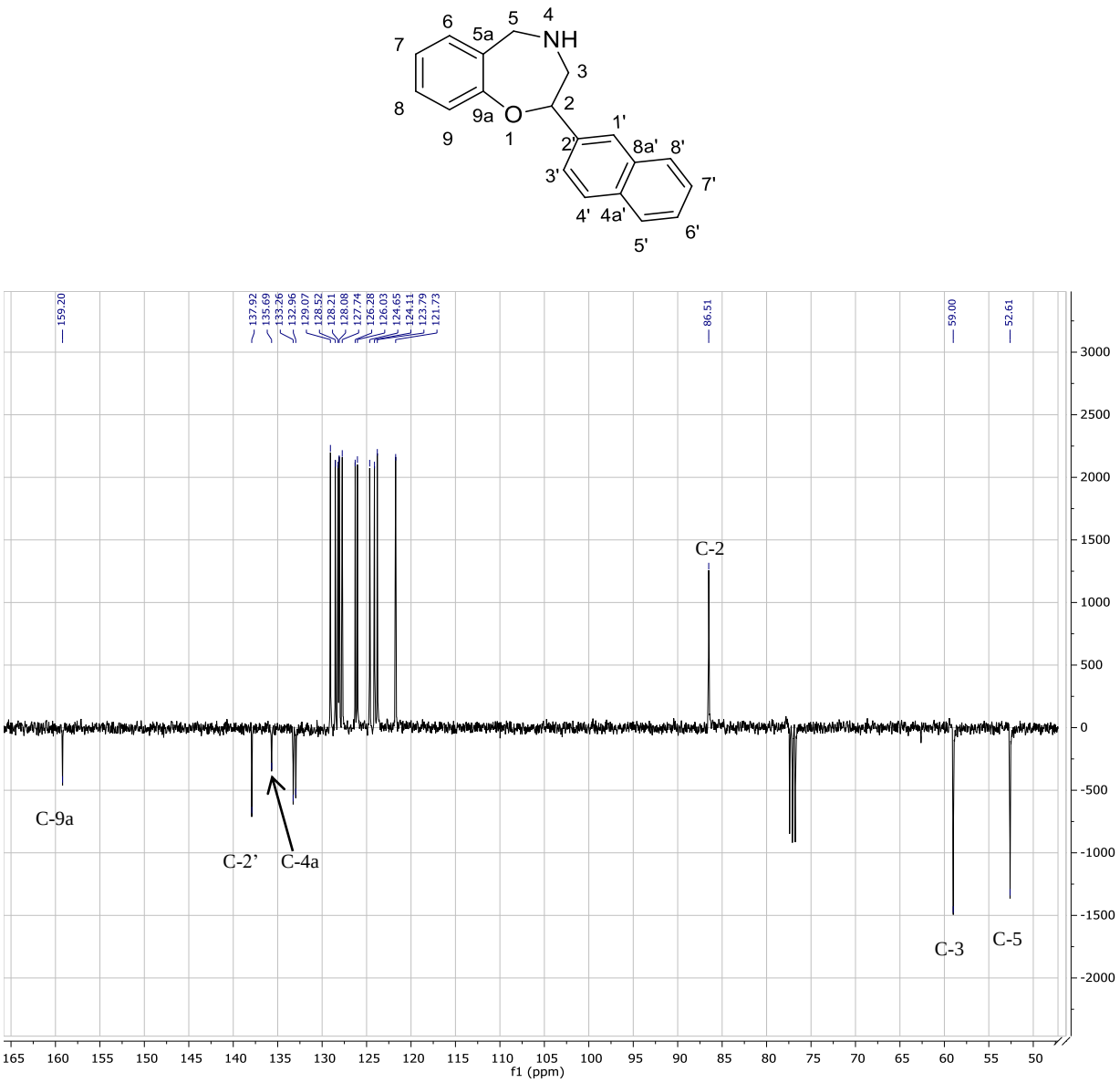

Figure S38. J-modulated ^{13}C-NMR spectrum of *rac*-**9c** measured in $CDCl_3$ (100 MHz)

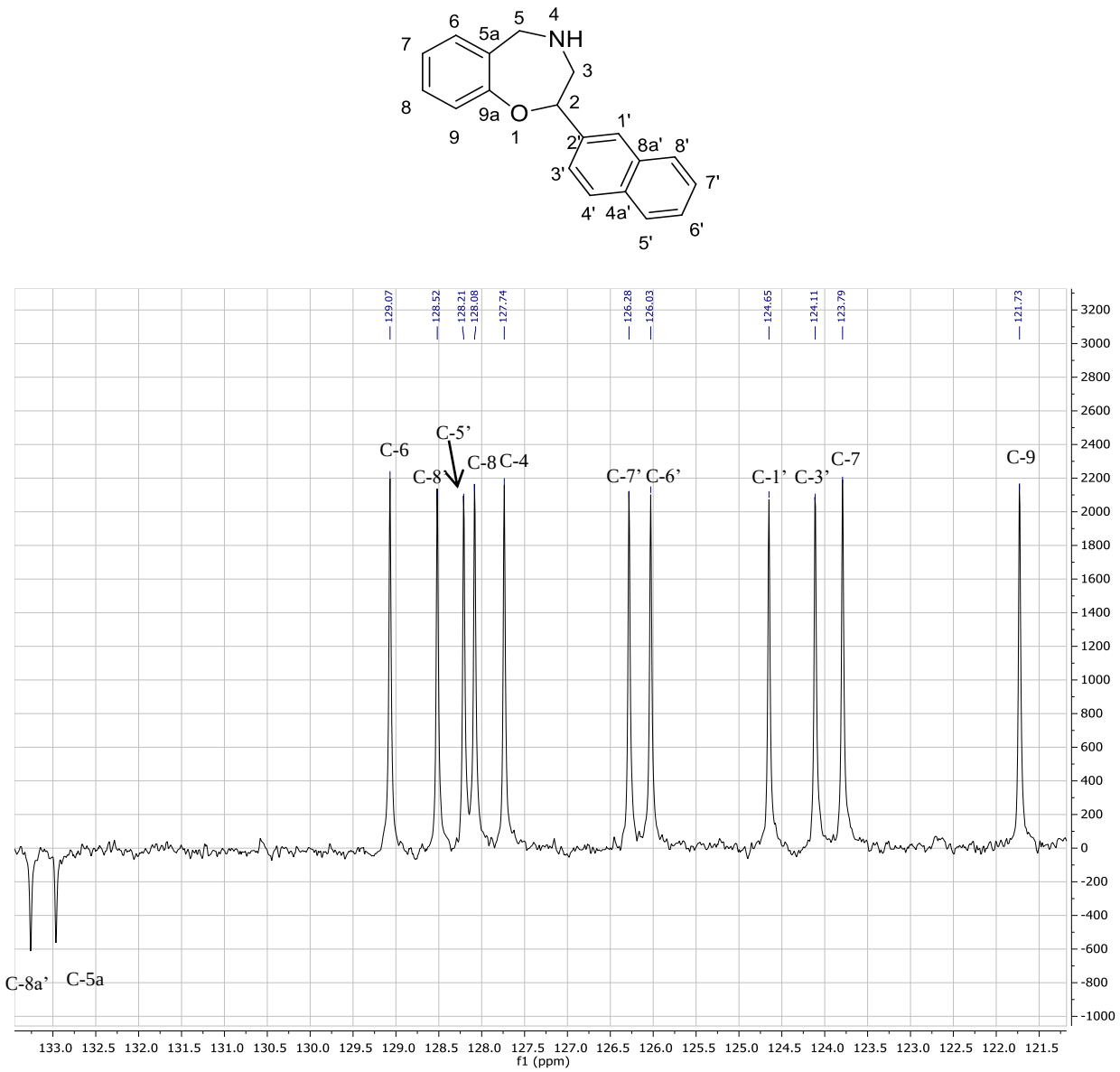

Figure S39. J-modulated ^{13}C-NMR spectrum of *rac*-**9c** measured in $CDCl_3$ (100 MHz)

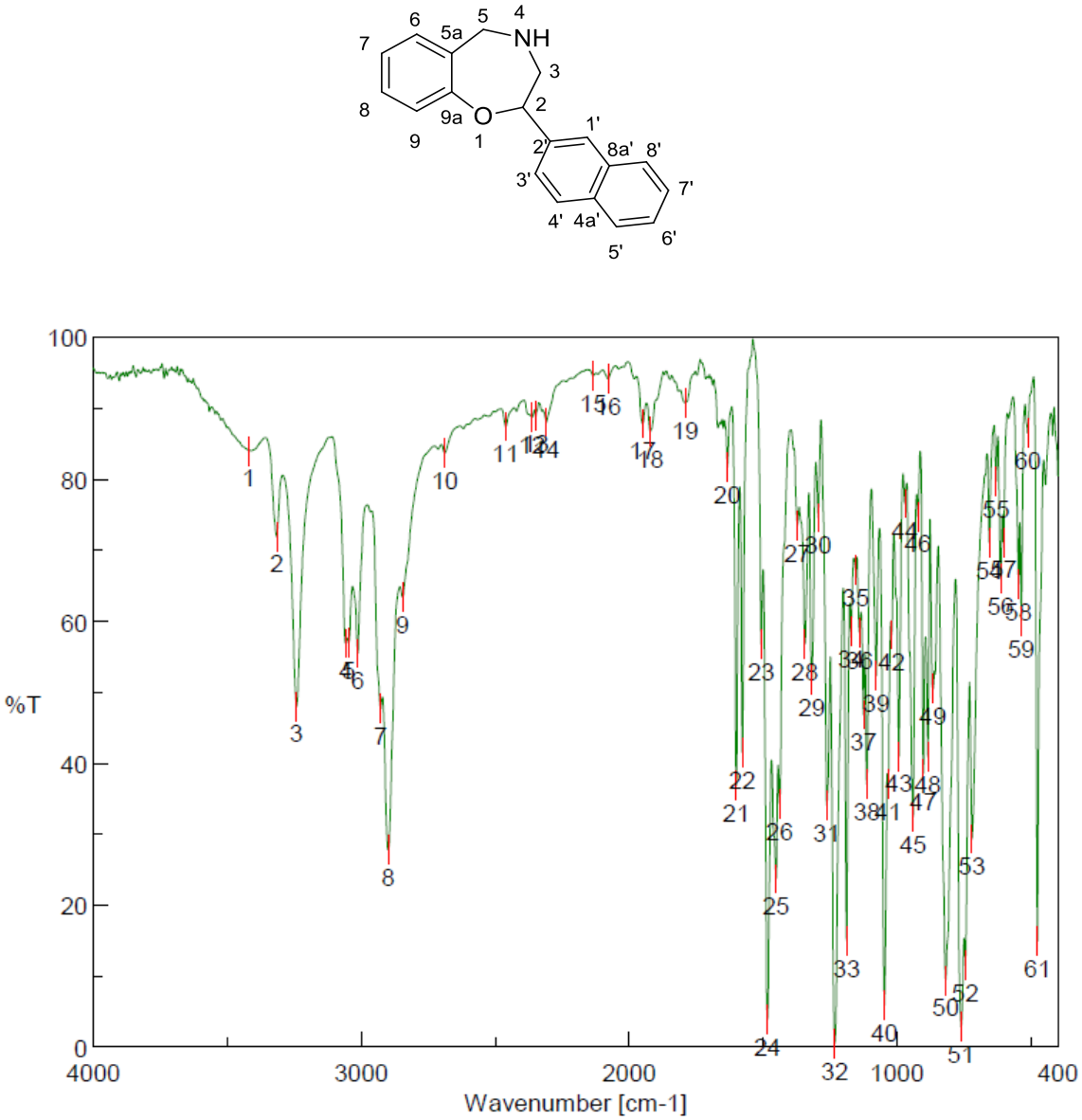

Figure S40. IR spectrum of *rac*-**9c** recorded as KBr disc

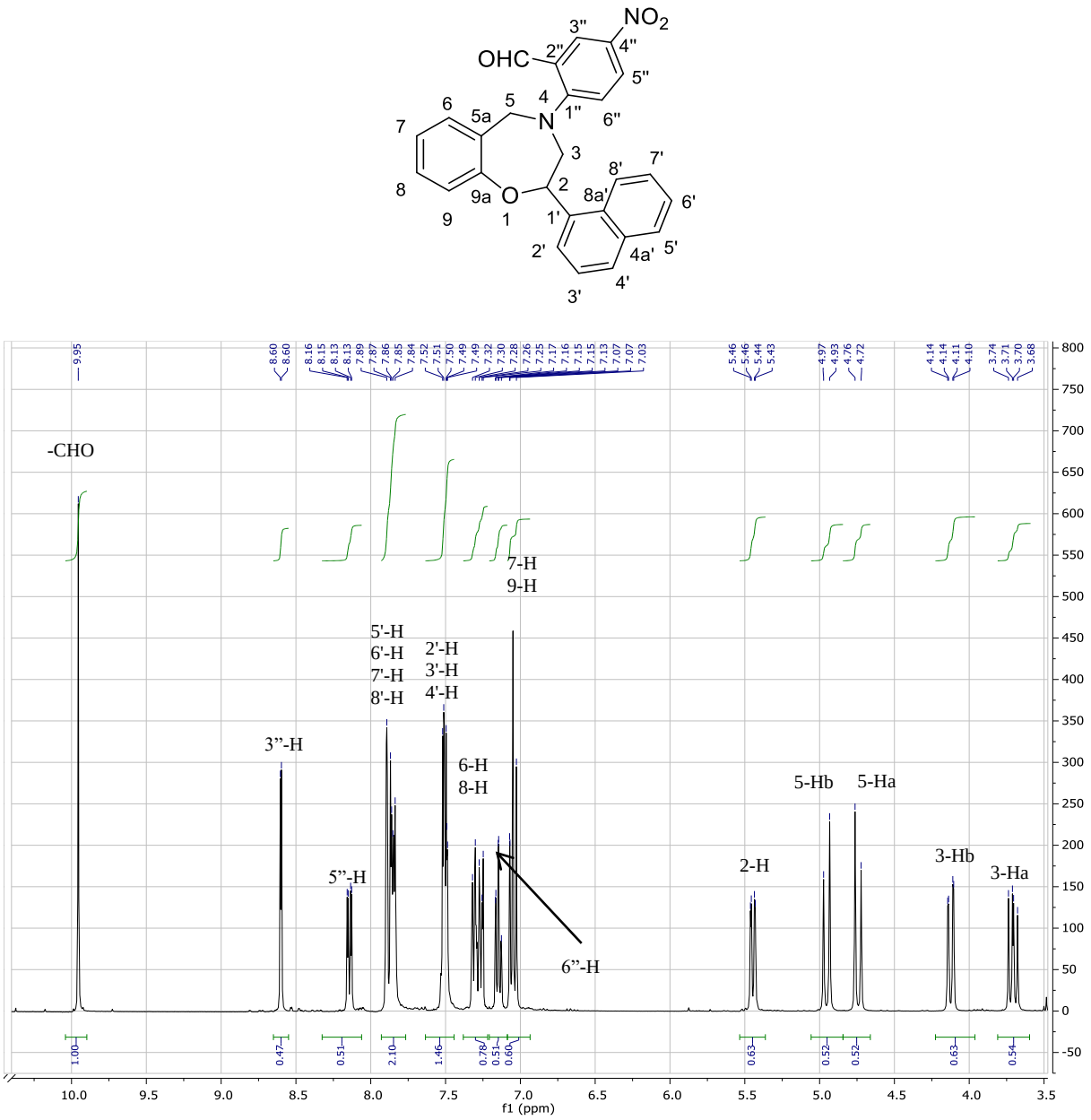

Figure S41. ^{1}H-NMR spectrum of *rac*-**1b** measured in $CDCl_3$ (400 MHz)

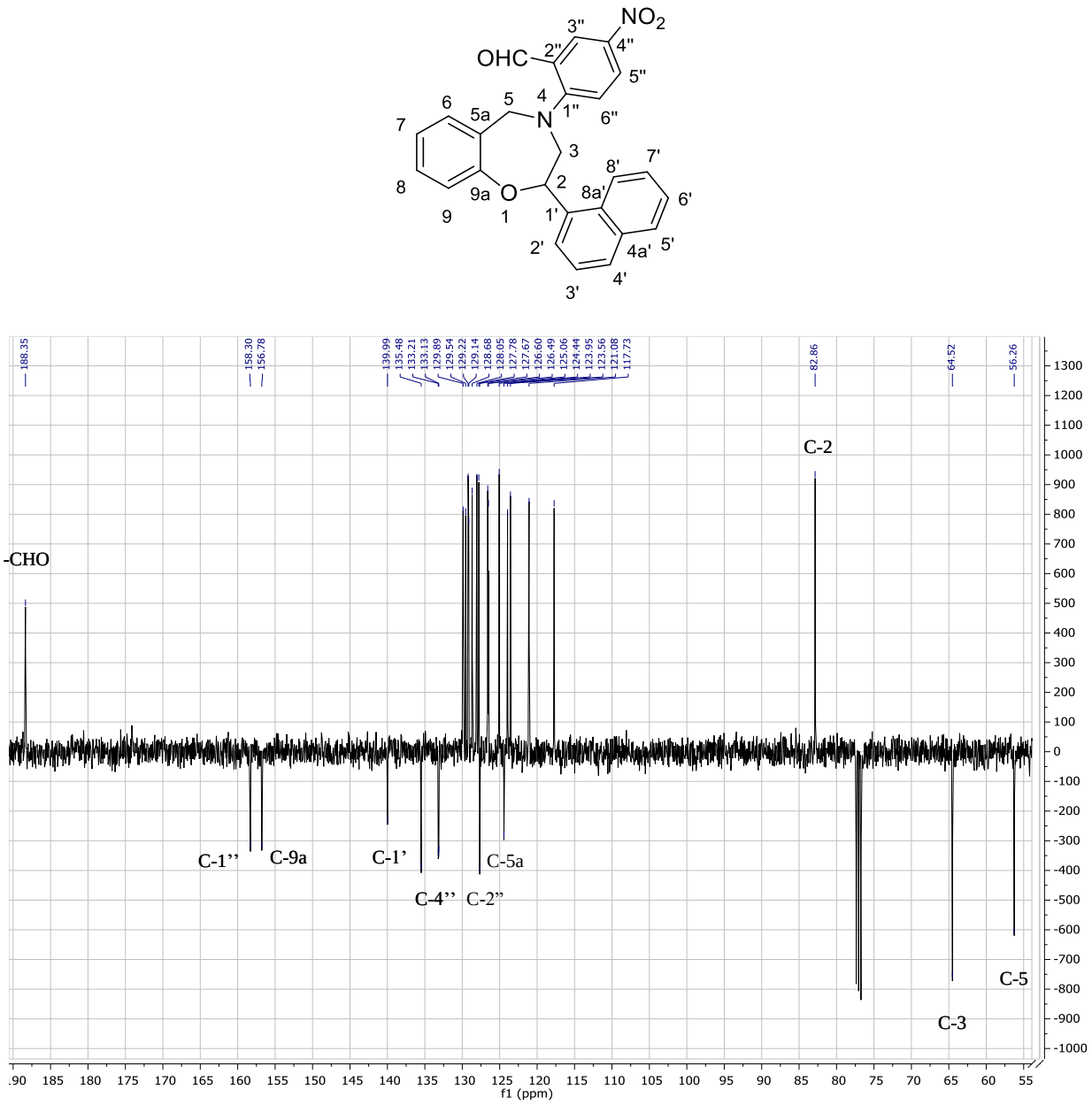

Figure S42. J-modulated ^{13}C-NMR spectrum of *rac*-**1b** measured in $CDCl_3$ (100 MHz)

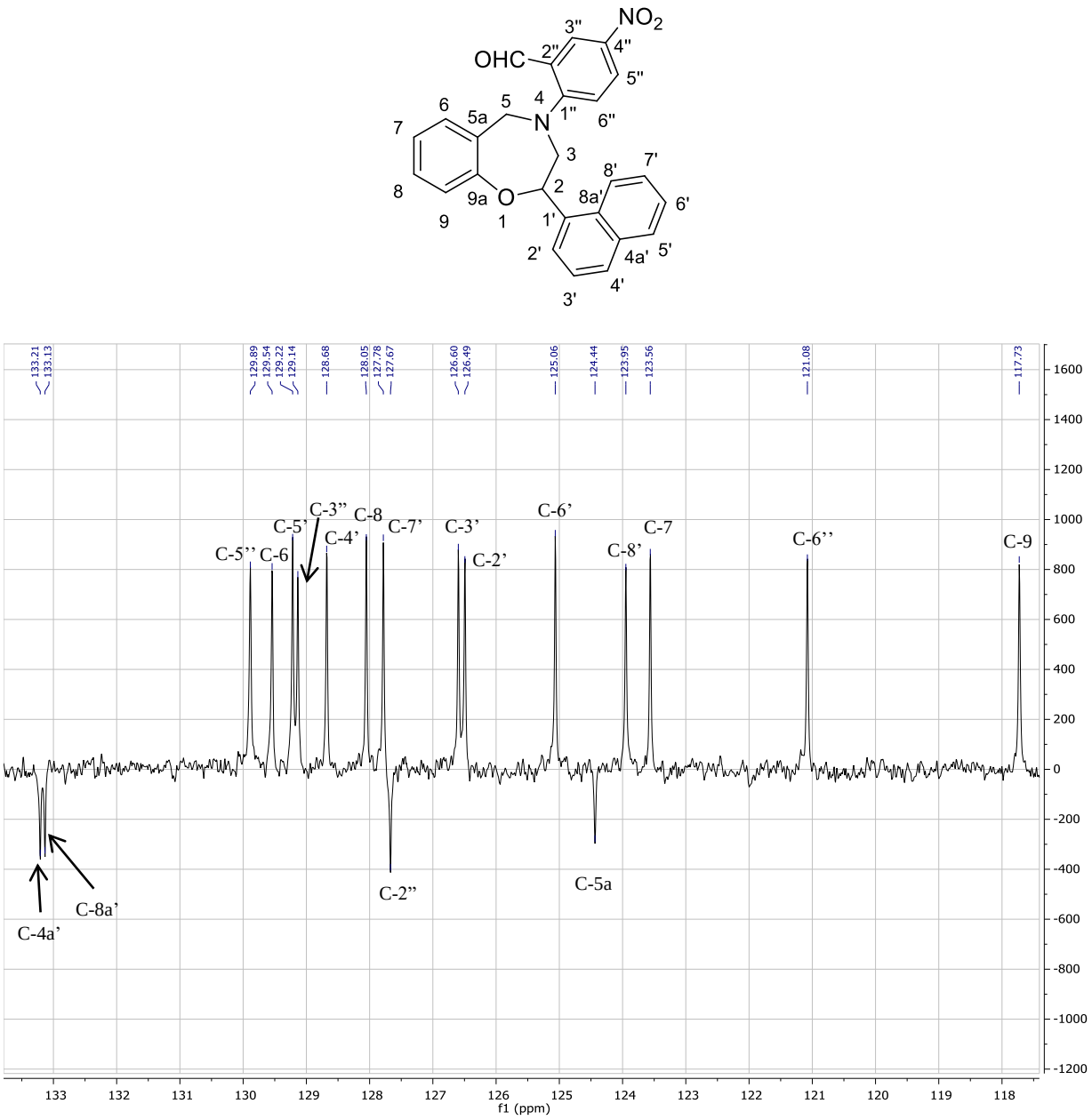

Figure S43. J-modulated ^{13}C-NMR spectrum of *rac*-**1b** measured in $CDCl_3$ (100 MHz)

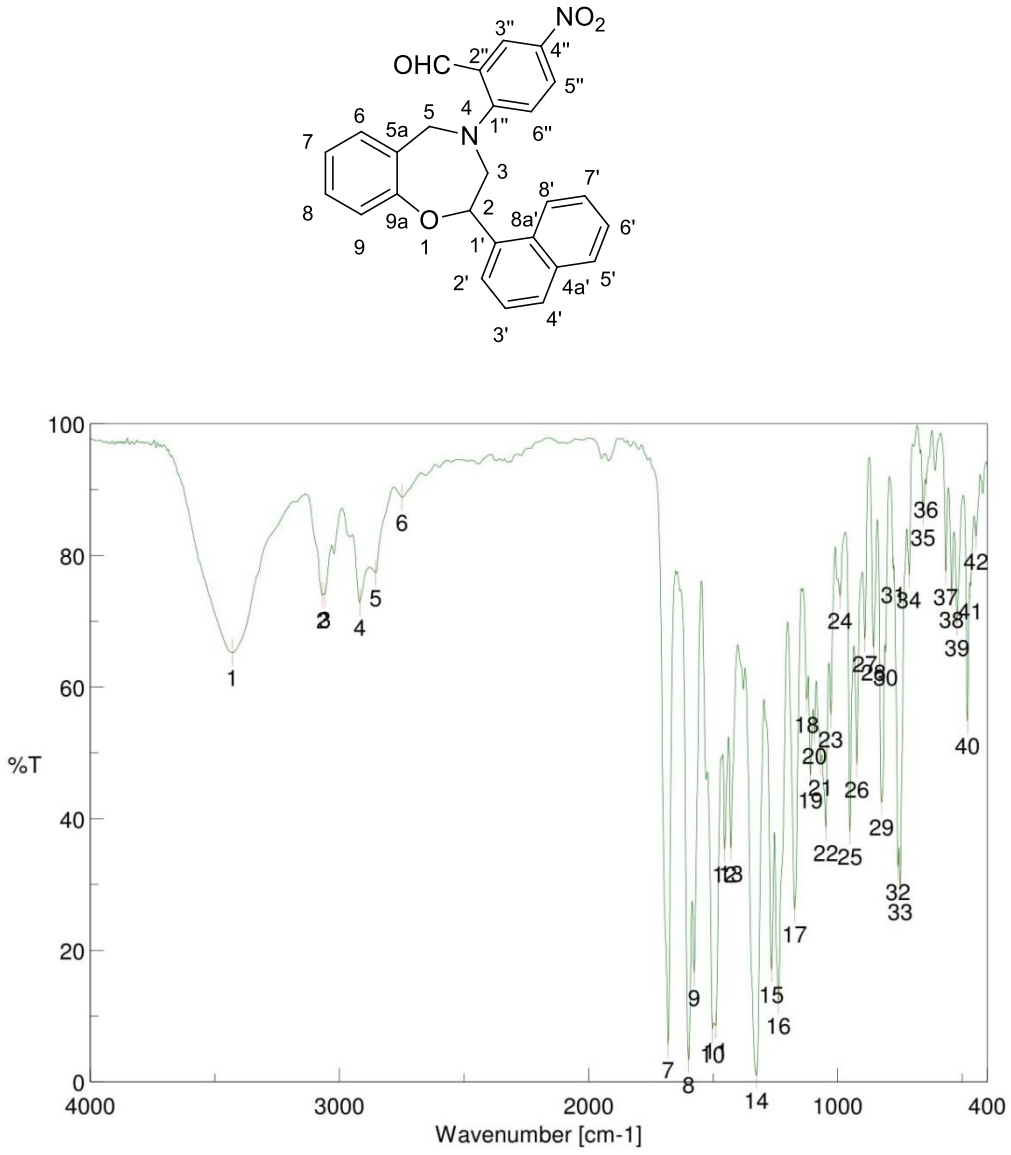

Figure S44. IR spectrum of *rac*-**1b** recorded as KBr disc

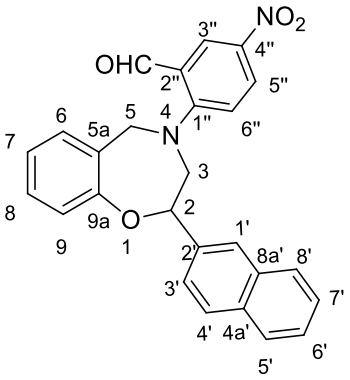

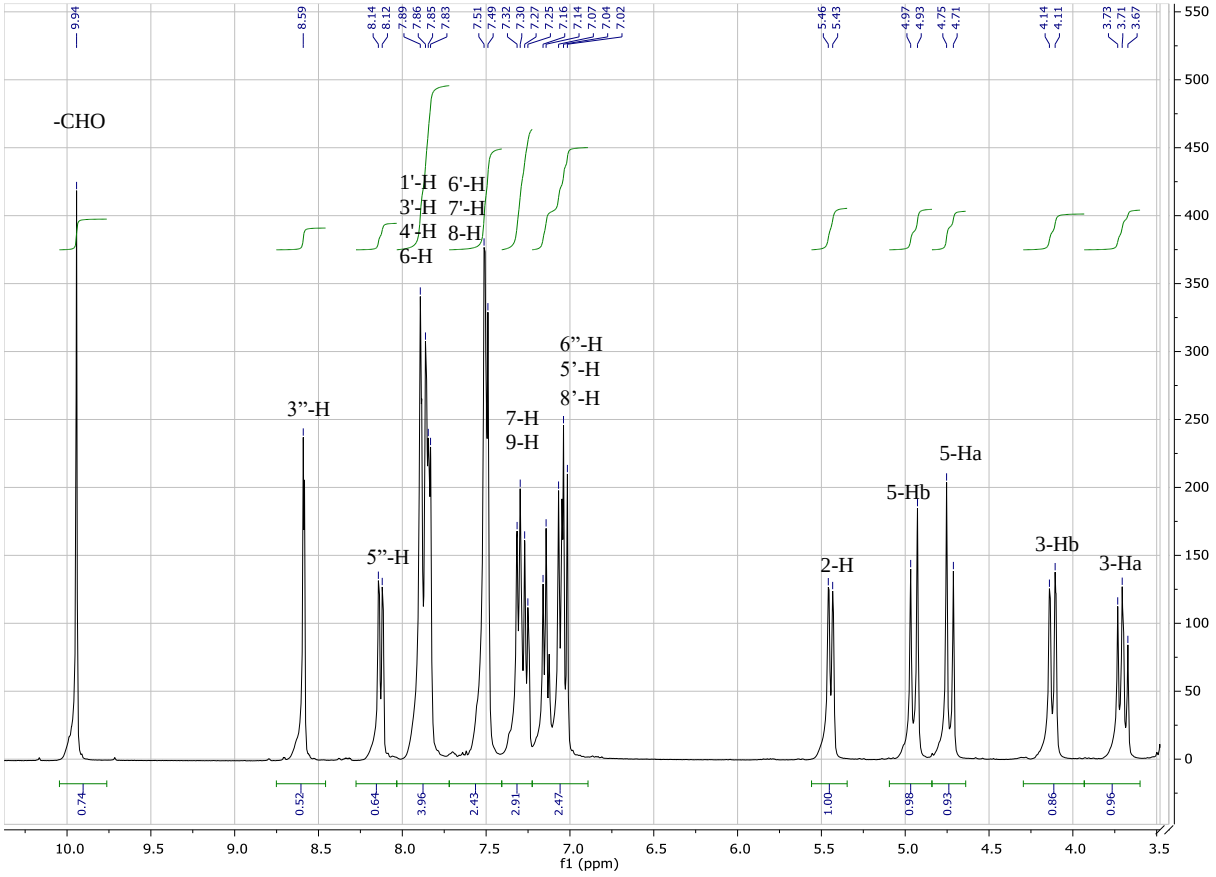

Figure S45. ^{1}H-NMR spectrum of *rac*-**1c** measured in $CDCl_3$ (400 MHz)

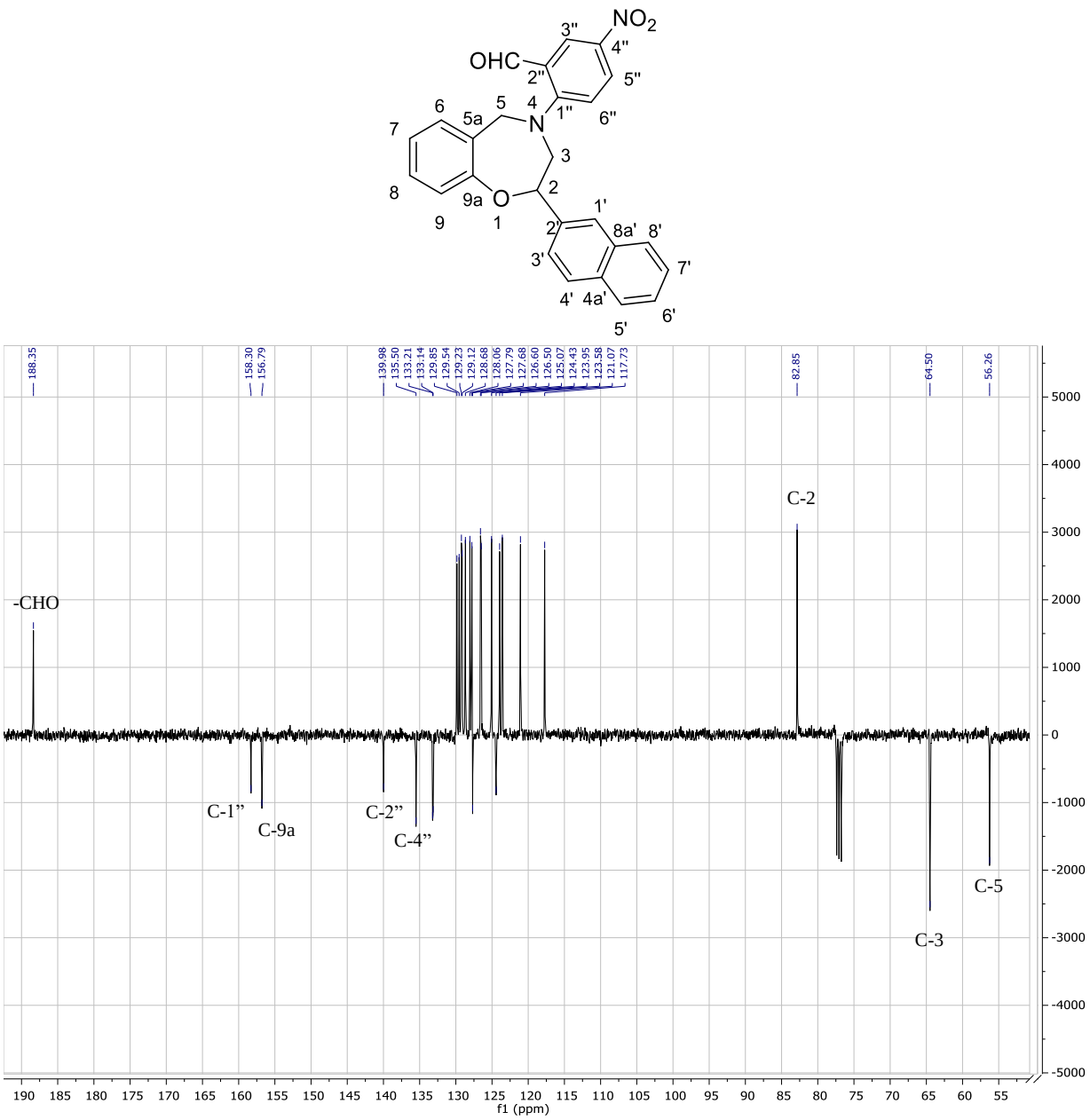

Figure S46. J-modulated ^{13}C-NMR spectrum of *rac*-**1c** measured in $CDCl_3$ (100 MHz)

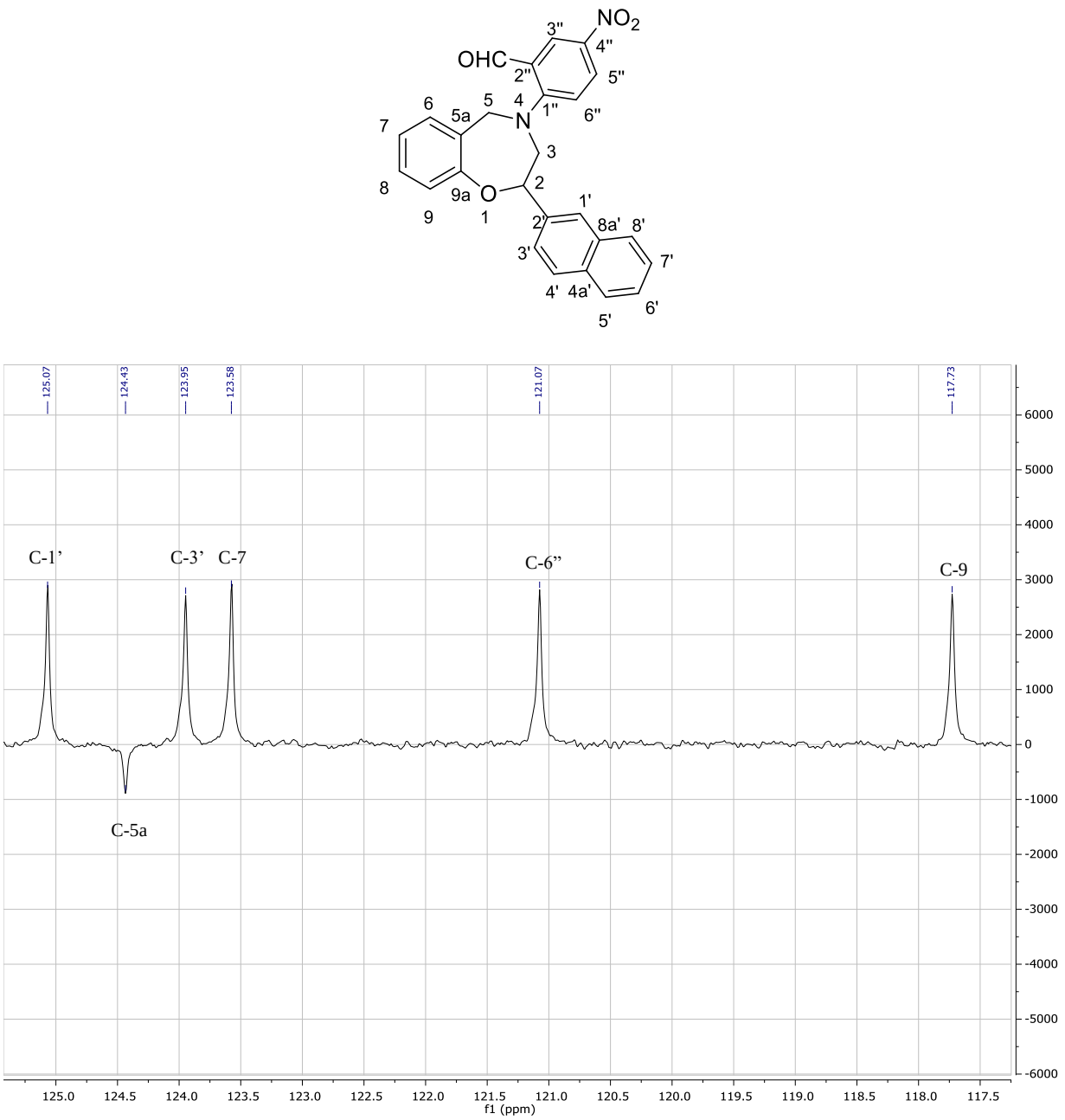

Figure S47. J-modulated ^{13}C-NMR spectrum of *rac*-**1c** measured in $CDCl_3$ (100 MHz)

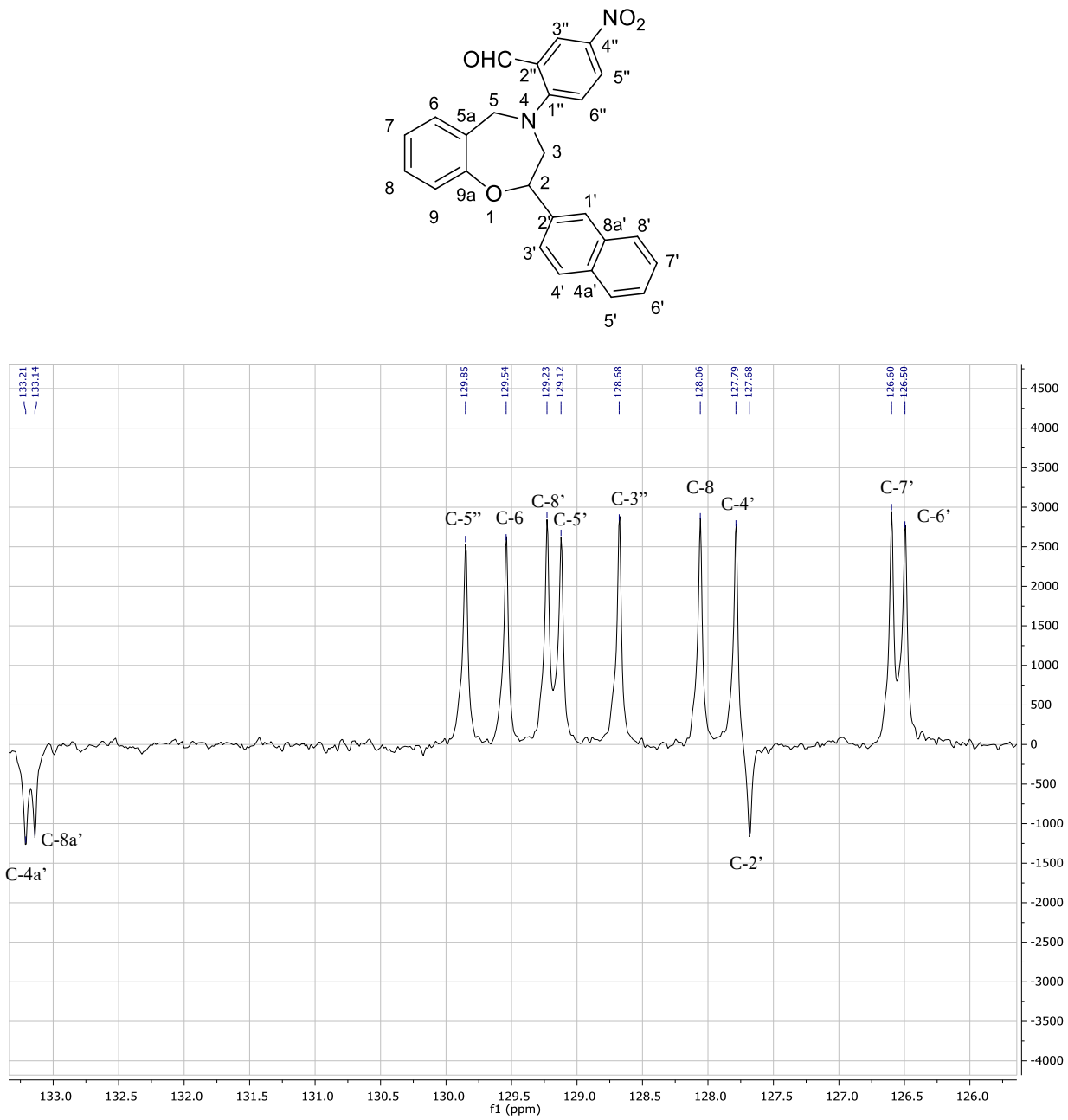

Figure S48. J-modulated ^{13}C-NMR spectrum of *rac*-**1c** measured in $CDCl_3$ (100 MHz)

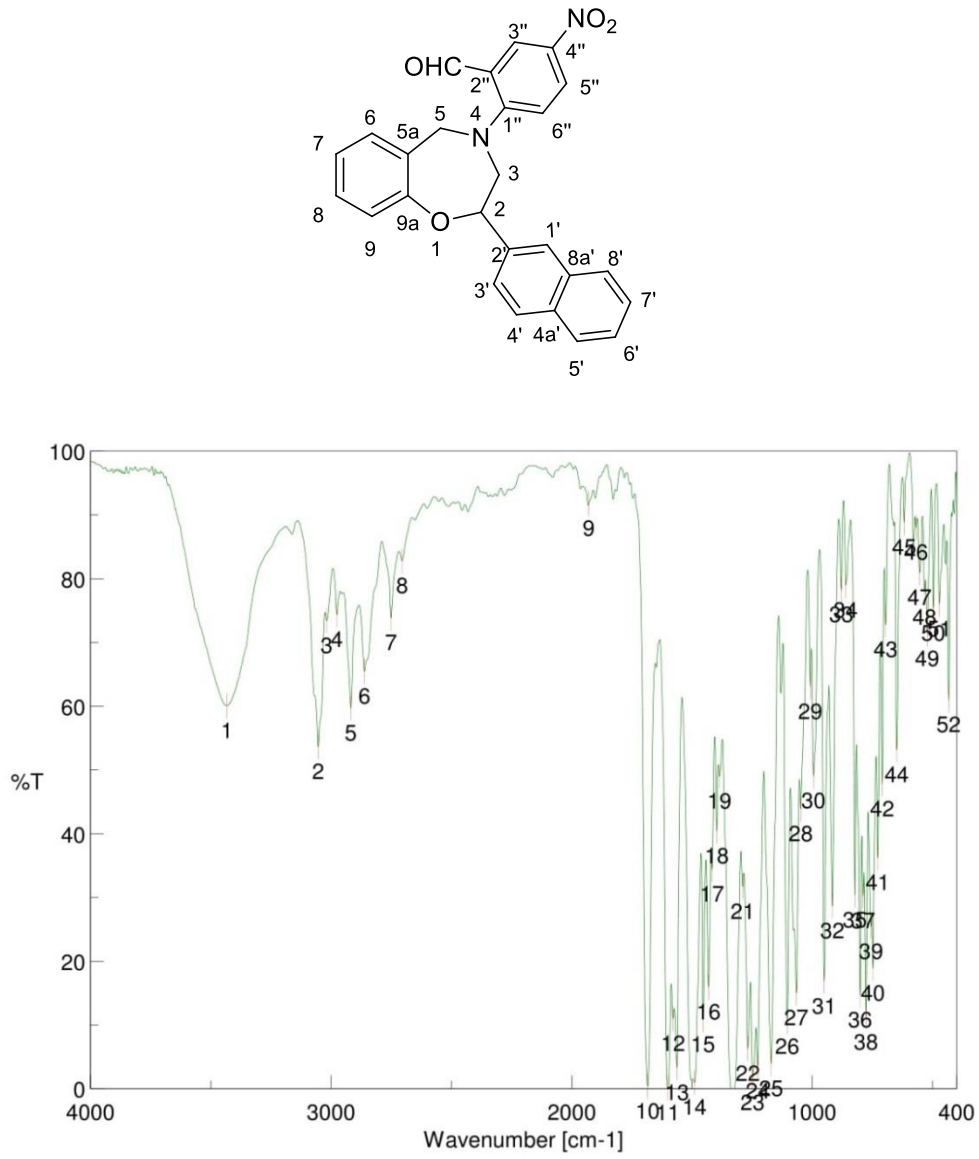

Figure S49. IR spectrum of *rac*-**1c** recorded as KBr disc

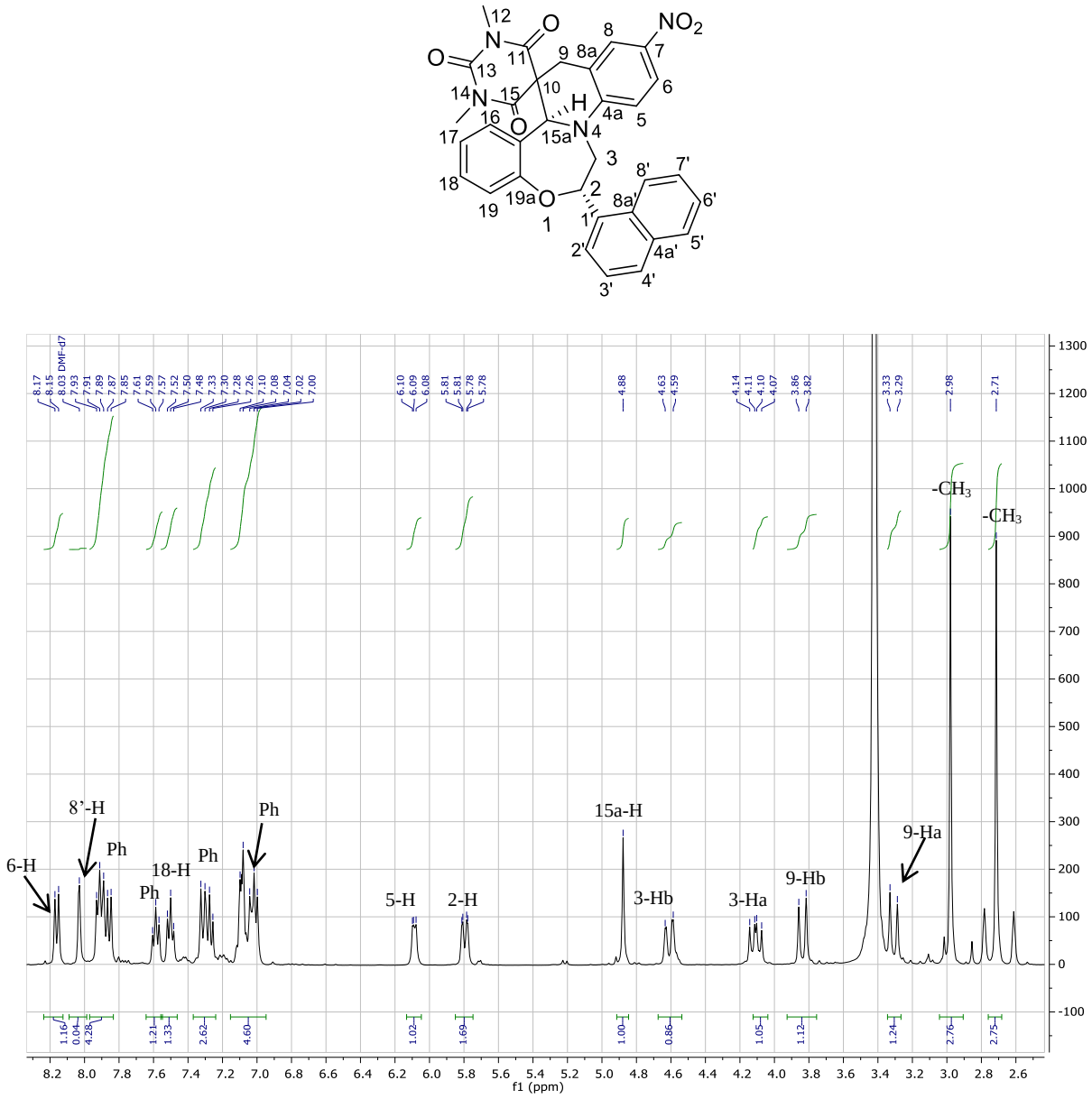

Figure S50. ^{1}H-NMR spectrum of *rac*-**10b** measured in DMF-d_7 (400 MHz)

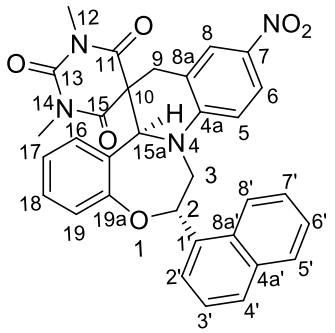

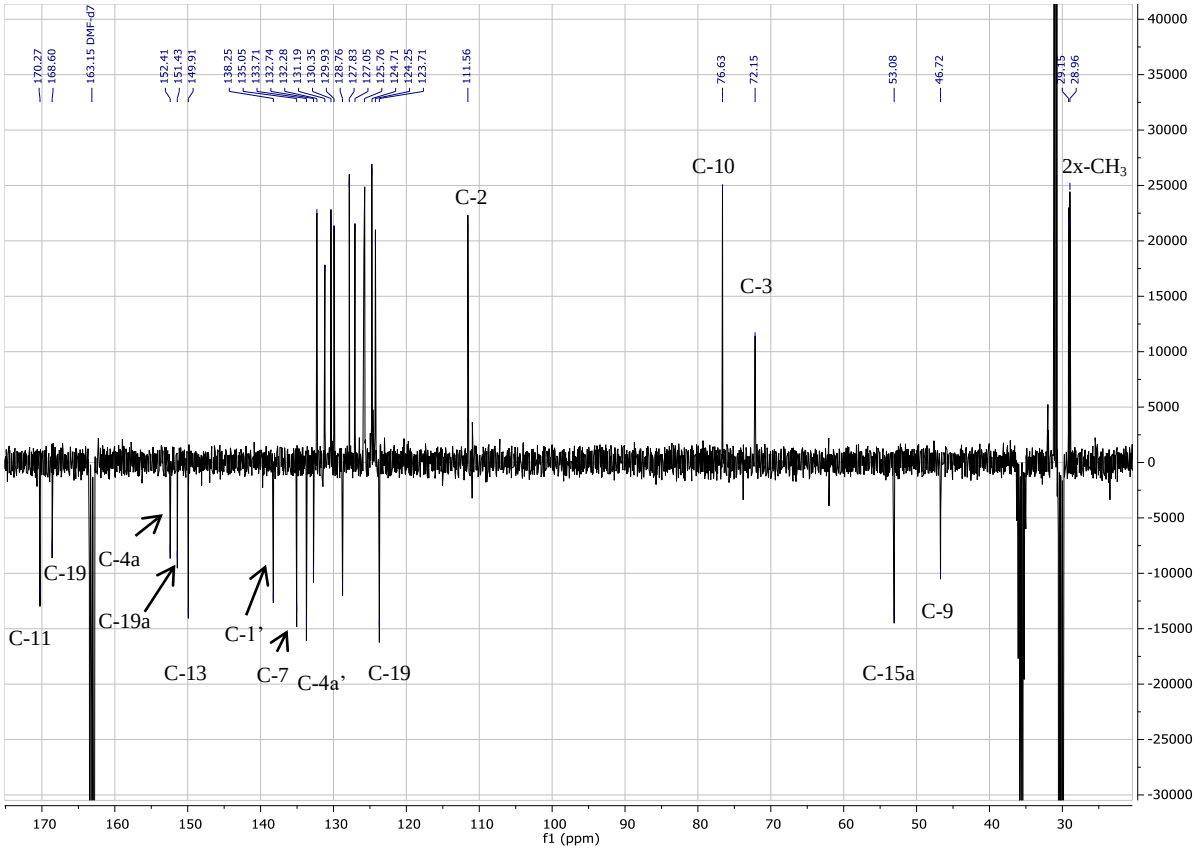

Figure S51. J-modulated ^{13}C-NMR spectrum of *rac*-**10b** measured in DMF-d_7 (100 MHz)

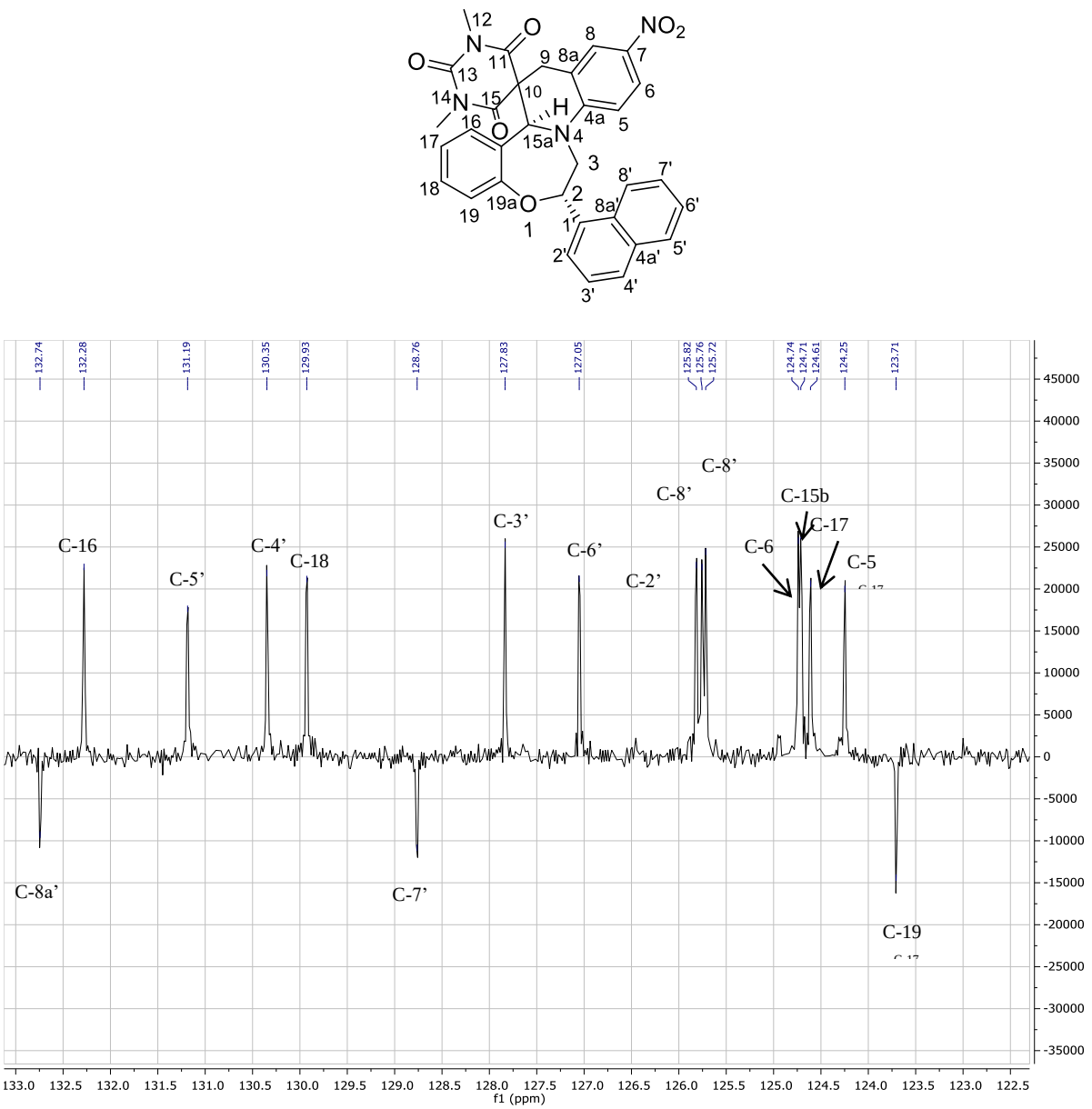

Figure S52. J-modulated ^{13}C-NMR spectrum of *rac*-**10b** measured in DMF-d_7 (100 MHz)

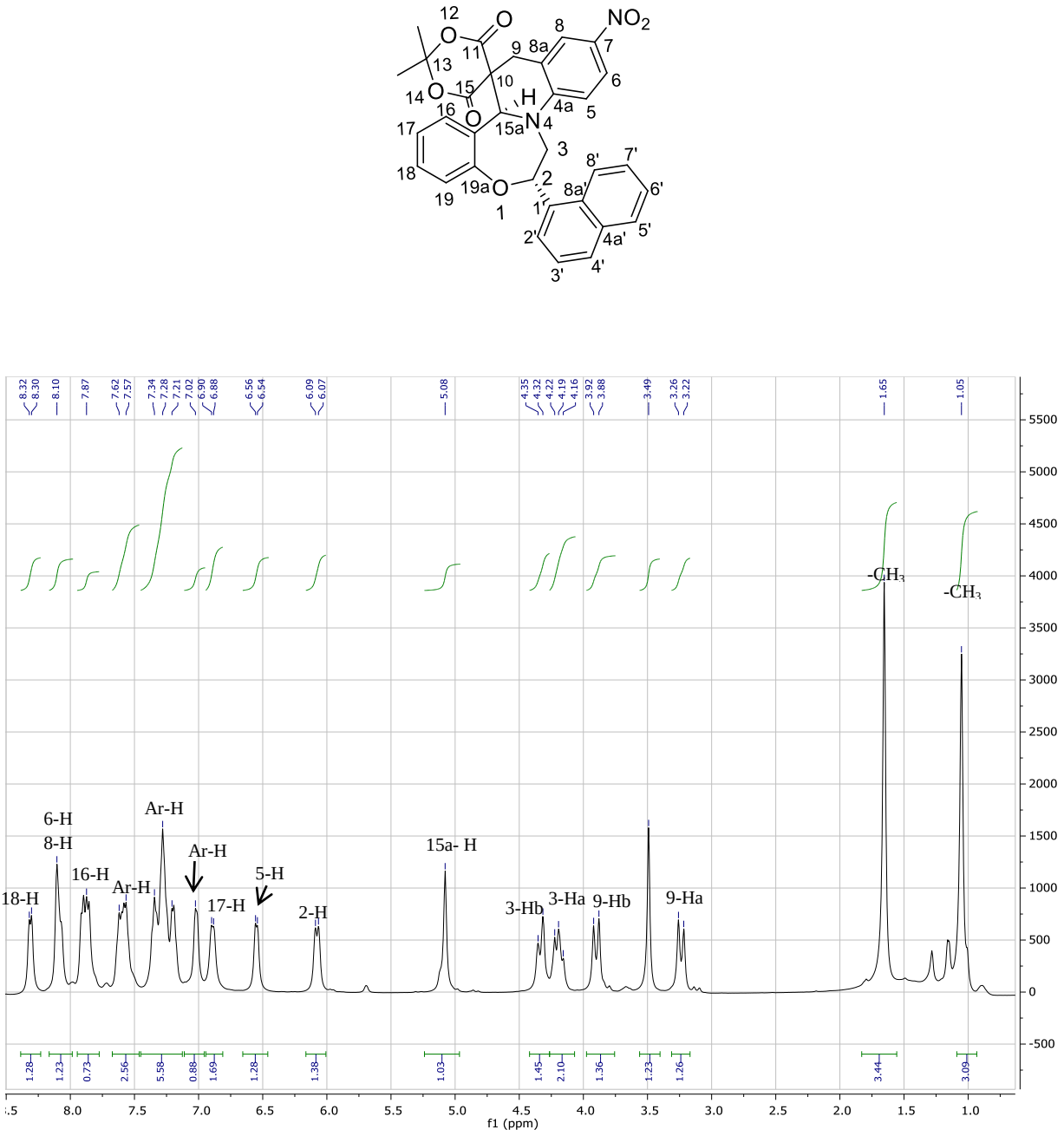

Figure S53. ^{1}H-NMR spectrum of *rac*-**11b** measured in $CDCl_3$ (400 MHz)

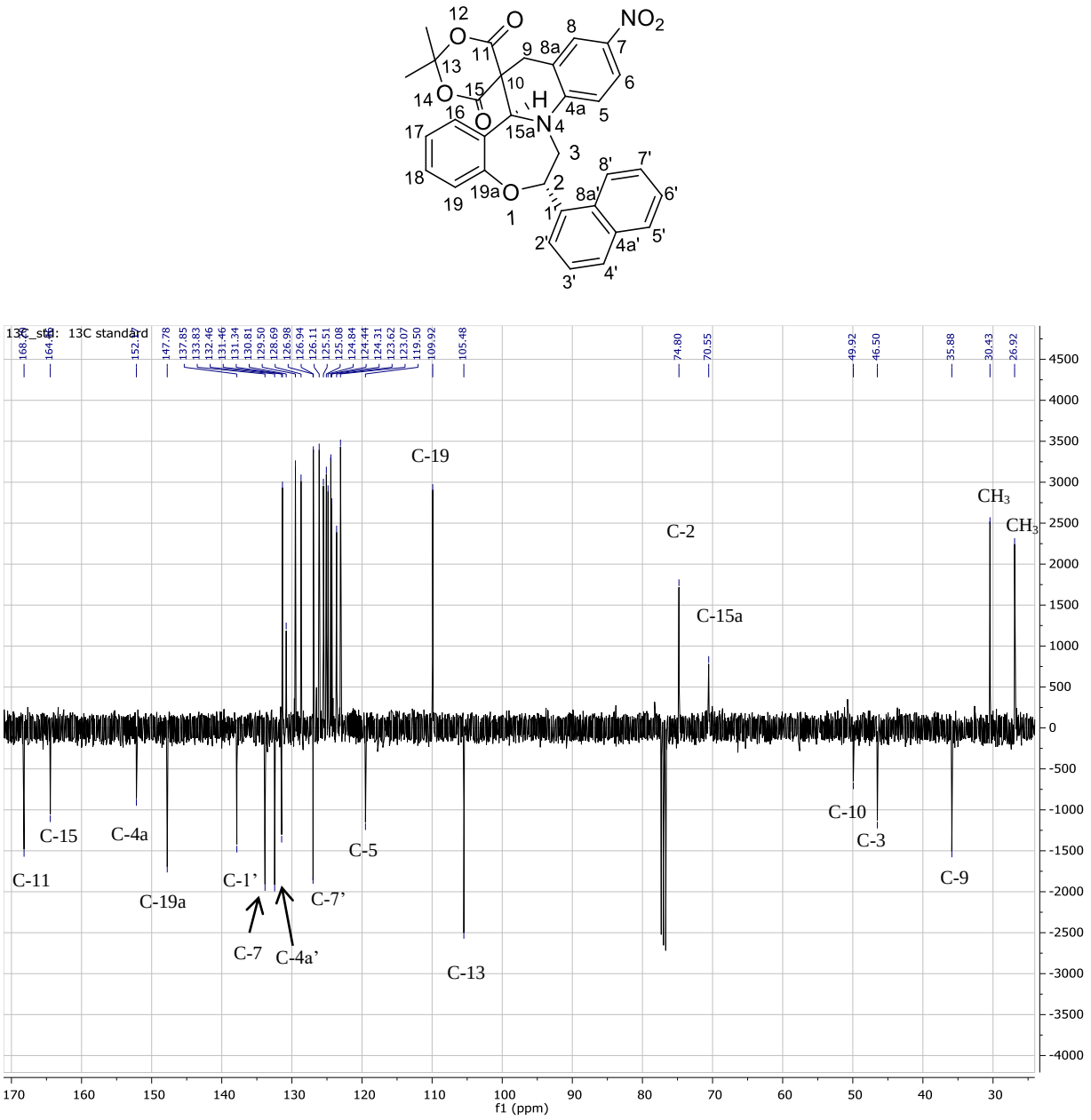

Figure S54. J-modulated ^{13}C-NMR spectrum of *rac*-**11b** measured in $CDCl_3$ (100 MHz)

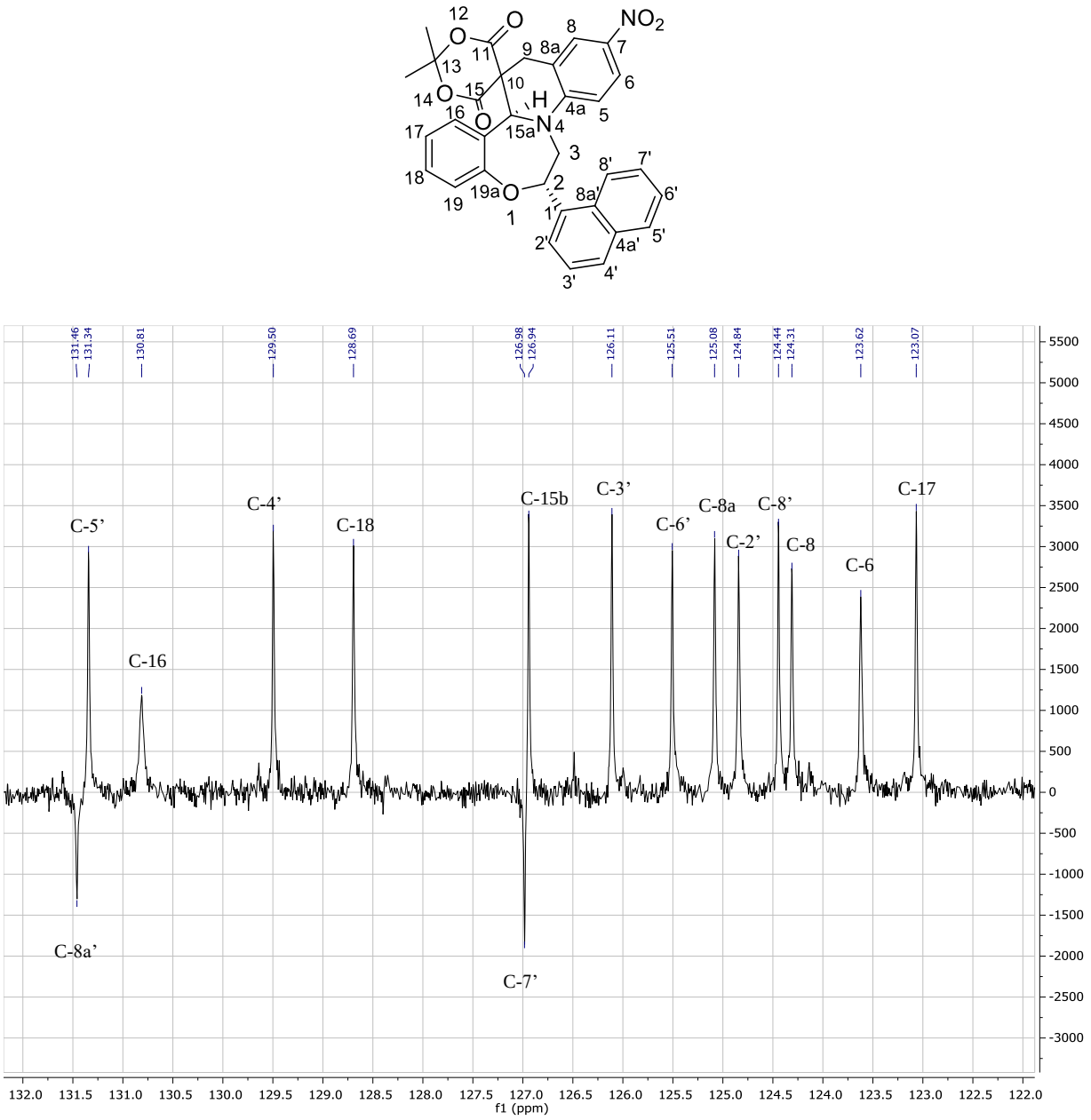

Figure S55. J-modulated ^{13}C-NMR spectrum of *rac*-**11b** measured in $CDCl_3$ (100 MHz)

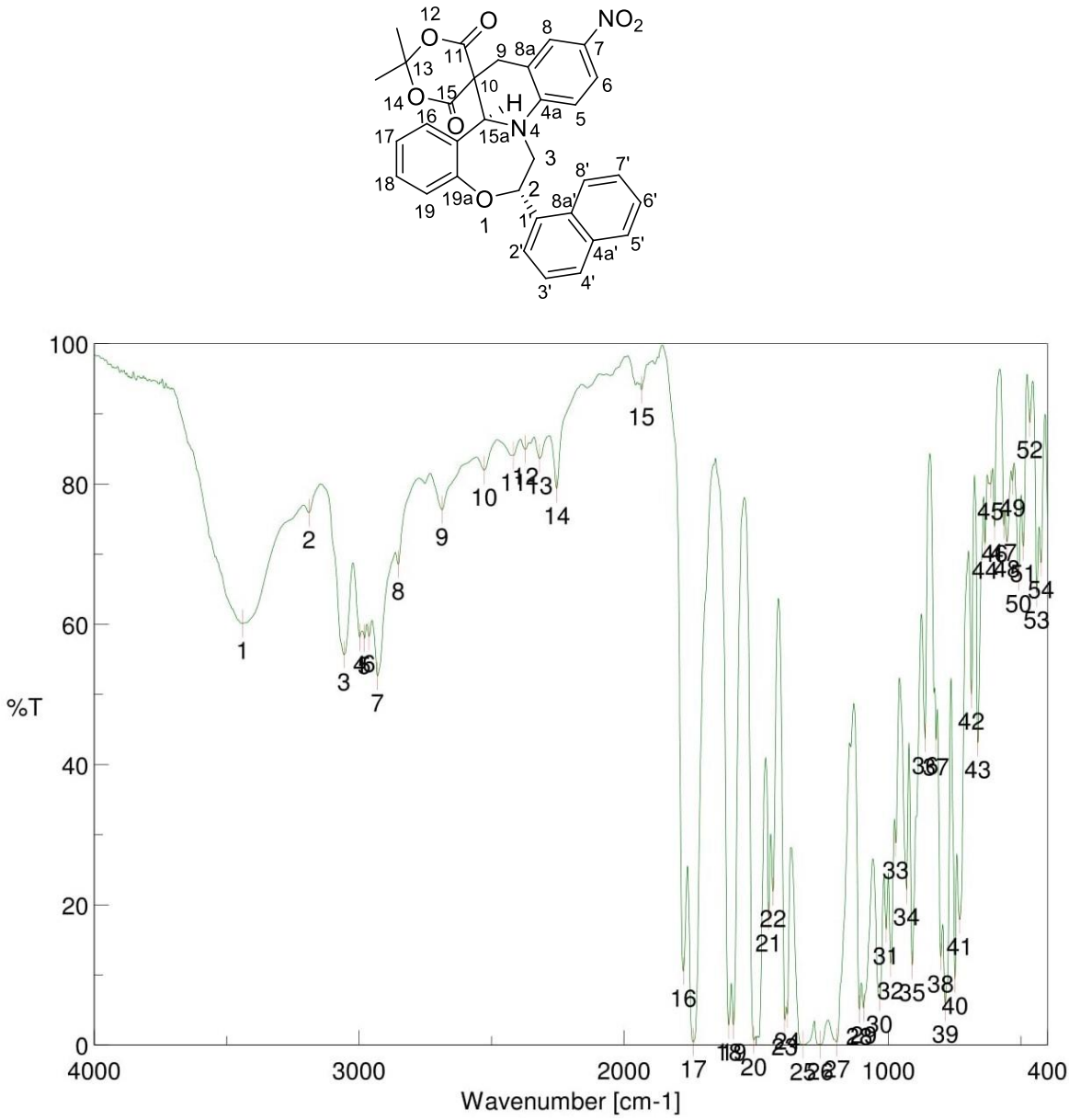

Figure S56. IR spectrum of *rac*-**11b** recorded as KBr disc

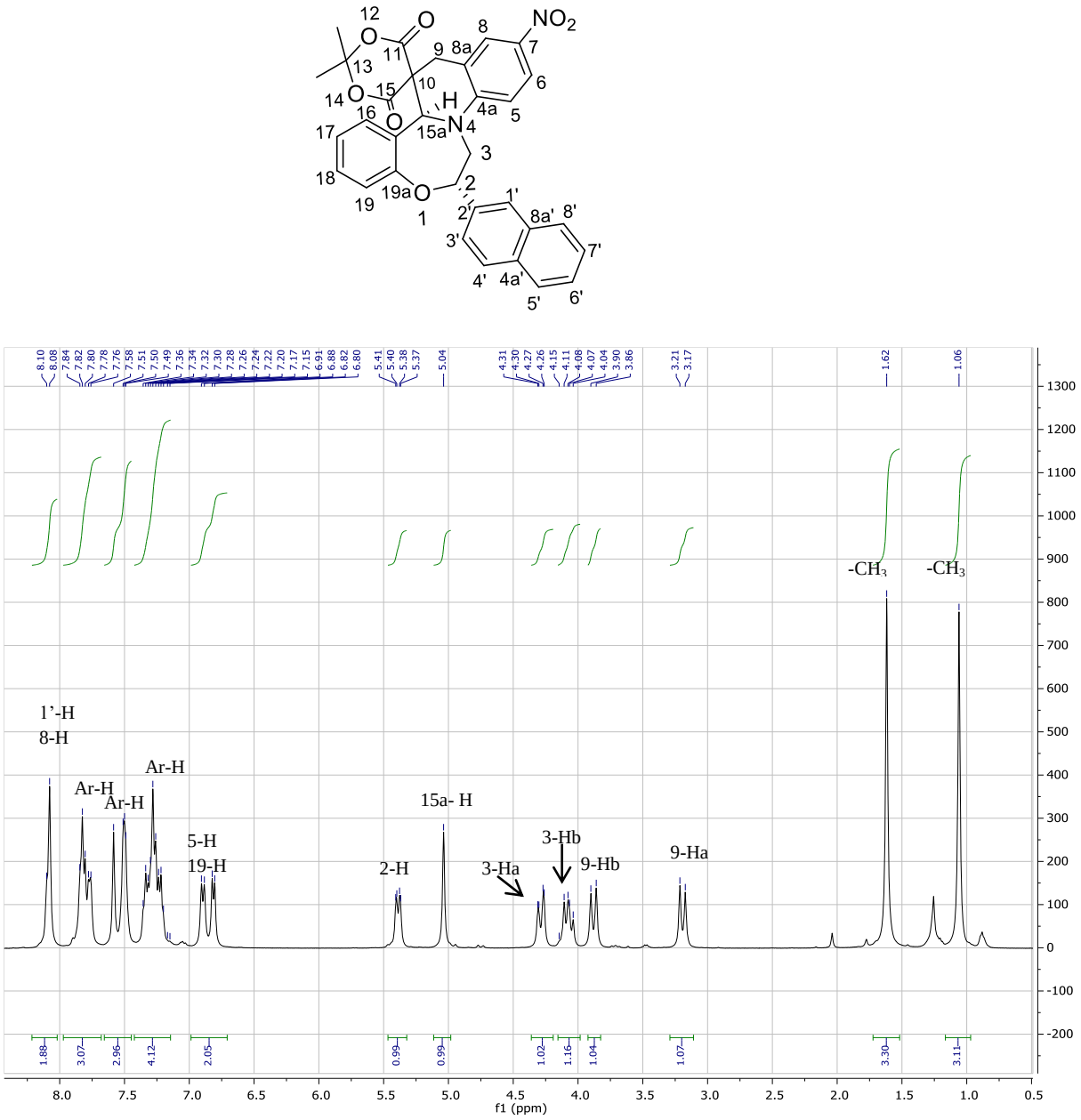

Figure S57. ^{1}H-NMR spectrum of *rac*-**11c** measured in $CDCl_3$ (400 MHz)

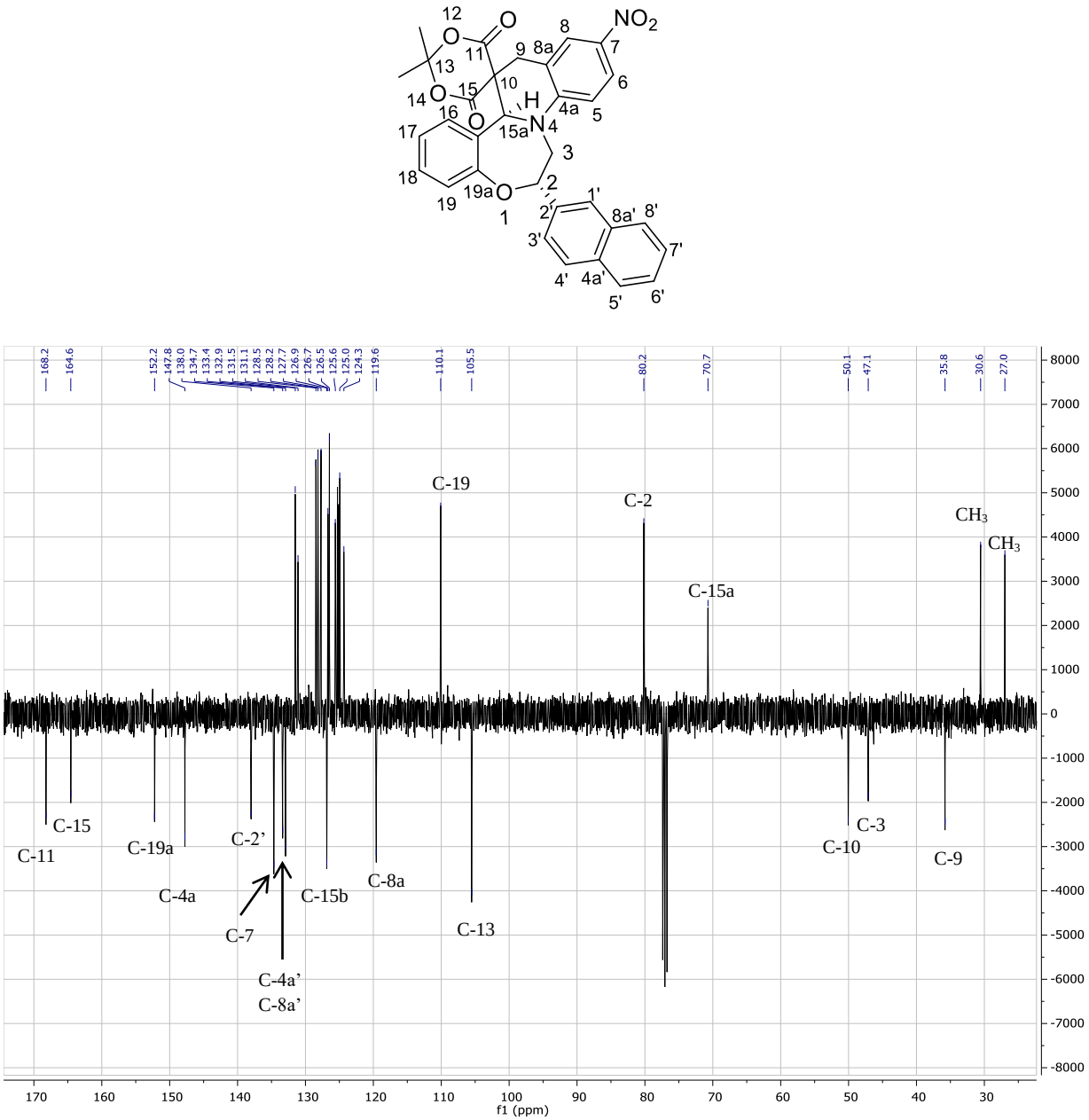

Figure S58. J-modulated ^{13}C-NMR spectrum of *rac*-**11c** measured in $CDCl_3$ (100 MHz)

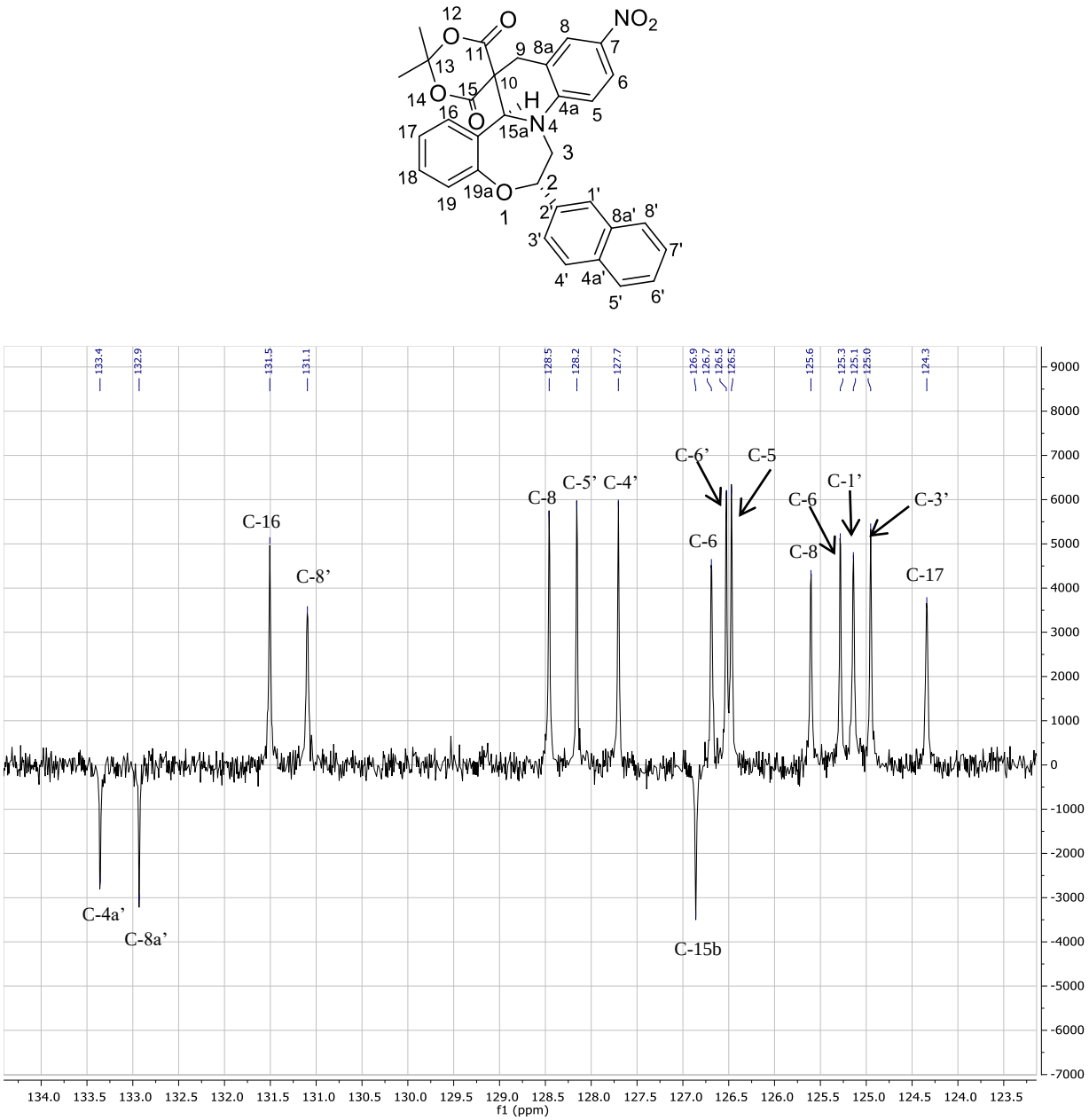

Figure S59. J-modulated ^{13}C-NMR spectrum of *rac*-**11c** measured in $CDCl_3$ (100 MHz)

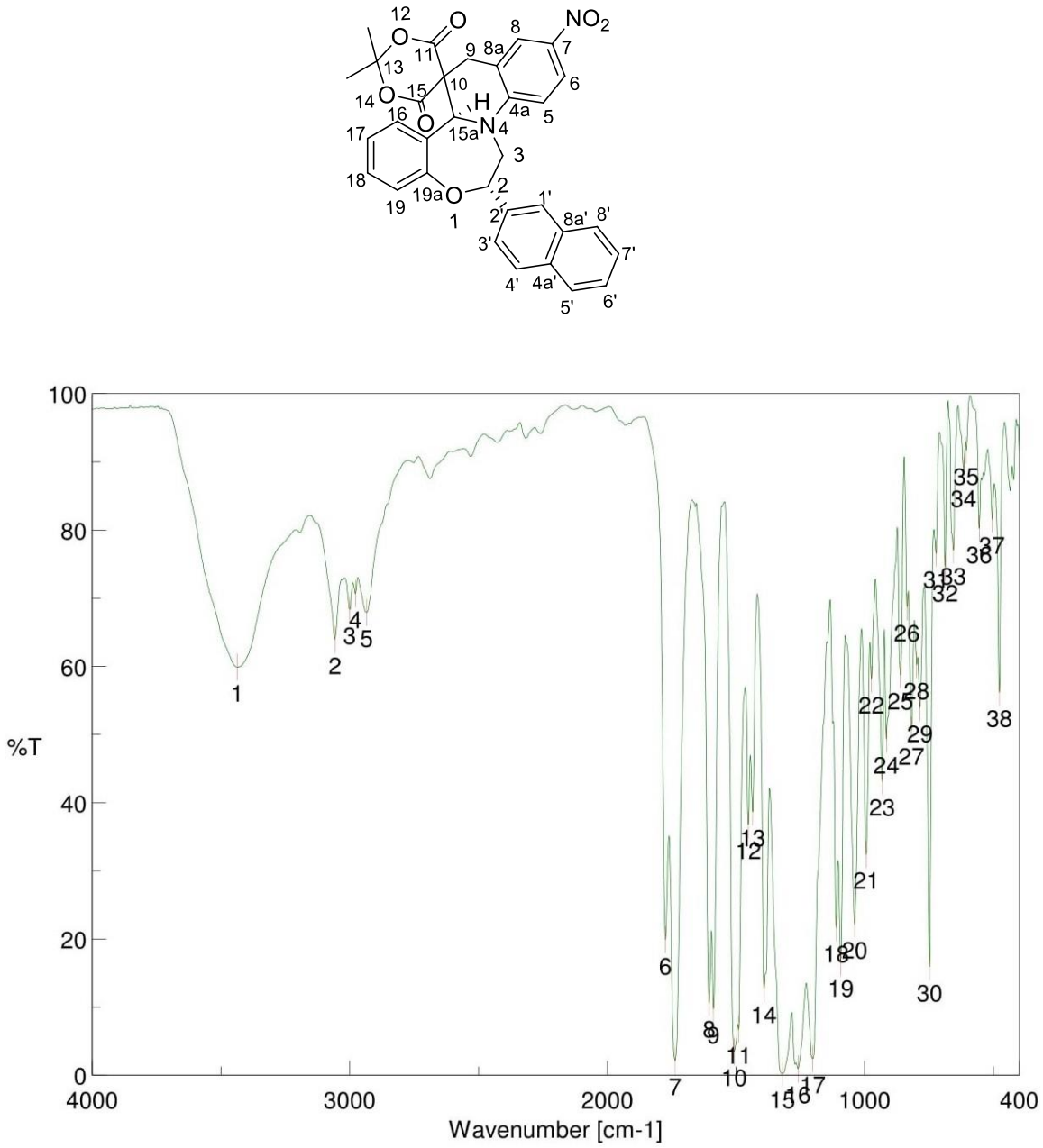

Figure S60. IR spectrum of *rac*-**11c** recorded as KBr disc

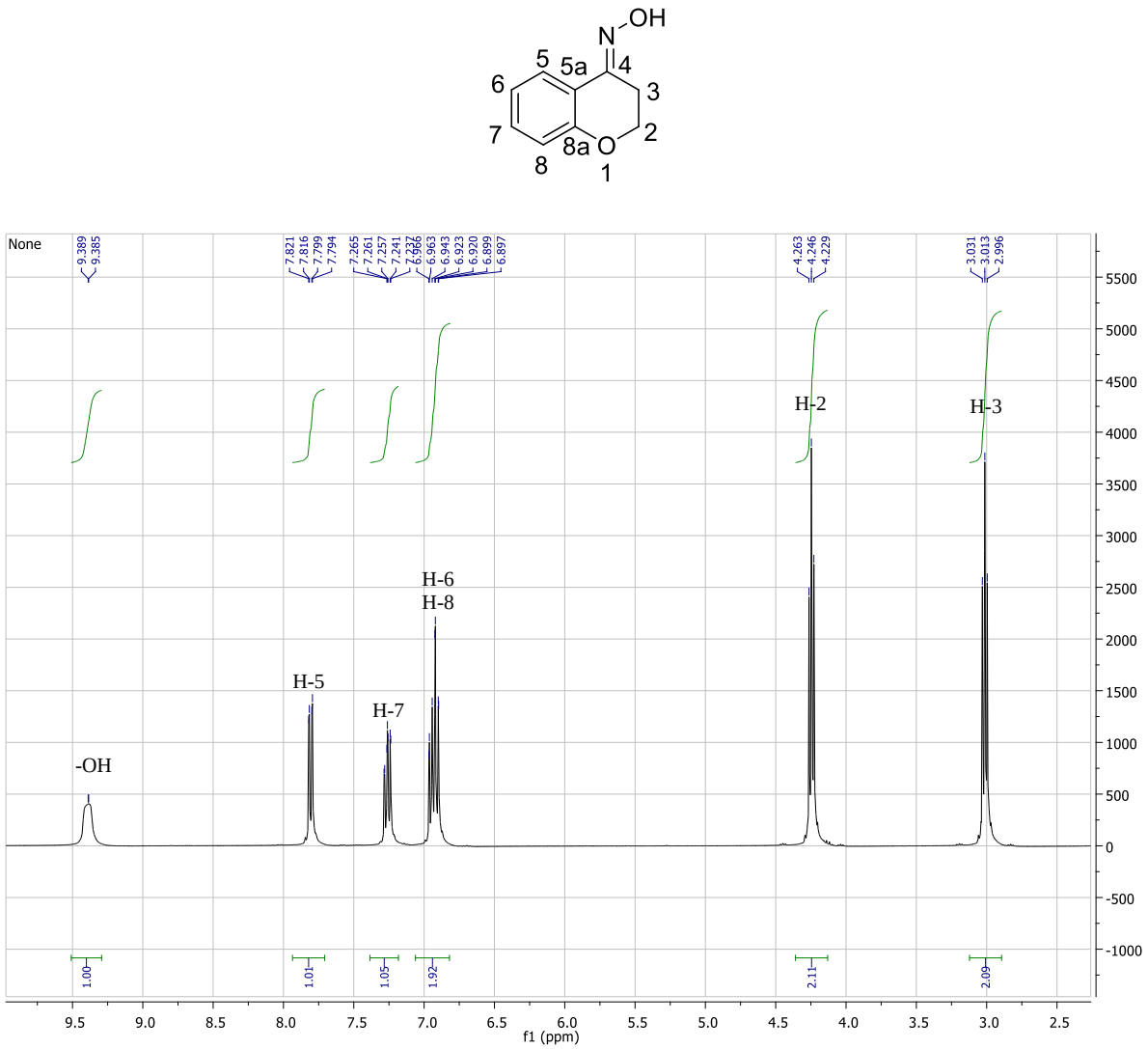

Figure S61. ^{1}H-NMR spectrum of **13** measured in $CDCl_3$ (360 MHz)

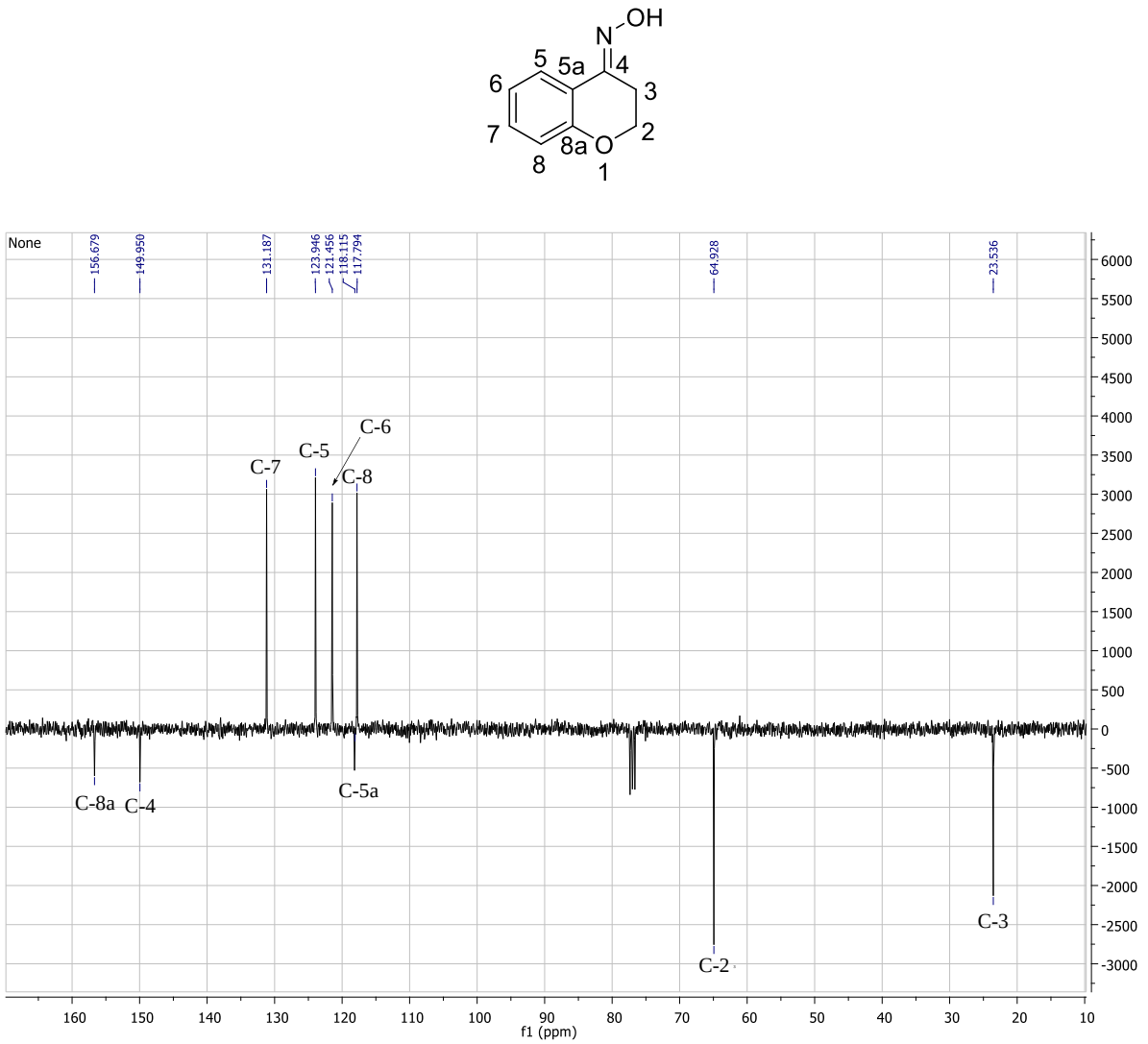

Figure S65. J-modulated ^{13}C-NMR spectrum of **13** measured in $CDCl_3$ (90 MHz)

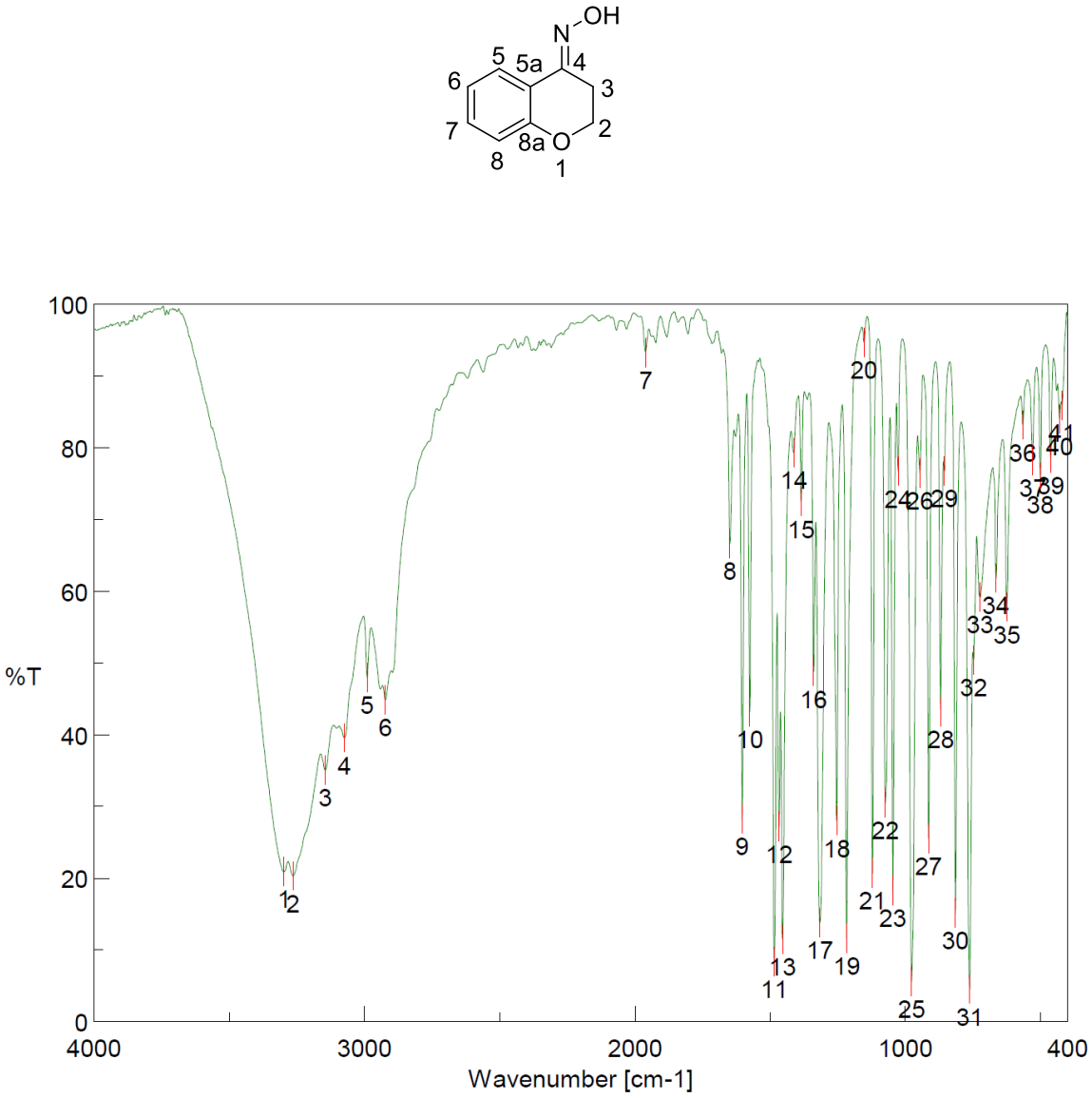

Figure S66. IR spectrum of **13** recorded as KBr disc

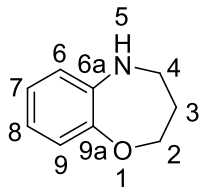

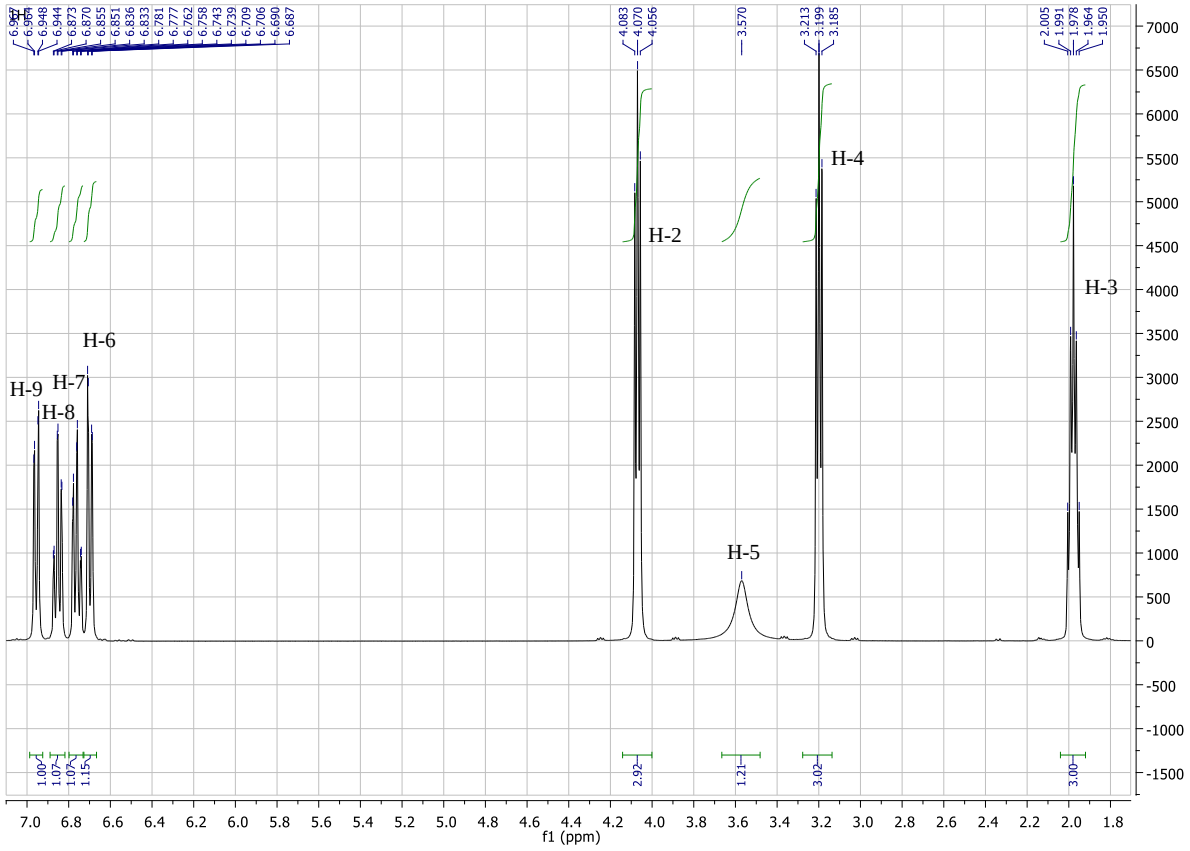

Figure S67. ^{1}H-NMR spectrum of **15** measured in $CDCl_3$ (400 MHz)

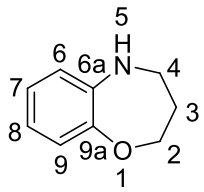

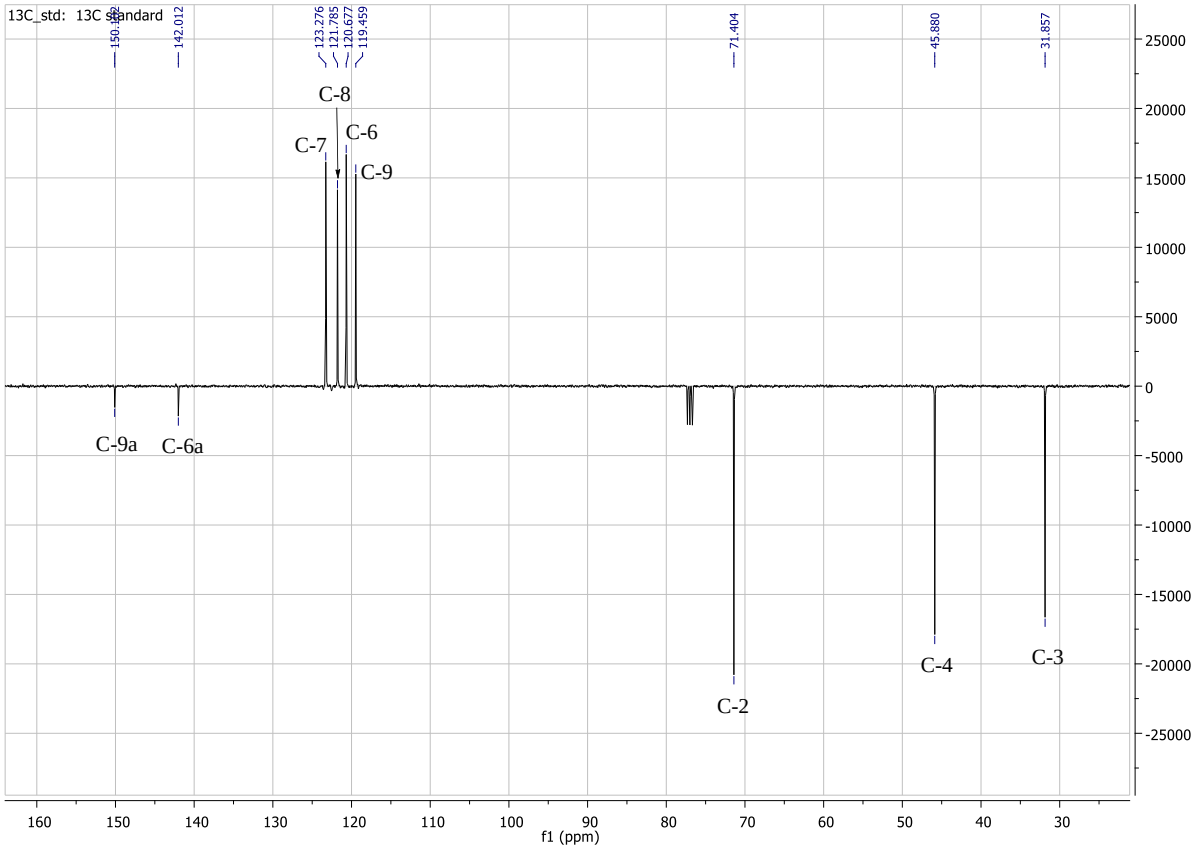

Figure S68. J-modulated ^{13}C-NMR spectrum of **15** measured in $CDCl_3$ (100 MHz)

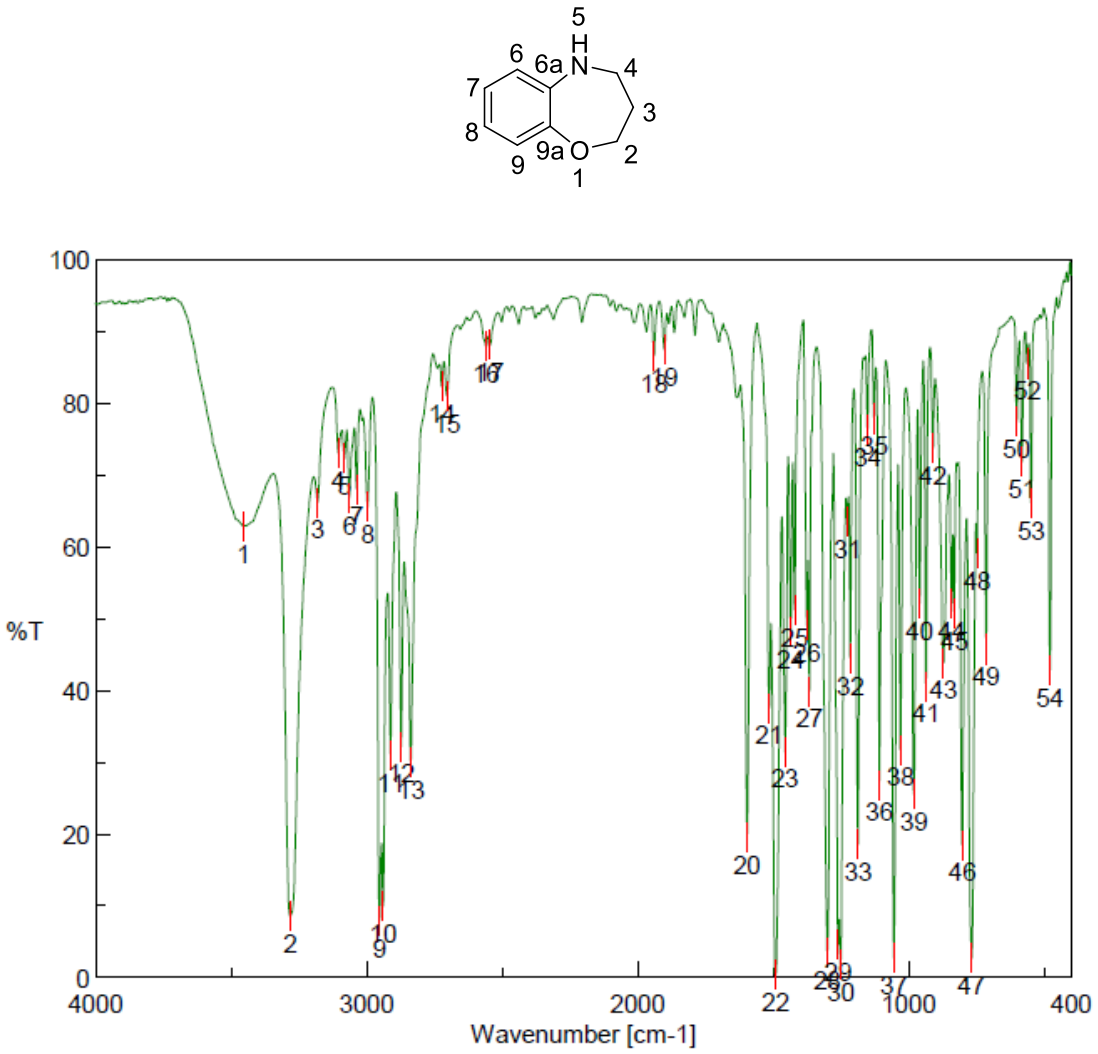

Figure S69. IR spectrum of **15** recorded as KBr disc

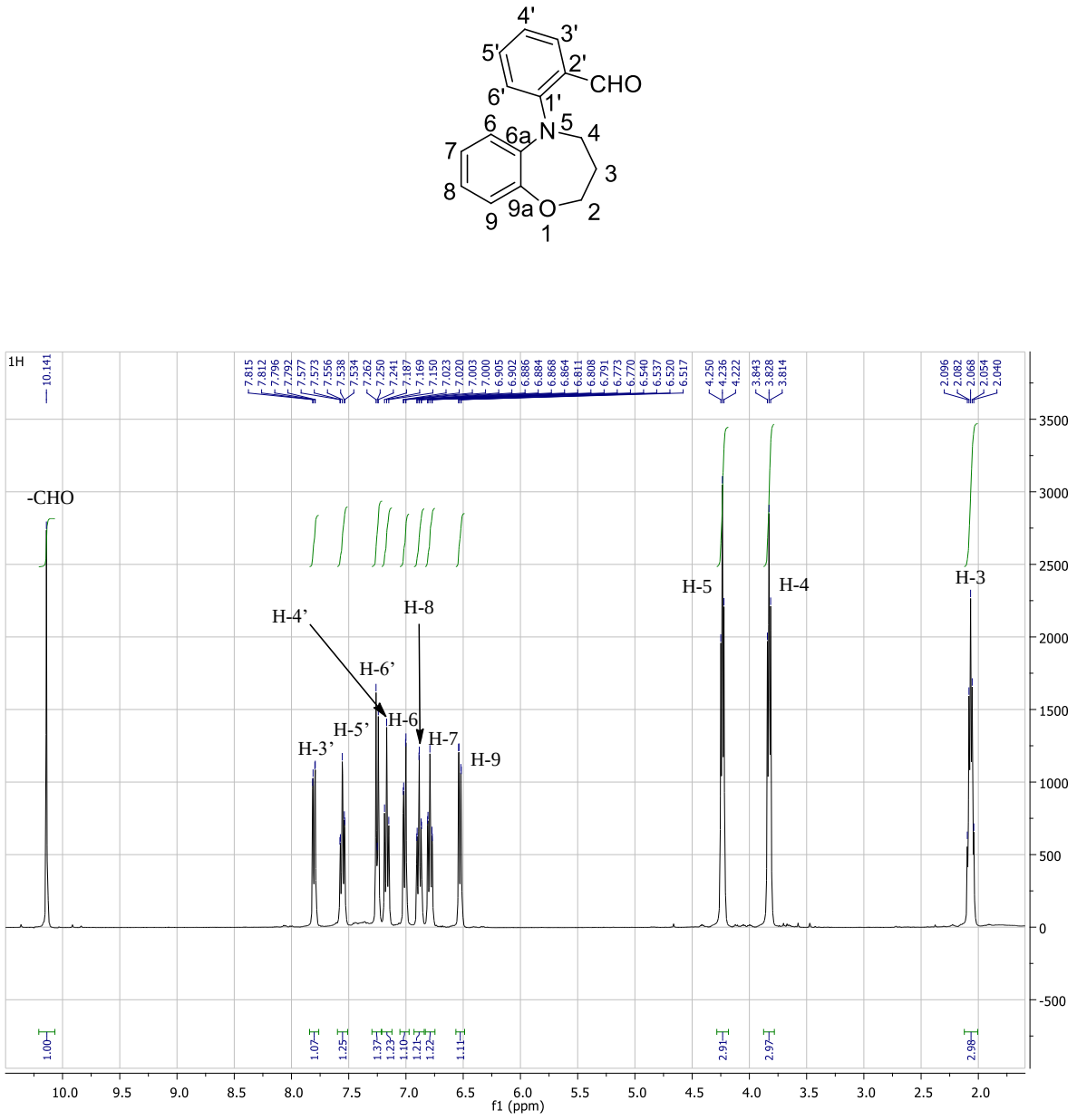

Figure S70. ^{1}H-NMR spectrum of **4** measured in $CDCl_3$ (400 MHz)

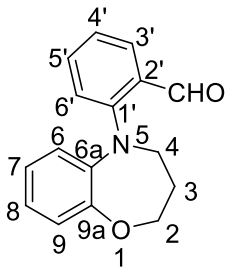

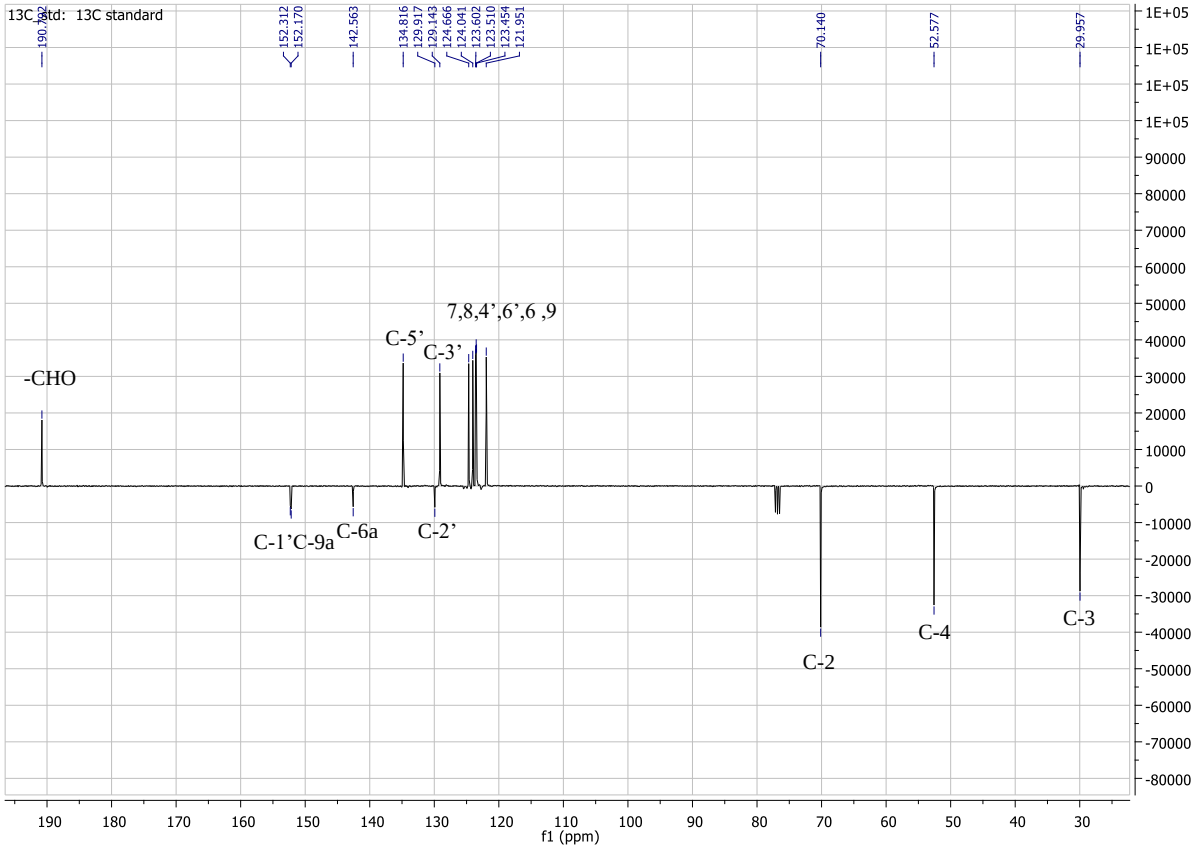

Figure S71. J-modulated ^{13}C-NMR spectrum of **4** measured in $CDCl_3$ (100 MHz)

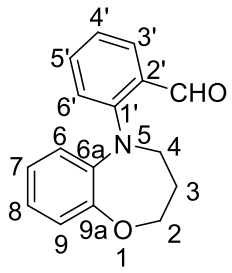

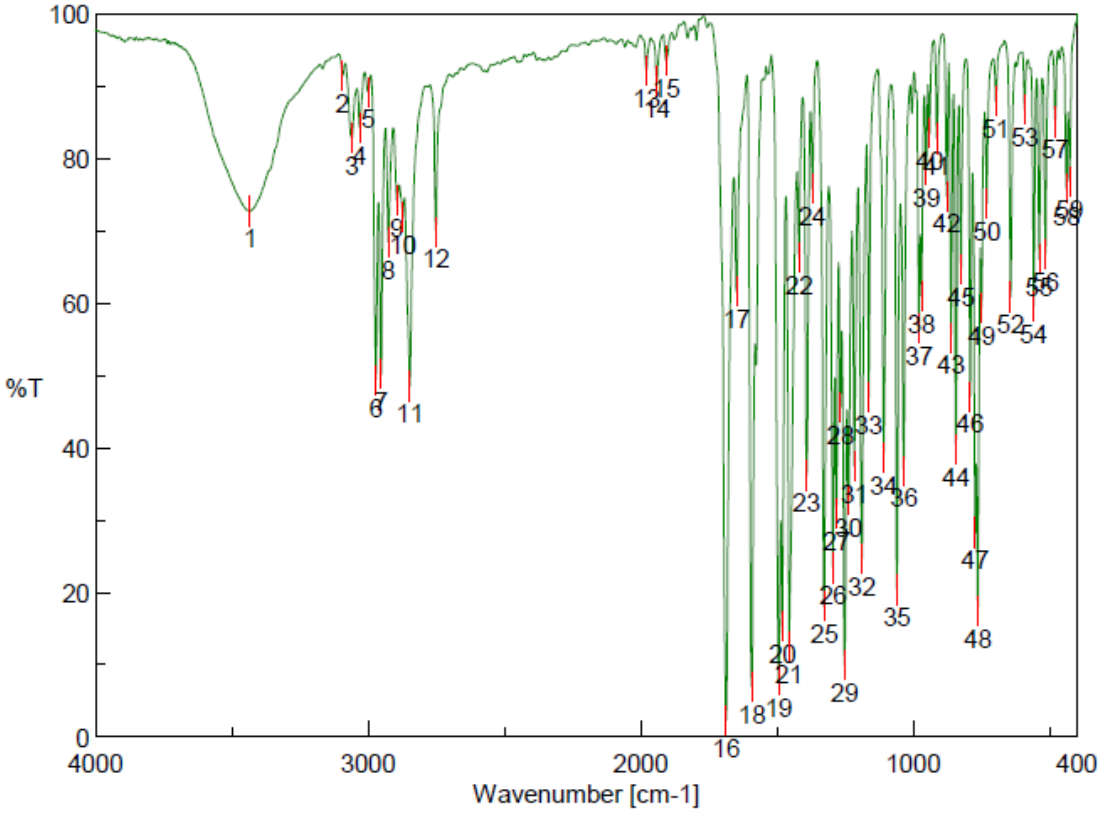

Figure S72. IR spectrum of **4** recorded as KBr disc

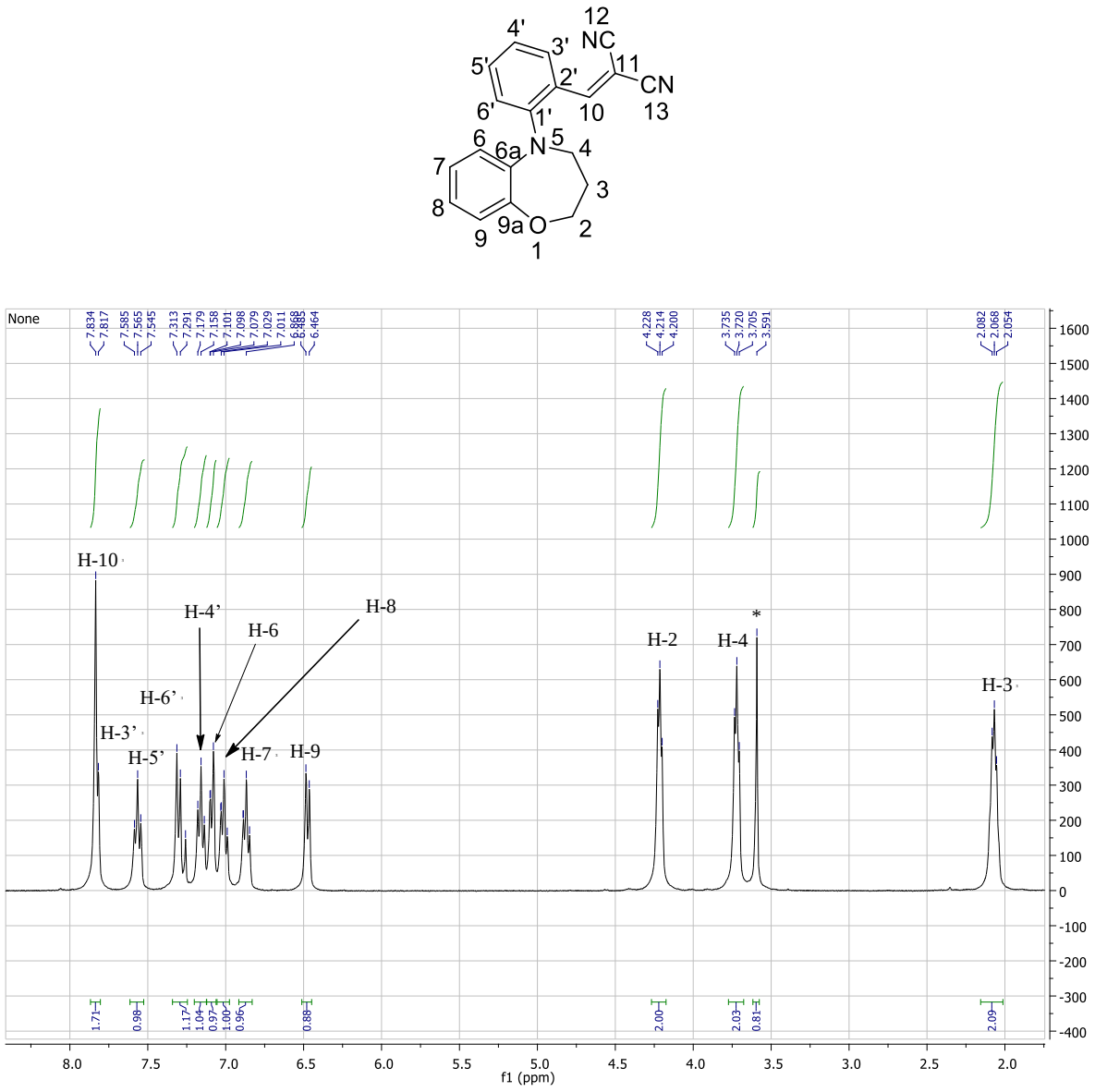

Figure S73. ^{1}H-NMR spectrum of **20** measured in $CDCl_3$ (360 MHz)

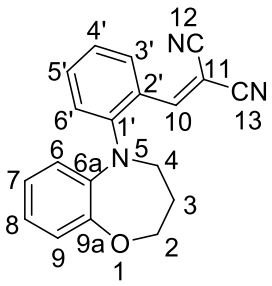

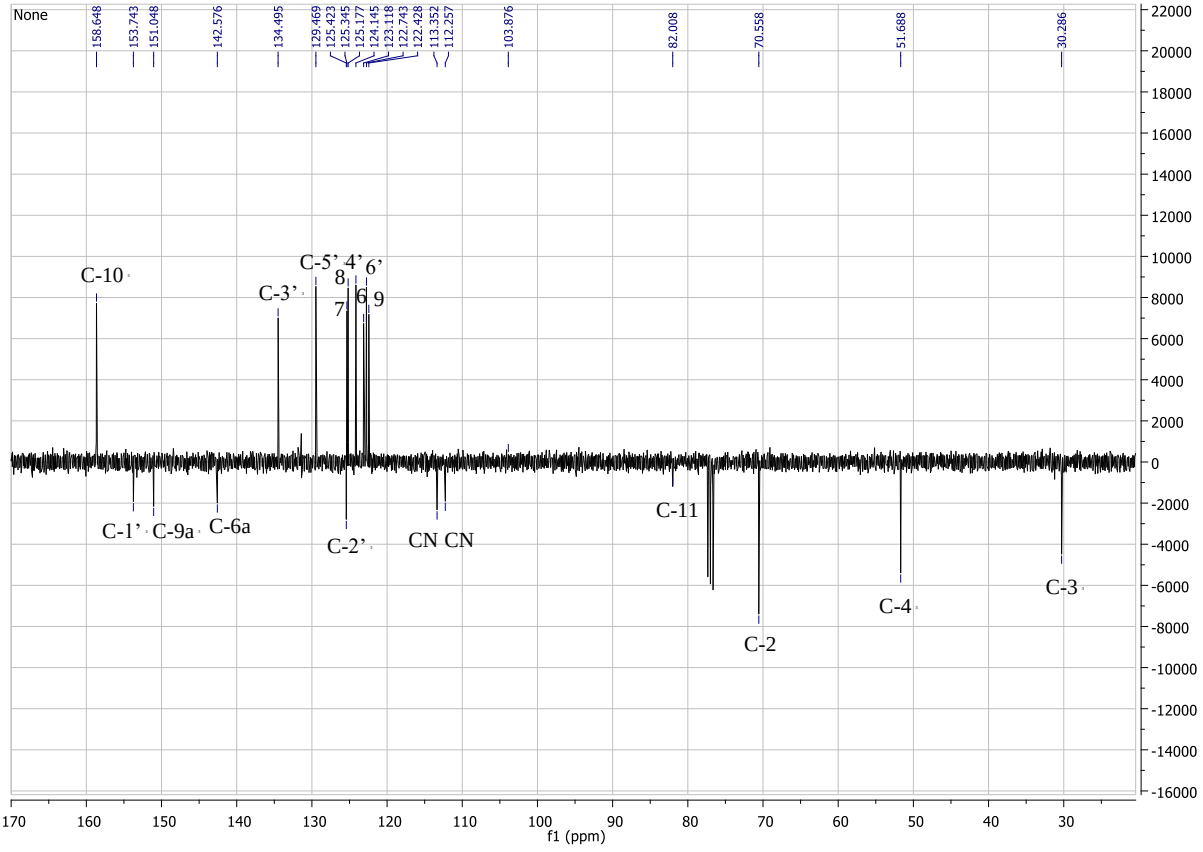

Figure S74. J-modulated ^{13}C-NMR spectrum of **20** measured in $CDCl_3$ (90 MHz)

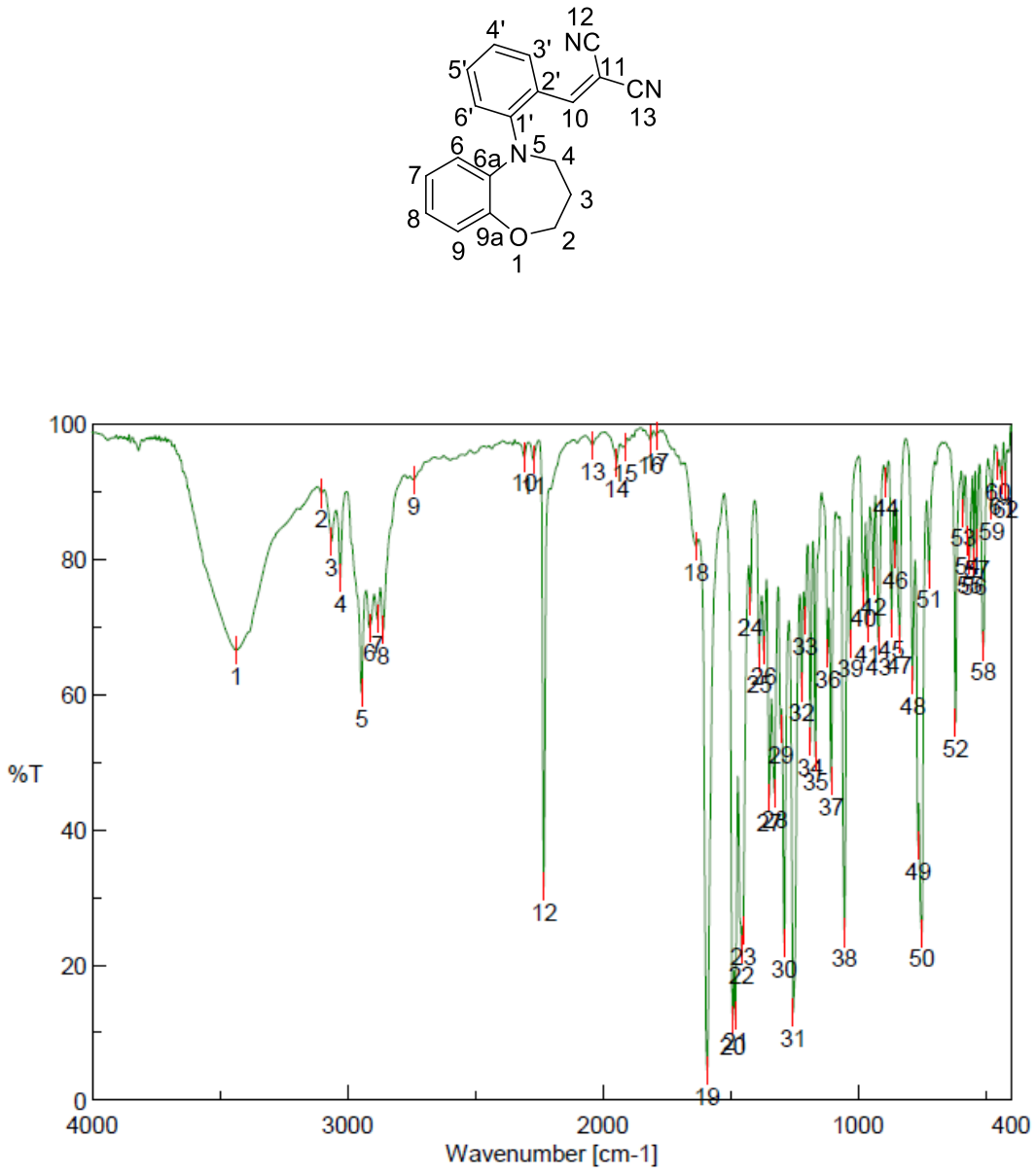

Figure S75. IR spectrum of **20** recorded as KBr disc

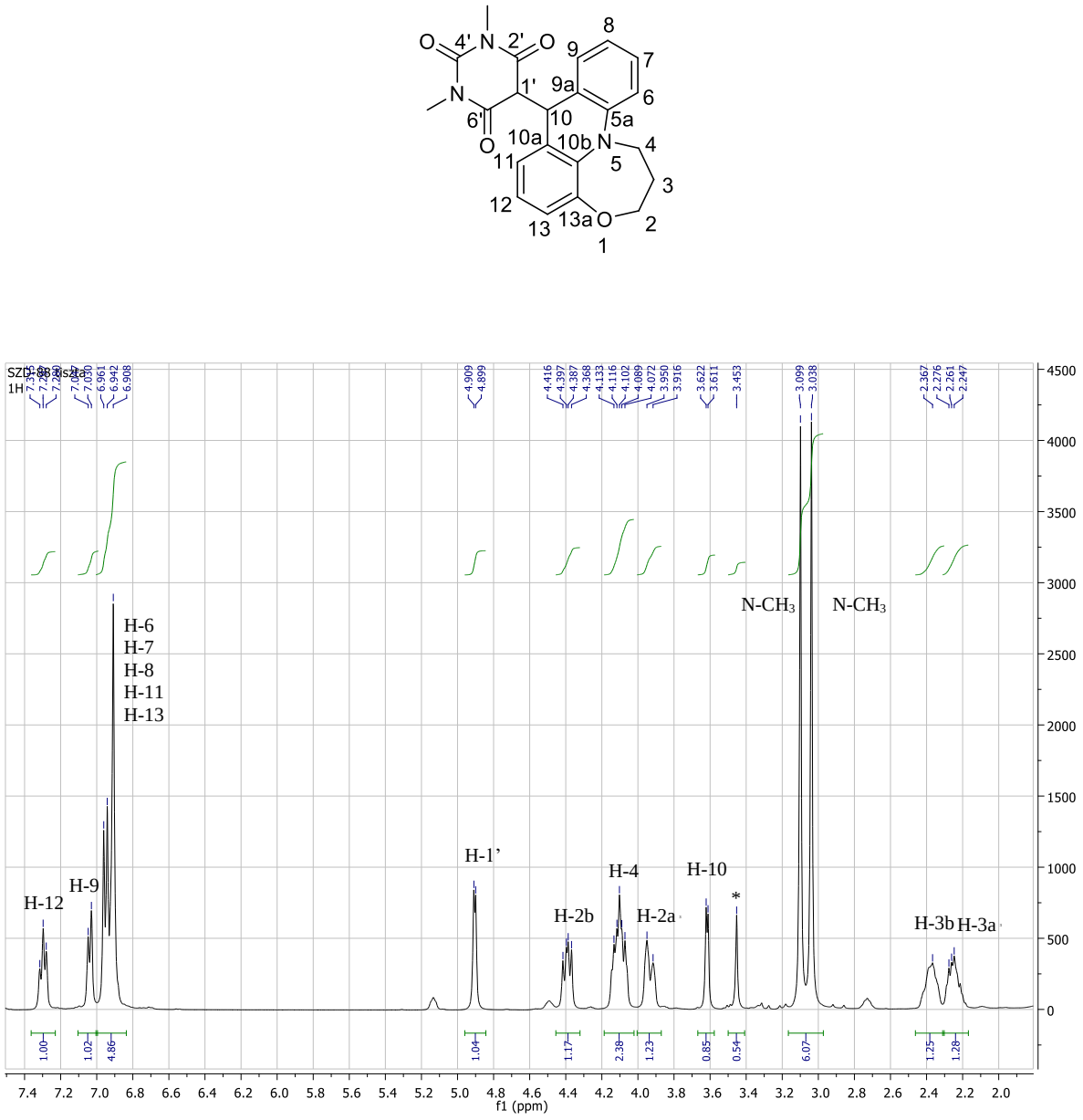

Figure S76. ^{1}H-NMR spectrum of **6** measured in $CDCl_3$ (400 MHz)

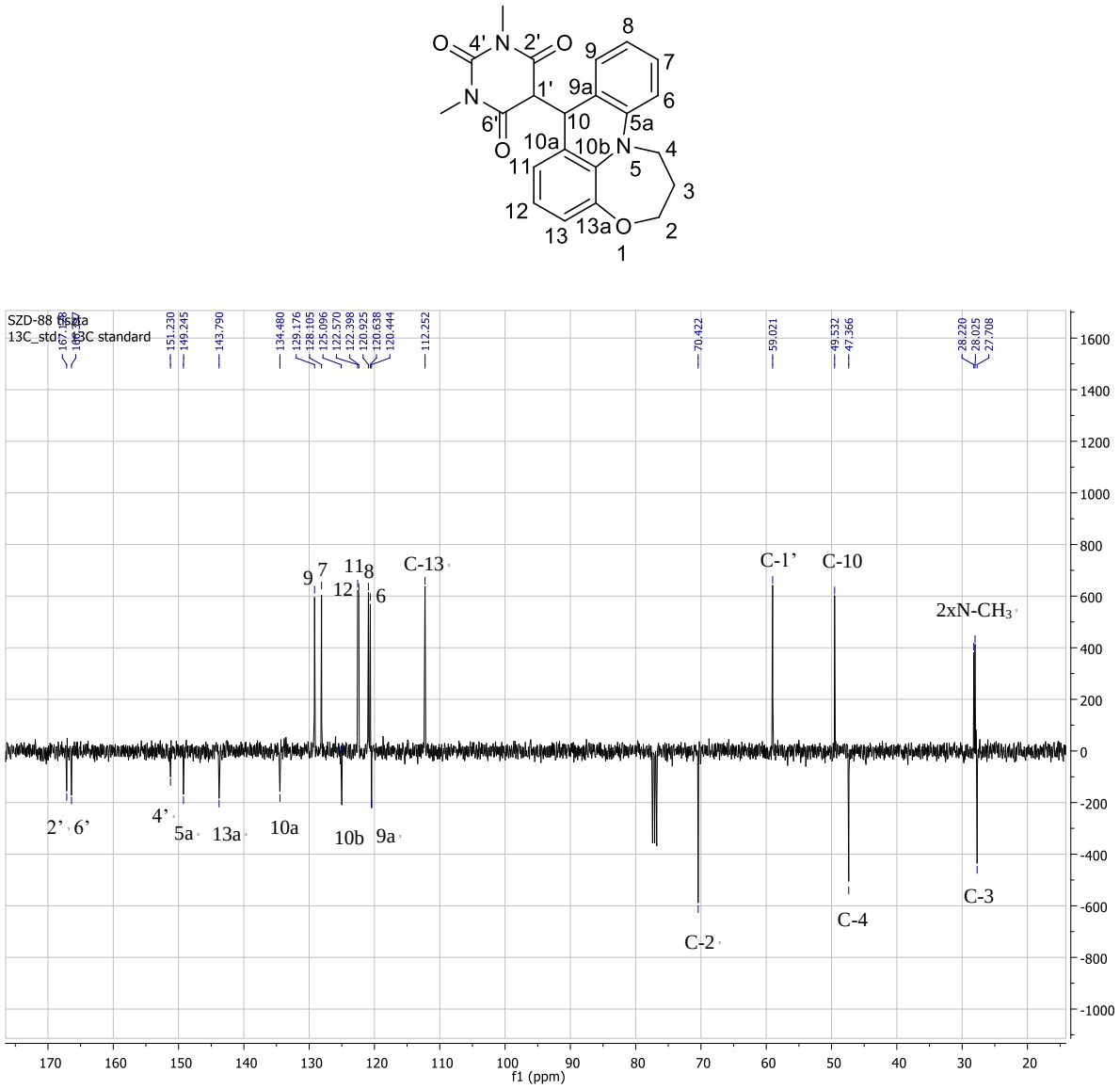

Figure S77. J-modulated ^{13}C-NMR spectrum of **6** measured in $CDCl_3$ (100 MHz)

organocatalyst	Reaction time (day)		Conversion (%)		ee (%)	
	A	B	A	B	A	B
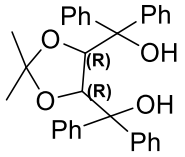	21	9	22	25	6.1	6.9
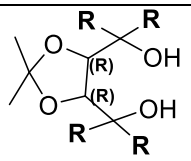 **R**: α-naftil	21	9	26	26	7.3	5.4
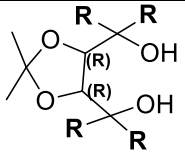 **R**: β-naftil	21	9	17	29	7.2	3.8
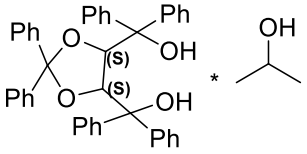	21	9	13	30	4.6	2.9
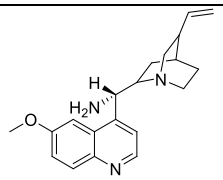	8	8	10	11	2.9	1.9
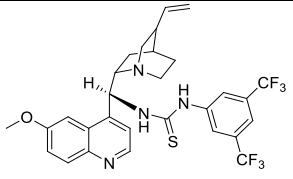	8	8	9	8	0.0	1.0

Table S1. Organocatalytic transformations of **1a** to *trans*-**10a** (columns A) and **1a** to **11a** (columns B); reaction condition: $MgSO_4/CHCl_3$, 0.3 equivalent of organocatalyst, rt.

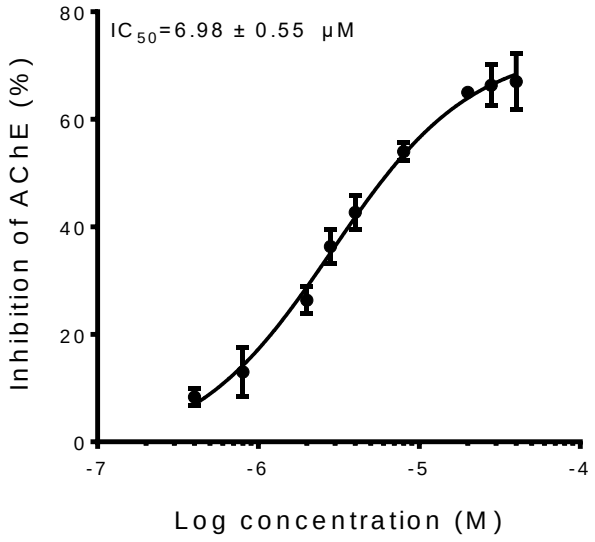

Figure S78. Concentration-dependent curve of **6** for the inhibition of AChE activity. IC_{50} of **6** was calculated to be 6.98 ± 0.55 µM. Every point is an average of three independent experiments (mean ± SD).